Journal of Chemistry

Antioxidants in Disease and Aging

Guest Editors: Qiusheng Zheng, Ji Li, Zhenhua Wang, and Chunming Wang

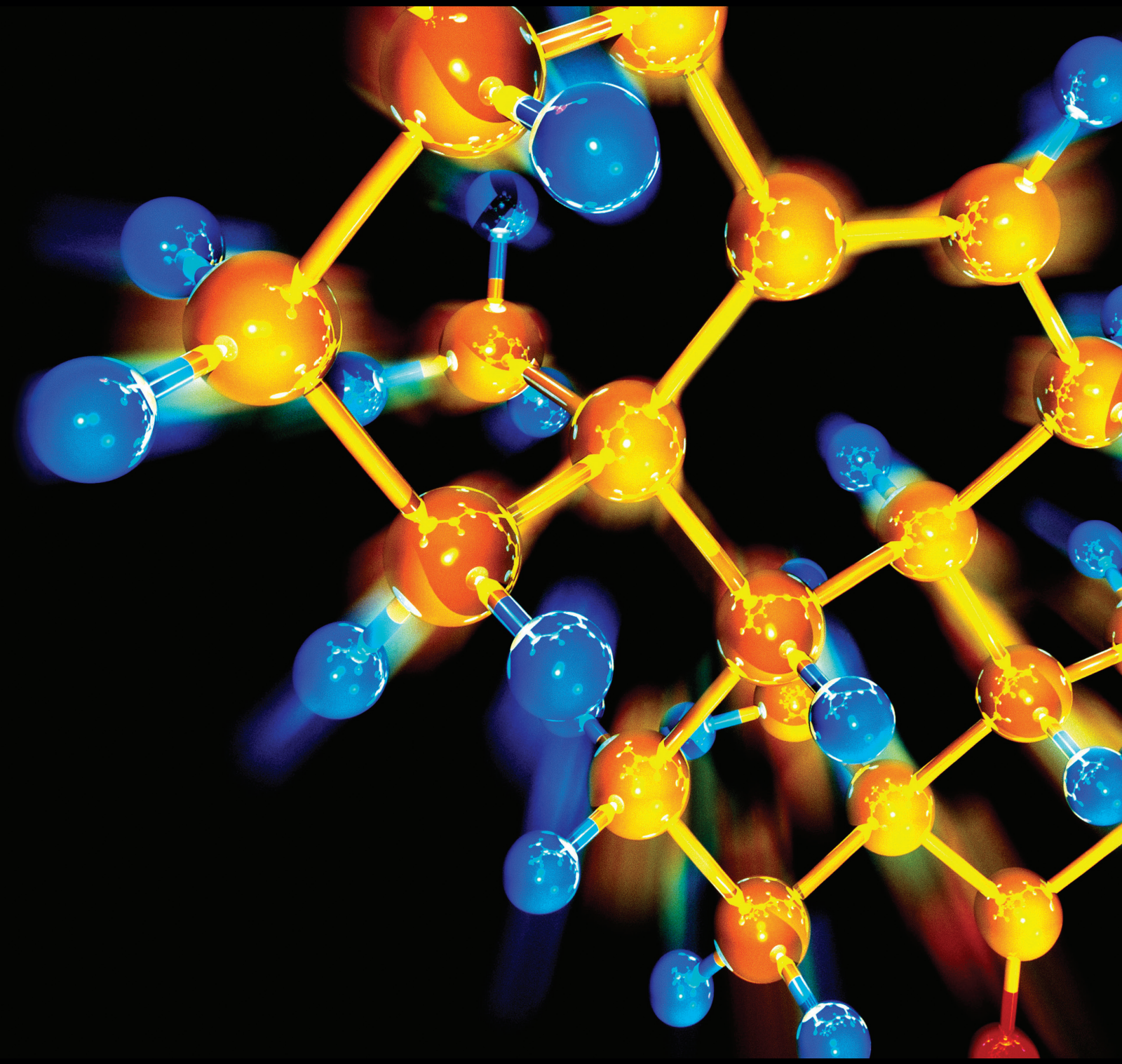

Antioxidants in Disease and Aging

Journal of Chemistry

Antioxidants in Disease and Aging

Guest Editors: Qiusheng Zheng, Ji Li, Zhenhua Wang, and Chunming Wang

Contents

Hindawi Publishing Corporation
Journal of Chemistry
Volume 2014, Article ID 235147, 2 pages
http://dx.doi.org/10.1155/2014/235147

Editorial

Antioxidants in Disease and Aging

Qiusheng Zheng,[1] Ji Li,[2] Zhenhua Wang,[3] and Chunming Wang[4]

[1] *Binzhou Medical University, Yantai 264005, China*
[2] *School of Medicine and Biomedical Sciences, State University of New York (SUNY) at Buffalo, Buffalo, NY 14214, USA*
[3] *Life Sciences School, Yantai University, Yantai 264005, China*
[4] *Life Sciences School, Lanzhou University, Lanzhou 730000, China*

Correspondence should be addressed to Qiusheng Zheng; johnsonjem@hotmail.com

Received 22 August 2014; Accepted 22 August 2014; Published 1 September 2014

Free radicals and related reactive species, especially reactive oxygen and nitrogen species (ROS/RNS), are able to cause damage to biomolecules, leading to cell and tissue injury in mammals, including humans. Thus, a number of endogenous antioxidant defenses have been evolved in mammals to protect against the damage caused by ROS/RNS; a variety of antioxidants has been applied to the treatment and prevention of disease. In addition, antioxidants have been widely used in food, medicine, and cosmetics industry.

As a result, "antioxidants" became a buzzword in the 1990s, and their benefits were glorified by the media, by the food industry which began labeling foods as "rich in antioxidants," and by the supplement industry as they began hyping the health benefits of antioxidant supplements. They were even promoted as antiaging ingredients in beauty products. It is very necessary for seeking new bioactive antioxidants and studying their chemical and biological properties, their chemical basis of security, and the interaction between them. Thus, in this special issue, we have published a series of papers that address such issues.

One paper of this special issue introduces the antioxidant constituents and pharmacological effects of Sijunzi decoction by looking up literatures in recent years. Research on the antioxidant components of Sijunzi decoction and their targets is a promising study area in the future.

Another paper presents the study on stress-induced ROS changes DNA methylation patterns; this paper developed a protocol combining methylation-sensitive restriction endonuclease digestion with suppression subtractive hybridization to construct the differential-methylation subtractive library.

Another paper clarified the cardioprotective property of the aqueous extract of *Elaeagnus angustifolia* L. leaf (EA) against myocardial ischemia/reperfusion injury in isolated rat heart. Another paper evaluated the cardioprotective property of the aqueous extract of lavender flower (LFAE) on myocardial ischemia/reperfusion (I/R) injury of rat using Langendorff retrograde perfusion technology. The result of these two articles showed that EA and LFAE provide protection for heart against the I/R injury via the improvement of myocardial oxidative stress states.

One paper clarified that water extract of *Chorispora bungeana* treatment significantly reduced neurological deficit scores and infarct size through antioxidant and antiapoptotic activities. Another paper revealed that the antioxidant enzymes of halophyte used in traditional Chinese medicine for clearing heat and for detoxification are activated under NaCl stress. Another paper clarified the protection of ginsenoside Rg3 against oxidative stress in human neuroblastoma SK-N-SH cells. Both 20 (R)-Rg3 and 20 (S)-Rg3 had obvious protection against H_2O_2-induced oxidative stress in SK-N-SH cells.

Another paper uncovered that ophiurasaponin from *Ophiopholis mirabilis* had obvious antioxidant activities and antimicrobial activities which could provide the theoretical basis for further research and development of antioxidant and antimicrobial marine drugs. Another paper made clear

that five compounds with antioxidant and anti-inflammatory activities were isolated for the first time from Styela clava.

Another paper systematically evaluated the antioxidant activity of Xanthohumol using three systems; results showed that different methods for evaluation of antioxidant capicity may have led to a different conclusion.

Qiusheng Zheng
Ji Li
Zhenhua Wang
Chunming Wang

Hindawi Publishing Corporation
Journal of Chemistry
Volume 2014, Article ID 278318, 10 pages
http://dx.doi.org/10.1155/2014/278318

Review Article

Pharmacological Activities of Sijunzi Decoction Which Are Related to Its Antioxidant Properties

Lei Ye,[1] Jianwei Gong,[1] Yonghua Wang,[2] and Xiling Sun[1]

[1] *Department of Chinese Medicine Integrated with Western Medicine, Binzhou Medical University, Yantai, Shandong 264003, China*
[2] *School of Biosciences, Northwest A&F University, Xi'an, Shanxi 710000, China*

Correspondence should be addressed to Xiling Sun; sunxilingsun@sohu.com

Received 18 May 2014; Accepted 5 July 2014; Published 23 July 2014

Academic Editor: Qiusheng Zheng

This paper introduces the antioxidant constituents and pharmacological effects of Sijunzi decoction by looking up literatures in recent years. Sijunzi decoction is composed of Ginseng, Atractylodes, Tuckahoe, and Glycyrrhiza. The antioxidant ingredients of Sijunzi decoction include paeonol, dauricine, naringin, and isoliquiritigenin. The study has proved that it possesses wide pharmacological effects of anticardiovascular diseases, antinervous system disease, antidiabetes, antimetabolic syndrome, and antitumor. Research on the antioxidant components of Sijunzi decoction and their targets is a promising study area in the future.

1. Introduction

Phagocytic cells release a significant amount of reactive oxygen species (ROS) through respiratory burst under the stimulus of pathogenic microorganisms when "spleen qi deficiency" occurs, which is often associated with gastrointestinal inflammation. Through NADPH oxidation, ROS can cause oxidative damage and further aggravate the inflammation. Studies have shown that Sijunzi decoction has evident antioxidant effects [1] and can eliminate or reduce biological membrane lipid peroxidation caused by free radicals [2]. Moreover, Sijunzi decoction can increase superoxide dismutase (SOD) activity and reduce MDA generation to speed up the elimination of free radicals and other harmful substances to protect biological macromolecules from damage and improve the DNA repair. Sijunzi decoction has an antioxidant effect because it contains a wide variety of free radical scavenging molecules. These antioxidant compounds possess anti-inflammatory, antiatherosclerotic, antitumor, antimutagenic, anticarcinogenic, or antibacterial properties. The antioxidants derived from Sijunzi decoction are summarized in this study. The source of antioxidants discussed in this study is shown in Table 1.

2. The Role of Antioxidants from Sijunzi Decoction

2.1. Antioxidants of Anticardiovascular Disease. Several components of Sijunzi soup have antioxidant activity and decrease the occurrence of cardiovascular diseases. Studies have shown that isoliquiritigenin, which is a natural antioxidant derived from liquorice, has a significant role in anticardiovascular disease through activation of the AMP-activated protein kinase (AMPK) and ERK signaling pathways and balance of cellular redox status [3]. Naringin derived from liquorice, which is the second most important antioxidant component, inhibits reactive oxygen species- (ROS-) activated MAPK pathway involved in high glucose-induced injuries of H9c2 cardiac cells [4]. Naringin mitigates hypertension and thrombosis by increasing the bioavailability of nitrogen oxide (NO) and protecting the endothelial function from ROS [5]. Moreover, naringin can improve redox-sensitive myocardial ischemia reperfusion injury [6]. Glabridin, which is derived from liquorice and is responsible for its antioxidative characteristics in low-density lipoprotein (LDL) oxidation, is also important [7]. Isorhamnetin, which is also derived from liquorice, can inhibit the H_2O_2-induced activation of the

Table 1

Source of ingredient	Antioxidant ingredient
Ginseng	Paeonol, dauricine, pancratistatin
Licorice	Isoliquiritigenin, naringin, glabridin, isorhamnetin, calycosin, pinocembrin, nicotiflorin, liquiritigenin, kaempferol, licoflavone, isobavachalcone, morusin, licochalcone A, licochalcone B, rutin, quercetin

intrinsic apoptotic pathway through ROS scavenging and ERK inactivation. Therefore, isorhamnetin is a promising reagent for the treatment of ROS-induced cardiomyopathy [8].

Paeonol, which is mainly collected from ginseng, affects the development of cardiovascular tissues. Paeonol has antioxidant and anti-inflammatory properties, which can be developed for use in anti-inflammatory and vascular disorders [9]. The therapeutic mechanism of paeonol prevents monocyte adhesion onto vascular endothelial cells (VECs) induced by ox-LDL [10]. Paeonol has a protective effect on the hypoxia/reoxygenation damage of myocardial cells; therefore, it can prevent myocardial infarction induced by isoproterenol in rats [11]. Paeonol can also decrease oxidative injury and repair blood vessel endothelium, as well as prevent the development of coronary diseases [12].

2.2. Antioxidants against Diabetes and Metabolic Syndrome. Metabolic syndrome is a low-grade inflammatory state, where oxidative stress is involved. Some of the antioxidants extracted from Sijunzi decoction exhibit antidiabetes activities or metabolic syndrome reversal. Isoliquiritigenin can significantly decrease the level of blood glucose [13]. Naringin exhibits significant antidiabetic effects by potentiating the antioxidant defense system and by suppressing proinflammatory cytokine production in a rat model of T2DM [14]. Naringin reverses the metabolic syndrome by decreasing inflammatory cell infiltration and plasma lipids; the process mitigates oxidative stress and improves mitochondrial function [15]. Glabridin, which is a major active flavonoid in *Glycyrrhiza glabra* (licorice), improves learning and memory in mice. Glabridin reverses learning and memory defects in diabetic rats. Glabridin treatment partially improves the reduced body weight and hyperglycemia of diabetic rats. Their mechanisms may be related to the combination of antioxidant, neuroprotective, and anticholinesterase properties of glabridin [16] or as an activator of AMP-activated protein kinase (AMPK) [17].

2.3. Antioxidants of Antineurological Diseases. Clinically, Sijunzi decoction is often used to treat several neurological diseases. Calycosin, which is derived from licorice, has a neuroprotective effect against cerebral ischemia/reperfusion injury through its antioxidant effects [55]. Isoliquiritigenin protects HT22 hippocampal neuronal cells from oxidative stress-induced glutamate. The mechanisms are related to the reversed ROS production and mitochondrial depolarization induced by glutamate, as well as the regulation expression of the apoptotic regulators, Bcl-2 and Bax [31]. Isoliquiritigenin can protect dopaminergic cells from oxidative injury and prevent Aβ(25–35)-induced neuronal apoptotic death by interfering with the increase of [$Ca2^{+}$] and ROS [32]. Liquiritigenin is derived from licorice; this compound improves behavioral performance and attenuates neuronal loss in the brain of rats [64]. Pinocembrin derived from licorice has a significant role in neurovascular protection by protecting the cerebral ischemia and increasing the viability of the mitochondrial membrane [57, 58, 80, 81]. Pinocembrin abrogates the effects of the neurotoxin 1-methyl-4-phenylpyridinium, which mimics Parkinson's disease with an elevation of intracellular ROS level and apoptotic death [82]. This phenomenon might be another mechanism for pinocembrin in mitigating nervous system diseases.

Nicotiflorin, which is derived from licorice, markedly reduces brain infarct volume and neurological deficits immediately following its administration after the onset of ischemia. Nicotiflorin also protects against memory dysfunction, energy metabolism failure, oxidative stress in multi-infarct dementia model rats, cerebral ischemic damage, aluminum chloride-induced cognitive dysfunction, and mitochondrial oxidative damage [61, 62]. Investigations about the protective mechanism of kaempferol glycosides showed the involvement of their antioxidative activity, blockage of caspase cascades, attenuation of NMDA-induced neuronal toxicity, inhibition of monoamine oxidase (MAO), excessive NO production, and others [63].

Naringin may be beneficial in mitigating 3-NP-induced neurodegeneration through its antioxidant and antiapoptotic effects [39, 40].

Glabridin has a neuroprotective effect because of the modulation of multiple pathways associated with apoptosis. Glabridin significantly attenuates the level of brain malonyldialdehyde (MDA) in MCAO rats; however, it elevates the levels of two endogenous antioxidants in the brain, namely, SOD and reduced glutathione [48].

Dauricine is derived from ginseng and has cerebral ischemia-reperfusion injury protection effect, which may be related to its inhibition of neuron apoptosis [22]. Paeonol mitigates neuronal damage not only by decreasing ROS overgeneration, but also by regulating expression of apoptosis proteins and neurotrophic factors [18, 19].

2.4. Antioxidants of Antirespiratory Diseases. Three components from Sijunzi soup have significant roles in preventing respiratory diseases.

Naringin has antitussive, anti-AHR, and anti-inflammation effects on chronic cigarette smoke exposure-induced chronic bronchitis in guinea pigs; this compound improves SOD activity in lung tissue and increases the content of lipoxin A4 in bronchoalveolar lavage fluid (BALF) in a guinea pig model for chronic bronchitis [41, 42]. Dauricine induces glutathione depletion and apoptosis in lungs of CD-1 mice and in cultured human lung cells [23]. Liquiritigenin can protect human lung cells (A549) from a hemolysin-mediated injury [65].

2.5. Antioxidants against Digestive System Diseases. Several components of Sijunzi soup are also involved in antidigestive system diseases.

Liquiritigenin has a choleric effect and exhibits the ability to induce hepatic transporters and phase-II enzymes, which are a group of antioxidant systems that function against oxidative stress, carcinogenesis, mutagenesis, and other forms of toxicity [66]. Isoliquiritigenin, which is similar with liquiritigenin, can repress LXRα-dependent hepatic steatosis through JNK1 inhibition and protect hepatocytes from oxidative injury inflicted by fat accumulation [33].

The induction of HO activity by pinocembrin has a protective effect against hepatic damage associated with oxidative stress in rats. Pinocembrin challenges hepatocarcinogens and may exhibit anticarcinogenic effects [59]. Dauricine is subject to oxidative bioactivation in human liver microsomes in vitro and in rats in vivo [24].

Licoflavone, isobavachalcone, and quercetin are derived from licorice. Licoflavone feeding suppresses gastric mucosa injury and protects and restores injured mucosa in rats with chronic superficial gastritis. These effects are related with the upregulation of serum PGE2 levels [69]. Isobavachalcone shows broad antioxidative activities in rat liver microsomes and mitochondria [70]. Quercetin has beneficial effects on liver fibrosis in rats by enhancing antioxidant enzyme activity and reducing the prooxidant effects [79].

Several studies have demonstrated that isorhamnetin is efficient in protecting hepatocytes against oxidative stress by Nrf2 activation and in inducing the expression of its downstream genes [50].

Paeonol can inhibit HSC proliferation and induce mitochondrial apoptosis by disrupting the NF-κB pathway, which is probably the mechanism of paeonol reduction of liver fibrosis [20].

2.6. Antioxidants of Antitumors. Natural compounds isolated from Sijunzi decoction, which are rich sources of novel anticancer drugs, have gained increasing interest.

Isoliquiritigenin significantly inhibits the proliferation of C4-2 prostate cancer cells in IEC-6 normal epithelial cells in vitro, increases intracellular ROS levels, and causes SKOV-3 and hela cell apoptosis [34–36]. The prodifferentiation effect of isoliquiritigenin on HL-60, particularly the role of redox homeostasis in regulating HL-60 cell differentiation by modulation of the Nrf2/ARE pathway, has been investigated [37, 38].

Licochalcone A and licochalcone B are derived from licorice. Licochalcone A has potent antitumor effects in prostate, breast, and bladder cancer, as well as in leukemia cell lines [74]. A study has shown that the induction of endoplasmic reticulum stress through a PLC γ1-, Ca^{2+}-, and ROS-dependent pathways may be significant when licochalcone A induces apoptosis in HepG2 hepatocellular carcinoma cells [75]. Furthermore, licochalcone B inhibits the concentration-dependent bladder cancer cell proliferation; this antiproliferative effect is caused by the induction of S-phase arrest and apoptotic cell death [77].

Dauricine can inhibit the proliferation activity of urinary tract tumor cells. By inhibiting the NF-κB signaling pathway in colon cancer cells, dauricine inhibits proliferation and invasion of the cancer [25, 26]. Furthermore, dauricine inhibits human breast cancer angiogenesis by suppressing hypoxia inducible factor-1α (HIF-1α) protein accumulation and vascular endothelial growth factor (VEGF) expression [27].

Naringin can induce receptor death and mitochondria-mediated apoptosis in human cervical cancer cells [43]. Naringin reduces the growth potential of human triple-negative breast cancer cells by targeting the β-catenin signaling pathway [44]. Naringin is effective in reducing the number of preneoplastic lesions in rats exposed to 1,2-dimethylhydrazine. Several of these effects may be caused by reduced cellular proliferation and tissue levels of iron and the recovery of antioxidant mineral levels induced by this flavonoid [45].

Pancratistatin is derived from ginseng and may be a novel mitochondria-targeting compound that selectively induces apoptosis in cancer cells and significantly reduces tumor growth [28, 29]. Pancratistatin treatment in cancer cell lines results in increased ROS production and reduction of mitochondrial membrane potential [30]. Morusin, which is derived from licorice, significantly inhibits the growth and clonogenicity of HT-29 human colorectal cancer cells, as well as the human cervical cancer stem cell growth and migration [72, 73].

Calycosin is an indispensable element in antitumor activities. Calycosin inhibits breast cancer growth and is obtained by estrogen receptor (ER) β-mediated regulation of the IGF-1R signaling pathways and miR-375 expression [56]. Isorhamnetin exhibits antioxidant and antiproliferative activities in a variety of cancer cell lines [51–53].

Glabridin is a novel anticancer agent for treating breast cancer in three different manners, namely, inhibition of migration, invasion, and angiogenesis [49]. Pinocembrin triggers Bax-dependent mitochondrial apoptosis in colon cancer cells [60]. Isobavachalcone induces apoptotic cell death in neuroblastoma through the mitochondrial pathway and is not cytotoxic against normal cells [71]. Paeonol has significant growth-inhibitory and apoptosis-inducing effects in gastric cancer cells, both in vitro and in vivo [21].

2.7. Antioxidants against Inflammation. The components of Sijunzi soup have a significant role against inflammation.

Naringin is an effective anti-inflammatory compound for attenuating the chronic pulmonary neutrophilic inflammation in CS-induced rats. The oxidative stress caused by cigarette smoke (CS) exposure increases inflammatory cell influxes in the lungs, followed by lipid peroxidation, and increases proinflammatory cytokines, such as the tumor necrosis factor-α [46]. Liquiritigenin has an anti-inflammatory effect, as shown by the inhibition of nitric oxide and tumor necrosis factor-production, which is induced by the lipopolysaccharides in macrophages [67]. Licochalcone A protects BALB/c mice from lipopolysaccharide-(LPS-) induced endotoxin shock by inhibiting the production

Table 2

Antioxidant ingredient	Structure of compound	Pharmacological activity	References
Paeonol	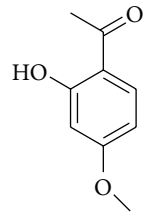	(1) Antioxidant and anti-inflammatory properties (2) Treatment for vascular disorders (3) Protection against atherosclerosis. (4) Neuroprotection (5) Protection against hypoxia/reoxygenation damage (6) Growth-inhibitory and apoptosis-inducing effects on cancer cells	[9–12, 18–21]
Dauricine	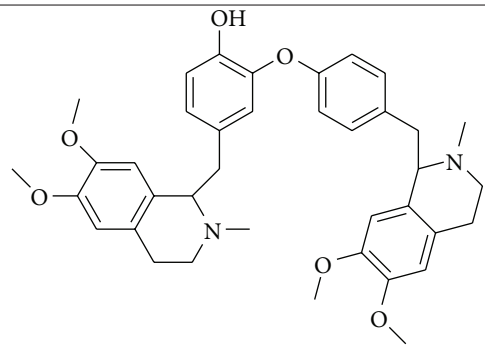	(1) Inhibition of neuron apoptosis (2) Induction of glutathione depletion and apoptosis in cancer cells (3) Inhibition of tumor cell proliferation (4) Inhibition of cancer angiogenesis (5) Induction of tumor cell apoptosis	[22–27]
Pancratistatin	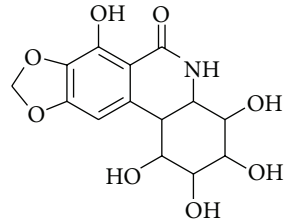	(1) Increased reactive oxygen species (ROS) production (2) Induction of mitochondrial membrane collapse (3) Potential induction of tumor apoptosis (4) Reduction of tumor growth	[28–30]
Isoliquiritigenin	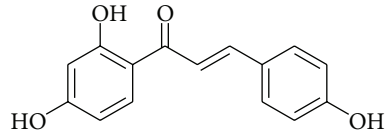	(1) Cardioprotection against ischemic injury (2) Decreased blood glucose level (3) Prevention of neurodegenerative diseases (4) Prevention of neuronal apoptotic death (5) Repression of liver X receptor-α-dependent hepatic steatosis (6) Induction of apoptosis (7) Inhibition of cancer cell proliferation (8) Enhancement of HepG2 cell radiosensitivity	[3, 13, 31–38]
Naringin	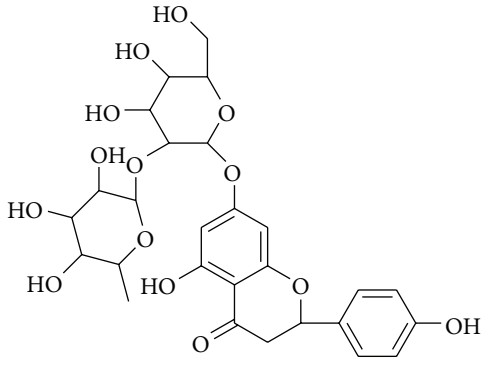	(1) Inhibition of ROS-activated MAPK pathway (2) Antihypertensive and antithrombotic effects (3) Protection of endothelial function from ROS (4) Protection against myocardial ischemia reperfusion injury (5) Antidiabetic effect (6) Decreased inflammatory cell infiltration (7) Neuroprotective effect (8) Anti-inflammatory effect (9) Protection against pulmonary fibrosis (10) Induction of cancer cell apoptosis (11) Attenuation of chronic pulmonary neutrophilic inflammation (12) Mitigation of erythrocyte aging	[4–6, 14, 15, 39–47]

Table 2: Continued.

Antioxidant ingredient	Structure of compound	Pharmacological activity	References
Glabridin	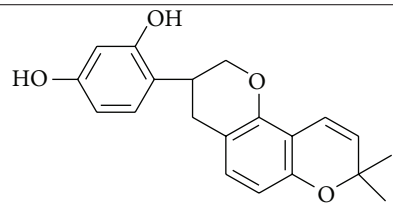	(1) Antioxidation (2) Protection against obesity-related metabolic disorders (3) Neuroprotective effect (4) Anti-inflammatory effect (5) Anticancer effect	[7, 16, 17, 48, 49]
Isorhamnetin	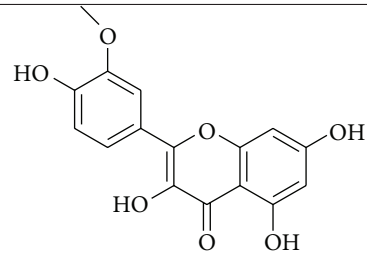	(1) Inhibition of ROS-induced apoptotic pathway (2) Anti-ROS-induced cardiomyopathy (3) Protection of hepatocytes against oxidative stress (4) Antioxidant and antiproliferative effects (5) Modulation of the peroxisome proliferator-activated receptor pathway in gastric cancer	[8, 50–54]
Calycosin	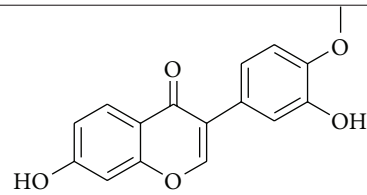	(1) Neuroprotection (2) Inhibition of breast cancer growth	[55, 56]
Pinocembrin	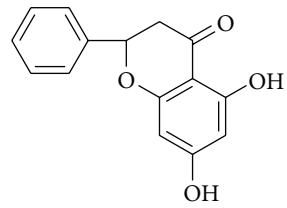	(1) Neurovascular protection (2) Protection of cerebral ischemia (3) Increased viability and mitochondrial membrane potential of cultured rat cerebral microvascular endothelial cells (4) Protection of rat brain against oxidation and apoptosis (5) Abrogation of neurotoxin effects (6) Improvement of rat cognitive impairments (7) Anticarcinogenic effects (8) Triggering mitochondrial apoptosis in cancer cells	[57–60]
Nicotiflorin	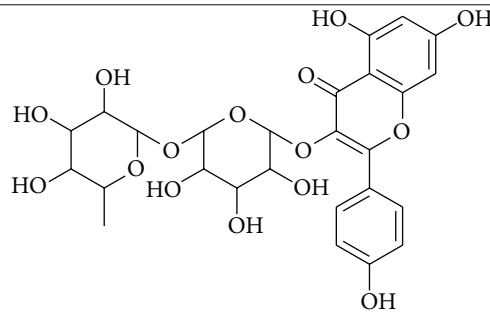	(1) Improvement of brain infarct volume and neurological deficits (2) Protection against memory dysfunction, energy metabolism failure, and oxidative stress (3) Protection against cerebral ischemic damage	[61–63]
Liquiritigenin	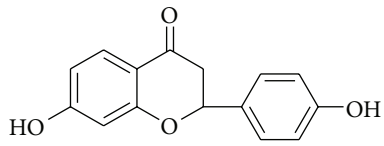	(1) Improvement of behavioral performance and attenuation of neuronal loss in the brain (2) Protection of human lung cells (A549) (3) Choleretic effect and induction of hepatic transporters and phase-II enzymes (4) Induction of apoptosis in the mitochondrial pathway (5) Anti-inflammatory effect (6) Protection of osteoblast against cytotoxicity	[64–68]

Table 2: Continued.

Antioxidant ingredient	Structure of compound	Pharmacological activity	References
Kaempferol	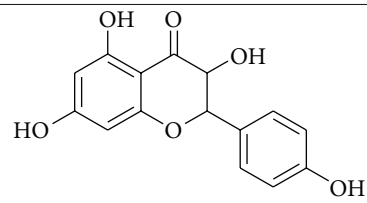	(1) Attenuation of neuronal toxicity (2) Inhibition of monoamine oxidase and excessive NO production	[63]
Licoflavone	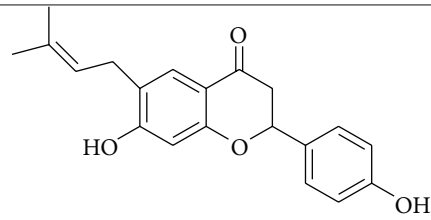	(1) Suppression of gastric mucosa injury	[69]
Isobavachalcone	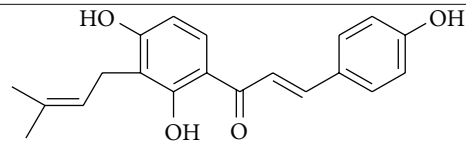	(1) Antioxidant effects on rat liver microsomes and mitochondria (2) Induction of neuroblastoma apoptosis	[70, 71]
Morusin	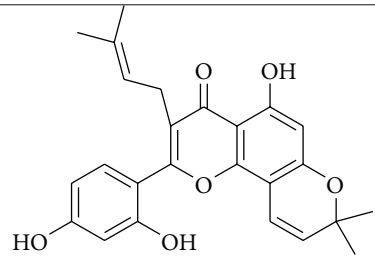	(1) Anticancer properties	[72, 73]
Licochalcone A	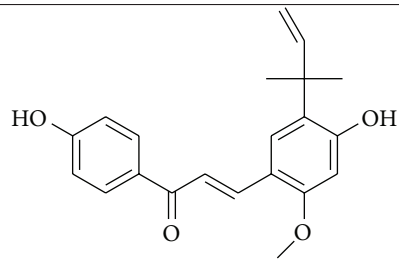	(1) Antitumor and antimetastatic properties (2) Apoptosis-promotion (3) Inhibition of inflammatory cytokines and ROS production	[74–76]
Licochalcone B	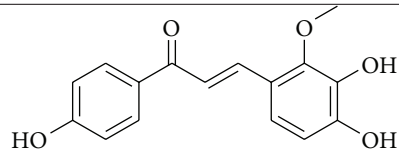	(1) Inhibition of cancer cell proliferation	[77]
Rutin	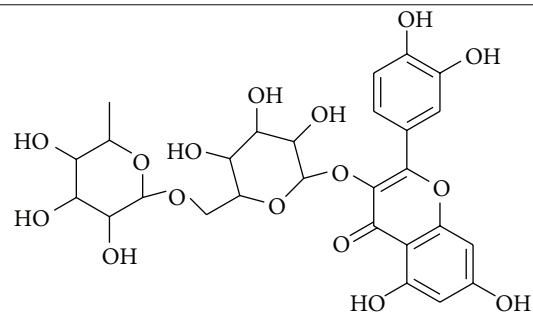	(1) Inhibition of primary humoral immune response	[78]

Table 2: Continued.

Antioxidant ingredient	Structure of compound	Pharmacological activity	References
Quercetin	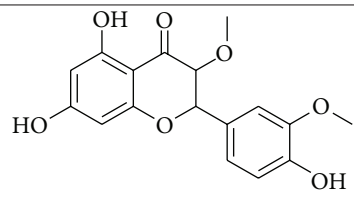	(1) Antiliver fibrosis properties (2) Modulation of degranulation and oxidative burst	[54, 69, 79]

of inflammatory cytokines and ROS [76]. Quercetin and kaempferol can modulate the degranulation and oxidative burst of stimulated human neutrophils. Rutin, which is derived from licorice, inhibits the primary humoral immune response in mice [78]. The induction of HO-1 by isorhamnetin may reduce ROS production, and the antioxidant property of isorhamnetin might inhibit the COX-2 expression in response to inflammation [54].

2.8. Others. The Sijunzi soup has a significant role in other aspects, such as the mitigation of musculoskeletal diseases and the progression of hematological system diseases.

The modulation of PI3K antioxidant effects and the attenuation of mitochondrial dysfunction by liquiritigenin represent an important mechanism for the protection of osteoblasts against cytotoxicity, which results from mitochondrial oxidative stress [68].

Naringin mitigates erythrocyte aging induced by paclitaxel (PTX), which suggests that naringin inhibits PTX-induced aging by reducing the PTX-induced oxidative stress [47].

3. Antioxidants List

See Tables 1 and 2.

4. Conclusion

The oxidative products of organisms cause several diseases. Several studies have been conducted on the effects of antioxidant-scavenging free radical. Sijunzi decoction contains a variety of antioxidants. The effects of these antioxidants have gained attention from scholars at home and abroad. Various research results have been obtained. The antioxidants in Sijunzi decoction decrease free radical content and enhance the free radical scavenging activities in the body by adjusting the activity of the antioxidative enzyme system when spleen deficiency occurs. The antioxidants in Sijunzi decoction eliminate the peroxidation damage in tissues, cells, and various types of biological macromolecules and protect the normal structure and function of the cell membrane. Sijunzi decoction improves the pathological changes of tissues and cells in the cardiovascular and respiratory systems, corrects the nerve and endocrine functions, strengthens digestion, and induces tumor cell apoptosis. Revealing mainly the antioxidant of Sijunzi decoction is necessary to understand its antioxidant effects. Research to discover the antioxidant components of Sijunzi decoction and their target research are areas of future study in this field.

Conflict of Interests

The authors declare that there is no conflict of interests regarding the publication of this paper.

References

[1] Y. Wei and W. Li, "The c orrelation of experimental spleen deficiency and free radical metabolism and t he adjustment of sijunzi decoction," *Acta Veterinaria et Zootechnica Sinica*, vol. 33, no. 1, pp. l00–104, 2002.

[2] W. Yanming and L. Wenguang, "Si Jun Zi decoction anti lipid peroxidation in vitro and the role of reactive oxygen free radicals," *Acta Veterinaria et Zootechnica Sinica*, vol. 33, no. 2, pp. 197–199, 2002.

[3] X. Zhang, P. Zhu, Y. Ma et al., "Natural antioxidant-isoliquiritigenin ameliorates contractile dysfunction of hypoxic cardiomyocytes via AMPK signaling pathway," *Mediators of Inflammation*, vol. 2013, Article ID 390890, 10 pages, 2013.

[4] J. Chen, R. Guo, H. Yan et al., "Naringin inhibits ROS-activated MAPK pathway in high glucose-induced injuries in H9c2 cardiac cells," *Basic & Clinical Pharmacology & Toxicology*, vol. 114, no. 4, pp. 293–304, 2014.

[5] M. Ikemura, Y. Sasaki, J. C. Giddings, and J. Yamamoto, "Preventive effects of hesperidin, glucosyl hesperidin and naringin on hypertension and cerebral thrombosis in stroke-prone spontaneously hypertensive Rats," *Phytotherapy Research*, vol. 26, no. 9, pp. 1272–1277, 2012.

[6] N. Rani, S. Bharti, M. Manchanda et al., "Regulation of heat shock proteins 27 and 70, p-Akt /p-eNOS and MAPKs by Naringin Dampens myocardial injury and dysfunction in vivo after ischemia/reperfusio," *PLoS ONE*, vol. 8, Article ID e82577, 2013.

[7] B. Fuhrman, S. Buch, J. Vaya et al., "Licorice extract and its major polyphenol glabridin protect low-density lipoprotein against lipid peroxidation: in vitro and ex vivo studies in humans and in atherosclerotic apolipoprotein E-deficient mice," *The American Journal of Clinical Nutrition*, vol. 66, no. 2, pp. 267–275, 1997.

[8] B. Sun, G. Sun, J. Xiao et al., "Isorhamnetin inhibits H_2O_2-induced activation of the intrinsic apoptotic pathway in H9c2 cardiomyocytes through scavenging reactive oxygen species and ERK inactivation," *Journal of Cellular Biochemistry*, vol. 113, no. 2, pp. 473–485, 2012.

[9] L. L. Pan and M. Dai, "Paeonol from Paeonia suffruticosa prevents TNF-α-induced monocytic cell adhesion to rat aortic endothelial cells by suppression of VCAM-1 expression," *Phytomedicine*, vol. 16, no. 11, pp. 1027–1032, 2009.

[10] Y.-Q. Wang, M. Dai, J.-C. Zhong, and D.-K. Yin, "Paeonol inhibits oxidized low density lipoprotein-induced monocyte adhesion to vascular endothelial cells by inhibiting the mitogen activated protein kinase pathway," *Biological and Pharmaceutical Bulletin*, vol. 35, no. 5, pp. 767–772, 2012.

[11] H. Li, Y. H. Xie, Q. Yang et al., "Cardioprotective effect of paeonol and danshensu combination on isoproterenol-induced myocardial injury in rats," *PloS ONE*, vol. 7, no. 11, Article ID e48872, 2012.

[12] Q. Yang, S. Wang, Y. Xie et al., "Effect of Salvianolic acid b and paeonol on blood lipid metabolism and hemorrheology in myocardial schemia rabbits induced by pituitruin," *International Journal of Molecular Sciences*, vol. 11, no. 10, pp. 3696–3704, 2010.

[13] R. Gaur, K. S. Yadav, R. K. Verma, N. P. Yadav, and R. S. Bhakuni, "In vivo anti-diabetic activity of derivatives of isoliquiritigenin and liquiritigenin," *Phytomedicine*, vol. 21, no. 4, pp. 415–422, 2014.

[14] A. M. Mahmoud, M. B. Ashour, A. Abdel-Moneim, and O. M. Ahmed, "Hesperidin and naringin attenuate hyperglycemia-mediated oxidative stress and proinflammatory cytokine production in high fat fed/streptozotocin-induced type 2 diabetic rats," *Journal of Diabetes and its Complications*, vol. 26, no. 6, pp. 483–490, 2012.

[15] M. A. Alam, K. Kauter, and L. Brown, "Naringin improves diet-induced cardiovascular dysfunction and obesity in high carbohydrate, high fat diet-fed rats," *Nutrients*, vol. 5, no. 3, pp. 637–650, 2013.

[16] P. Hasanein, "Glabridin as a major active isoflavan from Glycyrrhiza glabra (licorice) reverses learning and memory deficits in diabetic rats," *Acta Physiologica Hungarica*, vol. 98, no. 2, pp. 221–230, 2011.

[17] J. Lee, S. S. Choe, H. Jang et al., "AMPK activation with glabridin ameliorates adiposity and lipid dysregulation in obesity," *Journal of Lipid Research*, vol. 53, no. 7, pp. 1277–1286, 2012.

[18] J. Liu, L. Feng, D. Ma et al., "Neuroprotective effect of paeonol on cognition deficits of diabetic encephalopathy in streptozotocin-induced diabetic rat," *Neuroscience Letters*, vol. 549, pp. 63–68, 2013.

[19] N. N. Song, J. B. Wu, X. B. Wei, H. S. Guan, and X. M. Zhang, "Paeonol attenuates oxygen-glucose deprivation injury and inhibits NMDA receptor activation of cultured rat hippocampal neurons," *Yao Xue Xue Bao*, vol. 44, pp. 1228–1232, 2009.

[20] Y. W. Kim, H. E. Kang, M. G. Lee et al., "Liquiritigenin, a flavonoid aglycone from licorice, has a choleretic effect and the ability to induce hepatic transporters and phase-II enzymes," *American Journal of Physiology: Gastrointestinal and Liver Physiology*, vol. 296, no. 2, pp. G372–G381, 2009.

[21] N. Li, L. Fan, G. Sun et al., "Paeonol inhibits tumor growth in gastric cancer in vitro and in vivo," *World Journal of Gastroenterology*, vol. 16, no. 35, pp. 4483–4490, 2010.

[22] X. Yang, L. Zhang, S. Jiang, P. Gong, and F. Zeng, "Effect of dauricine on apoptosis and expression of apoptogenic protein after transient focal cerebral ischemia-reperfusion injury in rats," *Zhongguo Zhong Yao Za Zhi*, vol. 34, no. 1, pp. 78–83, 2009.

[23] H. Jin, S. Shen, X. Chen, D. Zhong, and J. Zheng, "CYP3A-mediated apoptosis of dauricine in cultured human bronchial epithelial cells and in lungs of CD-1 mice," *Toxicology and Applied Pharmacology*, vol. 261, no. 3, pp. 248–254, 2012.

[24] C. Punvittayagul, R. Wongpoomchai, S. Taya, and W. Pompimon, "Effect of pinocembrin isolated from Boesenbergia pandurata on xenobiotic-metabolizing enzymes in rat liver," *Drug Metabolism Letters*, vol. 5, no. 1, pp. 1–5, 2011.

[25] J. Wang, Y. Li, X. Zu, M. Chen, and L. Qi, "Dauricine can inhibit the activity of proliferation of urinary tract tumor cells," *Asian Pacific Journal of Tropical Medicine*, vol. 5, no. 12, pp. 973–976, 2012.

[26] Z. Yang, C. Li, X. Wang et al., "Dauricine induces apoptosis, inhibits proliferation and invasion through inhibiting NF-κB signaling pathway in colon cancer cells," *Journal of Cellular Physiology*, vol. 225, no. 1, pp. 266–275, 2010.

[27] X. D. Tang, X. Zhou, and K. Y. Zhou, "Dauricine inhibits insulin-like growth factor-I-induced hypoxia inducible factor 1α protein accumulation and vascular endothelial growth factor expression in human breast cancer cells," *Acta Pharmacologica Sinica*, vol. 30, no. 5, pp. 605–616, 2009.

[28] A. McLachlan, N. Kekre, J. McNulty, and S. Pandey, "Pancratistatin: A natural anti-cancer compound that targets mitochondria specifically in cancer cells to induce apoptosis," *Apoptosis*, vol. 10, no. 3, pp. 619–630, 2005.

[29] C. Griffin, A. Karnik, J. McNulty, and S. Pandey, "Pancratistatin selectively targets cancer cell mitochondria and reduces growth of human colon tumor xenografts," *Molecular Cancer Therapeutics*, vol. 10, no. 1, pp. 57–68, 2011.

[30] C. Griffin, J. McNulty, and S. Pandey, "Pancratistatin induces apoptosis and autophagy in metastatic prostate cancer cells," *International Journal of Oncology*, vol. 38, no. 6, pp. 1549–1556, 2011.

[31] E. J. Yang, J. S. Min, H. Y. Ku et al., "Isoliquiritigenin isolated from Glycyrrhiza uralensis protects neuronal cells against glutamate-induced mitochondrial dysfunction," *Biochemical and Biophysical Research Communications*, vol. 421, no. 4, pp. 658–664, 2012.

[32] H. K. Lee, E. Yang, J. Y. Kim, K. Song, and Y. H. Seong, "Inhibitory effects of glycyrrhizae radix and its active component, isoliquiritigenin, on Aβ(25-35)-induced neurotoxicity in cultured rat cortical neurons," *Archives of Pharmacal Research*, vol. 35, no. 5, pp. 897–904, 2012.

[33] Y. M. Kim, T. H. Kim, Y. W. Kim et al., "Inhibition of liver X receptor-α-dependent hepatic steatosis by isoliquiritigenin, a licorice antioxidant flavonoid, as mediated by JNK1 inhibition," *Free Radical Biology & Medicine*, vol. 49, no. 11, pp. 1722–1734, 2010.

[34] X. Yuan, B. Yu, Y. Wang et al., "Involvement of endoplasmic reticulum stress in isoliquiritigenin-induced SKOV-3 cell apoptosis," *Recent Patents on Anti-Cancer Drug Discovery*, vol. 8, no. 2, pp. 191–199, 2013.

[35] X. Yuan, B. Zhang, N. Chen et al., "Isoliquiritigenin treatment induces apoptosis by increasing intracellular ROS levels in HeLa cells," *Journal of Asian Natural Products Research*, vol. 14, no. 8, pp. 789–798, 2012.

[36] X. Zhang, E. D. Yeung, J. Wang et al., "Isoliquiritigenin, a natural anti-oxidant, selectively inhibits the proliferation of prostate cancer cells," *Clinical and Experimental Pharmacology and Physiology*, vol. 37, no. 8, pp. 841–847, 2010.

[37] X. Chen, B. Zhang, X. Yuan et al., "Isoliquiritigenin-induced differentiation in mouse melanoma B16F0 cell line," *Oxidative Medicine and Cellular Longevity*, vol. 2012, Article ID 534934, 11 pages, 2012.

[38] H. Chen, B. Zhang, X. Yuan et al., "Isoliquiritigenin-induced effects on Nrf2 mediated antioxidant defence in the HL-60 cell monocytic differentiation," *Cell Biology International*, vol. 37, no. 11, pp. 1215–1224, 2013.

[39] K. Gopinath and G. Sudhandiran, "Naringin modulates oxidative stress and inflammation in 3-nitropropionic acid-induced neurodegeneration through the activation of nuclear factor-erythroid 2-related factor-2 signalling pathway," *Neuroscience*, vol. 227, pp. 134–143, 2012.

[40] K. Gopinath, D. Prakash, and G. Sudhandiran, "Neuroprotective effect of naringin, a dietary flavonoid against 3-Nitropropionic acid-induced neuronal apoptosis," *Neurochemistry International*, vol. 59, no. 7, pp. 1066–1073, 2011.

[41] Y.-L. Luo, C.-C. Zhang, P.-B. Li et al., "Naringin attenuates enhanced cough, airway hyperresponsiveness and airway inflammation in a guinea pig model of chronic bronchitis induced by cigarette smoke," *International Immunopharmacology*, vol. 13, no. 3, pp. 301–307, 2012.

[42] Y. Chen, Y. Nie, Y. Luo et al., "Protective effects of naringin against paraquat-induced acute lung injury and pulmonary fibrosis in mice," *Food and Chemical Toxicology*, vol. 58, pp. 133–140, 2013.

[43] E. Ramesh and A. A. Alshatwi, "Naringin induces death receptor and mitochondria-mediated apoptosis in human cervical cancer (SiHa) cells," *Food and Chemical Toxicology*, vol. 51, no. 1, pp. 97–105, 2013.

[44] H. Li, B. Yang, J. Huang et al., "Naringin inhibits growth potential of human triple-negative breast cancer cells by targeting β-catenin signaling pathway," *Toxicology Letters*, vol. 220, no. 3, pp. 219–228, 2013.

[45] P. L. Sequetto, T. T. Oliveira, I. R. Maldonado et al., "Naringin accelerates the regression of pre-neoplastic lesions and the colorectal structural reorganization in a murine model of chemical carcinogenesis," *Food and Chemical Toxicology*, vol. 64, pp. 200–209, 2014.

[46] Y. Nie, H. Wu, P. Li et al., "Anti-inflammatory effects of naringin in chronic pulmonary neutrophilic inflammation in cigarette smoke-exposed rats," *Journal of Medicinal Food*, vol. 15, no. 10, pp. 894–900, 2012.

[47] G. I. Harisa, "Naringin mitigates erythrocytes aging induced by Paclitaxel: an in vitro study," *Journal of Biochemical and Molecular Toxicology*, vol. 28, no. 3, pp. 129–136, 2014.

[48] X. Q. Yu, C. C. Xue, Z. W. Zhou et al., "In vitro and in vivo neuroprotective effect and mechanisms of glabridin, a major active isoflavan from Glycyrrhiza glabra (licorice)," *Life Sciences*, vol. 82, no. 1-2, pp. 68–78, 2008.

[49] Y. L. Hsu, L. Y. Wu, M. F. Hou et al., "Glabridin, an isoflavan from licorice root, inhibits migration, invasion and angiogenesis of MDA-MB-231 human breast adenocarcinoma cells by inhibiting focal adhesion kinase/Rho signaling pathway," *Molecular Nutrition & Food Research*, vol. 55, no. 2, pp. 318–327, 2011.

[50] J. H. Yang, B. Y. Shin, J. Y. Han et al., "Isorhamnetin protects against oxidative stress by activating Nrf2 and inducing the expression of its target genes," *Toxicology and Applied Pharmacology*, vol. 274, pp. 293–301, 2014.

[51] C. Shi, L. Y. Fan, Z. Cai, Y. Y. Liu, and C. L. Yang, "Cellular stress response in Eca-109 cells inhibits apoptosis during early exposure to isorhamnetin.," *Neoplasma*, vol. 59, no. 4, pp. 361–369, 2012.

[52] J. Boubaker, M. B. Sghaier, I. Skandrani, K. Ghedira, and L. Chekir-Ghedira, "Isorhamnetin 3-O-robinobioside from Nitraria retusa leaves enhance antioxidant and antigenotoxic activity in human chronic myelogenous leukemia cell line K562," *BMC Complementary and Alternative Medicine*, vol. 12, article 135, 2012.

[53] L. Ramachandran, K. A. Manu, M. K. Shanmugam et al., "Sethi G.Isorhamnetin inhibits proliferation and invasion and induces apoptosis through the modulation of peroxisome proliferator-activated receptor? activation pathway in gastric cancer," *The Journal of Biological Chemistry*, vol. 287, pp. 38028–38040, 2012.

[54] K. Seo, J. H. Yang, S. C. Kim, S. K. Ku, S. H. Ki, and S.M. Shin, "The antioxidant effects of isorhamnetin contribute to inhibit COX-2 expression in response to inflammation: a potential role of HO-1," *Inflammation*, vol. 37, no. 3, pp. 712–722, 2014.

[55] C. Guo, L. Tong, M. Xi, H. Yang, H. Dong, and A. Wen, "Neuroprotective effect of calycosin on cerebral ischemia and reperfusion injury in rats," *Journal of Ethnopharmacology*, vol. 144, no. 3, pp. 768–774, 2012.

[56] J. Chen, X. Zhao, Y. Ye, Y. Wang, and J. Tian, "Estrogen receptor beta-mediated proliferative inhibition and apoptosis in human breast cancer by calycosin and formononetin," *Cellular Physiology and Biochemistry*, vol. 32, no. 6, pp. 1790–1797, 2013.

[57] M. Gao, R. Liu, S. Y. Zhu, and G. H. Du, "Acute neurovascular unit protective action of pinocembrin against permanent cerebral ischemia in rats," *Journal of Asian Natural Products Research*, vol. 10, no. 6, pp. 551–558, 2008.

[58] J. Qian, "Cardiovascular pharmacological effects of bisbenzylisoquinoline alkaloid derivatives," *Acta Pharmacologica Sinica*, vol. 23, no. 12, pp. 1086–1092, 2002.

[59] D. Kong, F. Zhang, D. Wei et al., "Paeonol inhibits hepatic fibrogenesis via disrupting nuclear factor-κB pathway in activated stellate cells: in vivo and in vitro studies," *Journal of Gastroenterology and Hepatology*, vol. 28, no. 7, pp. 1223–1233, 2013.

[60] M. A. S. Kumar, M. Nair, P. S. Hema, J. Mohan, and T. R. Santhoshkumar, "Pinocembrin triggers Bax-dependent mitochondrial apoptosis in colon cancer cells," *Molecular Carcinogenesis*, vol. 46, no. 3, pp. 231–241, 2007.

[61] R. Li, M. Guo, G. Zhang, X. Xu, and Q. Li, "Nicotiflorin reduces cerebral ischemic damage and upregulates endothelial nitric oxide synthase in primarily cultured rat cerebral blood vessel endothelial cells," *Journal of Ethnopharmacology*, vol. 107, no. 1, pp. 143–150, 2006.

[62] A. Prakash, B. Shur, and A. Kumar, "Naringin protects memory impairment and mitochondrial oxidative damage against aluminum-induced neurotoxicity in rats," *International Journal of Neuroscience*, vol. 123, no. 9, pp. 636–645, 2013.

[63] R. Li, M. Guo, G. Zhang, X. Xu, and Q. Li, "Neuroprotection of nicotiflorin in permanent focal cerebral ischemia and in neuronal cultures," *Biological and Pharmaceutical Bulletin*, vol. 29, no. 9, pp. 1868–1872, 2006.

[64] R. T. Liu, L. B. Zou, J. Y. Fu, and Q. J. Lu, "Effects of liquiritigenin treatment on the learning and memory deficits induced by amyloid β-peptide (25–35) in rats," *Behavioural Brain Research*, vol. 210, no. 1, pp. 24–31, 2010.

[65] X. H. Dai, H. E. Li, C. J. Lu et al., "Liquiritigenin prevents Staphylococcus aureus-mediated lung cell injury via inhibiting the production of α-hemolysin," *Journal of Asian Natural Products Research*, vol. 15, no. 4, pp. 390–399, 2013.

[66] M. Zhou, H. Higo, and Y. Cai, "Inhibition of hepatoma 22 tumor by liquiritigenin," *Phytotherapy Research*, vol. 24, no. 6, pp. 827–833, 2010.

[67] Y. W. Kim, R. J. Zhao, S. J. Park et al., "Anti-inflammatory effects of liquiritigenin as a consequence of the inhibition of NF-κB-dependent iNOS and proinflammatory cytokines production," *British Journal of Pharmacology*, vol. 154, no. 1, pp. 165–173, 2008.

[68] E. M. Choi, K. S. Suh, and Y. S. Lee, "Liquiritigenin restores osteoblast damage through regulating oxidative stress and mitochondrial dysfunction," *Phytotherapy Research*, vol. 28, no. 6, pp. 880–886, 2014.

[69] X. C. Lin, Y. Y. Chen, S. T. Bai, J. Zheng, and L. Tong, "Protective effect of licoflavone on gastric mucosa in rats with chronic superficial gastritis," *Nan Fang Yi Ke Da Xue Xue Bao*, vol. 33, pp. 299–304, 2013.

[70] H. Haraguchi, J. Inoue, Y. Tamura, and K. Mizutani, "Antioxidative components of Psoralea corylifolia (Leguminosae)," *Phytotherapy Research*, vol. 16, no. 6, pp. 539–544, 2002.

[71] R. Nishimura, K. Tabata, M. Arakawa et al., "Isobavachalcone, a chalcone constituent of Angelica keiskei, induces apoptosis in neuroblastoma," *Biological and Pharmaceutical Bulletin*, vol. 30, no. 10, pp. 1878–1883, 2007.

[72] J. Lee, S. Won, C. Chao et al., "Morusin induces apoptosis and suppresses NF-κB activity in human colorectal cancer HT-29 cells," *Biochemical and Biophysical Research Communications*, vol. 372, no. 1, pp. 236–242, 2008.

[73] L. Wang, H. Guo, L. Yang et al., "Morusin inhibits human cervical cancer stem cell growth and migration through attenuation of NF-κB activity and apoptosis induction," *Molecular and Cellular Biochemistry*, vol. 379, no. 1-2, pp. 7–18, 2013.

[74] M. M. Rafi, R. T. Rosen, A. Vassil et al., "Modulation of bcl-2 and cytotoxicity by licochalcone-A, a novel estrogenic flavonoid," *Anticancer Research*, vol. 20, no. 4, pp. 2653–2658, 2000.

[75] X. Yuan, D. Li, H. Zhao et al., "Licochalcone A-induced human bladder cancer T24 cells apoptosis triggered by mitochondria dysfunction and endoplasmic reticulum stress," *BioMed Research International*, vol. 2013, Article ID 474272, 9 pages, 2013.

[76] J. Kim, E. K. Shin, J. H. Park, Y. H. Kim, and J. H. Y. Park, "Antitumor and antimetastatic effects of licochalcone A in mouse models," *Journal of Molecular Medicine*, vol. 88, no. 8, pp. 829–838, 2010.

[77] X. Yuan, T. Li, E. Xiao et al., "Licochalcone B inhibits growth of bladder cancer cells by arresting cell cycle progression and inducing apoptosis," *Food and Chemical Toxicology*, vol. 65, pp. 242–251, 2014.

[78] P. Akbay, A. A. Basaran, U. Undeger, and N. Basaran, "In vitro immunomodulatory activity of flavonoid glycosides from Urtica dioica L.," *Phytotherapy Research*, vol. 17, no. 1, pp. 34–37, 2003.

[79] P. M. Amália, M. N. Possa, M. C. Augusto, and L. S. Francisca, "Quercetin prevents oxidative stress in cirrhotic rats," *Digestive Diseases and Sciences*, vol. 52, no. 10, pp. 2616–2621, 2007.

[80] R. Liu, M. Gao, Z. Yang, and G. Du, "Pinocembrin protects rat brain against oxidation and apoptosis induced by ischemia-reperfusion both in vivo and in vitro," *Brain Research*, vol. 1216, pp. 104–115, 2008.

[81] H.-M. Guang and G.-H. Du, "Protections of pinocembrin on brain mitochondria contribute to cognitive improvement in chronic cerebral hypoperfused rats," *European Journal of Pharmacology*, vol. 542, no. 1–3, pp. 77–83, 2006.

[82] Y. Wang, J. Gao, Y. Miao et al., "Pinocembrin protects SH-SY5Y cells against MPP+-induced neurotoxicity through the mitochondrial apoptotic pathway," *Journal of Molecular Neuroscience*, 2014.

Hindawi Publishing Corporation
Journal of Chemistry
Volume 2014, Article ID 536134, 8 pages
http://dx.doi.org/10.1155/2014/536134

Research Article

Construction of Differential-Methylation Subtractive Library

Wei Hu,[1] Xiaolei Liang,[1] Tian Dong,[1] Yanfeng Hu,[2] Jie Liu,[1] Lina Mao,[1] Xu Liu,[1] and Yurong Bi[1]

[1] *School of Life Sciences, Lanzhou University, Lanzhou 730000, China*
[2] *Key Laboratory of Mollisols Agroecology, Northeast Institute of Geography and Agroecology, Chinese Academy of Sciences, Nangang District, Harbin 150081, China*

Correspondence should be addressed to Yurong Bi; yrbi@lzu.edu.cn

Received 16 May 2014; Accepted 23 June 2014; Published 9 July 2014

Academic Editor: Wang Zhenhua

Stress-induced ROS changes DNA methylation patterns. A protocol combining methylation-sensitive restriction endonuclease (MS-RE) digestion with suppression subtractive hybridization (SSH) to construct the differential-methylation subtractive library was developed for finding genes regulated by methylation mechanism under cold stress. The total efficiency of target fragment detection was 74.64%. DNA methylation analysis demonstrated the methylation status of target fragments changed after low temperature or DNA methyltransferase inhibitor treatment. Transcription level analysis indicated that demethylation of DNA promotes gene expression level. The results proved that our protocol was reliable and efficient to obtain gene fragments in differential-methylation status.

1. Introduction

DNA methylation exists extensively in the genomes of bacteria, animals, and plants. In plants, about 20~30% cytosines are methylated in the nuclear genome [1]. In prokaryotes, modification of DNA prevents cleavage by the cognate restriction endonucleases [2]. In higher eukaryotes, DNA methylation is one of the epigenetic modifications which plays an important role in regulating development and developmental processes [3]. *Arabidopsis* decreased DNA methylation (ddm) mutants show pleiotropic phenotypes in development, such as early flowering, dwarfism, and irregular organ number [4]. In pumpkin, DNA methylation status changes were observed during somatic embryogenesis. DNA methylation reached the highest level in early embryo stages and decreased during embryo maturation [5]. Hypermethylation of promoter sequences is associated with transcriptional gene silencing while hypermethylation of transcribed or coding sequences is linked with posttranscriptional gene silencing [6]. In all, DNA methylation has been associated with many gene regulatory mechanisms including genomic imprinting, transcriptional regulation of genes and transposable elements, and gene silencing [6–10].

Animals and plants are constantly exposed to environmental stresses (biotic or abiotic). These stresses often lead to the increase in ROS level in cell. Growing evidence supports that stress-induced oxidative damage changes DNA methylation patterns, which in turn modulates gene expression [11]. Recent studies indicate that epigenetic mechanisms, such as DNA methylation, play a key role in regulating gene expression in response to environmental stresses [12]. When exposed to osmotic stress, a reversible hypermethylation of cytosine was observed in tobacco [13]. Long exposure to cold stress resulted in a stable transcription silencing of *FLC*, leading to flowering inhibition [14]. Dyachenko et al. [15] showed a twofold increase in CpNpG methylation level in nuclear genome of *M. crystallinum* plants exposed to high salinity. Choi and Sano [16] reported that environmental stimuli such as salinity, cold, and aluminum stress could cause demethylation in the coding region of *NtGPDL* and subsequently activated its expression. In rice, DNA methylation pattern changed in response to drought stress: the methylation level decreased and there was a large difference in DNA methylation/demethylation site in drought-tolerant and drought-sensitive lines under drought stress [12]. In wheat, salinity stress triggered the decrease in methylation

level [17]. Furthermore, changes in DNA methylation pattern can affect tolerance to stress. It was found that treatment with demethylating reagent, 5-azacytidine (5-Aza), resulted in wheat seedlings more tolerant to salt stress [18]. Exposure to zinc stress led to change in methylation patterns. This change could be stably inherited to progeny and caused progeny more tolerant to zinc stress [19].

Since DNA methylation plays an important role in numerous biological processes, more and more techniques such as MSAP, MS-RDA, bisulfite sequencing, and microarray analysis [20–23] are developed to analyze methylation patterns or to screen for genes regulated by methylation mechanism. However, MSAP may lead to loss of target genes because it is difficult to distinguish different sequences with the same length using these techniques. MS-RDA is technically complicated. Although bisulfite sequencing and microarray analysis can get more detailed information about the methylation site, these methods are relatively expensive. Therefore, a more efficient and economical method is necessary. Here, we described an approach combining methylation-sensitive restriction endonuclease (MS-RE) digestion with suppression subtractive hybridization (SSH) to generate a library for screening methylation-regulated genes.

2. Protocol Design

DNA methylation status is associated with gene expression. Methylation of DNA cytosine bases can repress the gene transcription, while demethylation can upregulate the gene transcription. Here, we design a protocol that combined the methylation-sensitive restriction endonuclease (MS-RE) digestion with suppression subtractive hybridization (SSH) to construct a differential-methylation subtractive library for finding genes upregulated by DNA demethylation.

2.1. Preparation of Drivers and Testers. Genomic DNA was extracted from *Arabidopsis* seedlings grown in different conditions and then was digested with Mse I, which recognizes and cuts the -TTAA- sequence in genome, to cut the genomic DNA into smaller fragments. The digested fragments from the plants grown in normal condition were ligated to different adapters to make two types of testers. The digested fragments from the plant grown in low temperature were ligated to the linker to produce the predrivers. Both testers and predrivers were digested with Hha I/Hpa II and then retrieved. The predrivers were amplified for 20 cycles to get drivers. All linkers, adapters, and primers used for SSH are listed in Table 1.

2.2. Subtractive Hybridization. Drivers were mixed with two groups of testers, respectively, at a ratio of 40 : 1 or higher. The mixtures were heat-denatured at 98°C for 15 min and allowed to anneal at 68°C for 9 h. After the first hybridization, the two mixtures were mixed and an equal volume of fresh hybridization buffer containing heat-denatured driver was added. The final mixture was allowed to hybridize at 68°C for another 9 h. At last, the mixture was diluted to 100 μL with dilution buffer (containing 20 mM Hepes (pH 8.3), 50 mM NaCl, and 0.2 mM EDTA) and heated at 68°C for 10 min and then stored at −20°C.

2.3. PCR Amplification and Cloning of Target. A nest-PCR was employed for the target amplification. The primary PCR contained 2 μL of diluted subtracted DNA, 1 μL of MP1 and MP2 (10 μM each), 2.5 μL of 10x PCR buffer, 1 μL of dNTP, and 0.5 μL of Taq in 25 μL volume. PCR was performed at 72°C for 15 min and then 95°C for 5 min, followed by 35 cycles of 95°C for 45 s, 66°C for 30 s, and 72°C for 1.5 min, with extension at 72°C for 10 min. The first PCR product was diluted 10 times with deionized water and used as the template in the secondary PCR under a similar condition to the primary PCR except for the primers replaced with MPN1 and MPN2, and the anneal temperature was set to 68°C. The secondary PCR products were ligated into the PMD-18 simple vector and then transformed into *E. coli* strain DH5α. The ampicillin resistant clones were selected for colony PCR test under a similar condition to the secondary PCR. The PCR positive clones were collected to generate the library.

3. Materials and Methods

3.1. Plant Material and Growth Condition. Seeds of wild type *Arabidopsis thaliana* (Columbia background, Col-0) were surface sterilized with 15% NaClO for 15 min, rinsed with sterilized water for 3 times, vernalized at 4°C for 2 days, and then transferred to Murashige and Skoog (MS) solid medium containing 3% sugar for germination. Plants were grown under long-day conditions (16 hours light/8 hours dark) at 23°C. For cold treatment, 7-day-old seedlings were transferred to a 4°C chamber with the same light condition for 3 days. For demethylation treatment, 7-day-old seedlings were transferred to MS medium containing 50 μM 5-azacytidine for 3 days.

3.2. DNA Isolation and Digestion with Restriction Enzymes. A modified CTAB method [24] was employed to isolate genomic DNA. A 5 μg aliquot of DNA was digested with MseI (Fermentas ER0981). Fragments retrieved using TIAN quick Midi Purification Kit (Tiangen DP204-02) were separated into two groups: group I (from plants grown at 4°C) was ligated to the linker and group II was ligated (from plants grown at 23°C) to adapters. After double digestion with two methylation-sensitive restriction enzymes, Hha I/Hpa II, group I fragments were retrieved for preamplification. Group II DNA was used as the tester.

3.3. Preamplification. 1 μg of digestion products was amplified by 20 cycles of PCR with oligonucleotide H24 as a primer. After retrieval, the PCR product was used as the driver.

3.4. Subtractive Library Construction and Sequencing. A subtractive library was constructed according to Diatchenko's protocol [25]. The ratio of driver to tester was about 60 : 1. The final PCR products were linked to PMD-18T simple vector (Takara, D-103A) and then transformed into *E. coli* strain DH5α. Ampicillin resistant single clones were selected. The

Table 1: Linkers, adapters, and primers used for SSH.

Group	Oligonucleotides	DNA sequence
Linker	Linker H24	AGGCAACTGTGCTATCCGAGGGAT
	Linker H12	TAATCCCTCGGA
Adapter	Ad1	CTACTACGTCGCACTGTTGGTTGGCGGGACGGCGCTCGTTAAGTC
	Ad1c	TAGACTTAACGAGC
	Ad2	TGTAGCGTGAAGACGACAGAAACCGCGTGGTGCTGAGGGCGTGAC
	Ad2c	TAGTCACGCCCT
Primer	MP1	CTACTACGTCGCACTGTTGGT
	MPN1	GCGGGACGGCGCTCGTTAAGTC
	MP2	TGTAGCGTGAAGACGACAGAA
	MPN2	CGCGTGGTGCTGAGGGCGTGAC

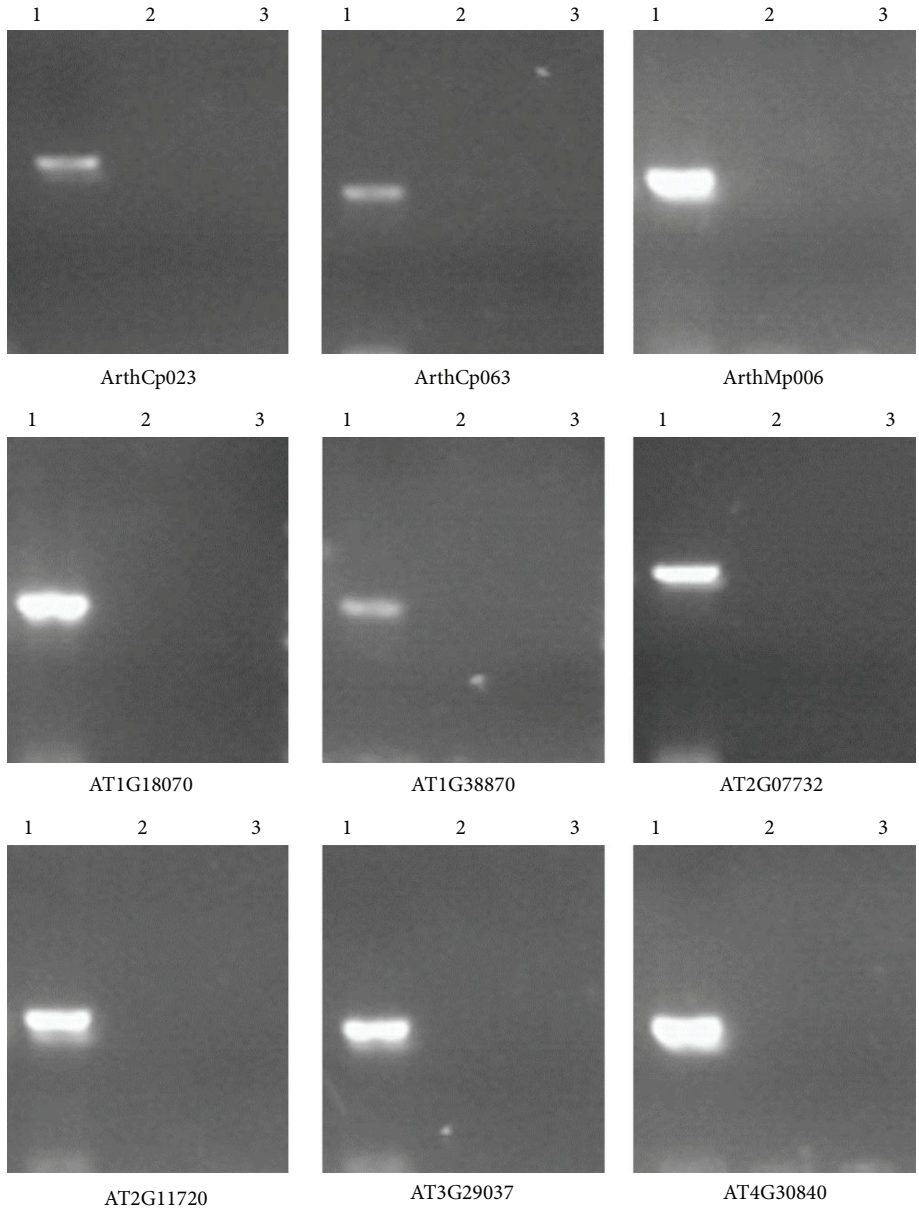

Figure 1: MS-RE PCR results of some genes under different conditions. Genomic DNA extracted from plants treated with cold (4°C) (Lane 2), 5-Aza (50 μM) (Lane 3) or normal conditions (Lane 1) were digested with Hha I/Hpa II, then taken PCR amplification.

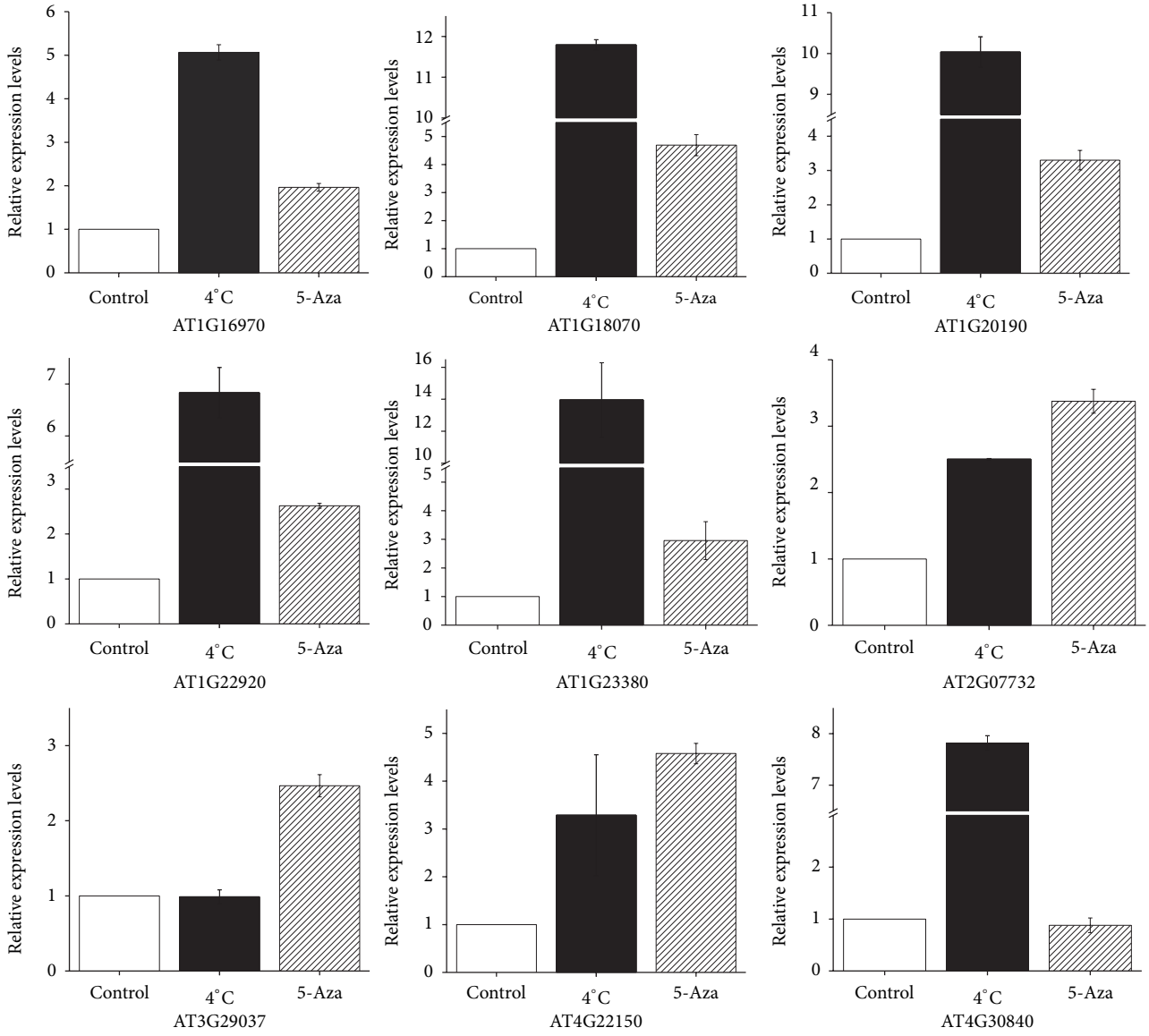

Figure 2: Transcript levels of some genes under different conditions.

second PCR primers were employed for bacteria liquid PCR test. The positive clones were stored to get the subtractive library and sent for sequencing.

3.5. Sequencing Results Analysis. Sequencing results were identified by BLAST searches against the *Arabidopsis thaliana* genome database from NCBI (http://blast.ncbi.nlm.nih.gov/Blast.cgi?PAGE_TYPE=BlastSearch&BLAST_SPEC=OGP__3702). Primers were designed according to the BLAST search results.

3.6. DNA Methylation Analysis. A MS-RE PCR was performed for DNA methylation analysis. Genomic DNA was digested with Hha I/Hpa II and then retrieved for PCR amplification. The primers for MS-RE PCR are listed in Table S1 (see Supplementary Material available online at http://dx.doi.org/10.1155/2014/536134).

3.7. Quantitative Real-Time RT-PCR Analysis. A two-step quantitative real-time RT-PCR was carried out for the expression analysis. Total RNA was extracted from 100 mg of fresh tissues with Trizol reagent (Invitrogen, 15596-026) and pretreated with RNA-free DNase (Promega, M6101) to eliminate gnomic DNA contamination. First strand cDNA was synthesized from 2 μg of total RNA using Takara primer script^{RT} master mix (Drr036A) according to the user's manual. The Takara SYBR Premix Ex Taq II (RR820A) was used for the PCR reaction. All reactions were carried out in 20 μL reaction mixtures with 2 μL of template DNAs, 1 μL of forward primer, and 1 μL of reverse primer (10 μM each). The running conditions were as follows: 95°C for 3 min,

Table 2: DNA sequences of some fragments from the differential-methylation subtractive library.

Clone	DNA sequence
1–35	ATGATTGAGTATAACAACTTAAACTGCAACCGG* ATCTTAAAGGCGTAAG AACTGTATCCTTGTTAGAA
2–26	GTTGTAAGGTCAGCATTTTCACTTTTCCCGGAATGAGAGATTATCAGACT TTACATGTTGATAAGGGTAATGTTTTT
2–32	ATGATCATGGACTTATCCTACATGAGAACGCCAATGAGGATCAA*GCGCGC* CTCAAT*GCGC*** AATTAGCTGCAAGAGATGCAGCAGGGCTCGGTGTC
3–32	TAAATTAGGCATGGAACGGAGCCACTACGAAGAAGTTCCGGGGGGTTACG AAGGAAACTTCGAGTTCATATTGGTCAT
4–1	ATACAACACGAGGACTTCCCGGGAGGTGACCCATCCTAGTACTACTCCC TCCCAAGCATGTTAACTGTGGAGTTCTGATGGGATCCGGTGCATTAGTGC TGGTATGATTGCATCCGTTA
5–86	TTCCGAATCAATCATTGTTAACGTCACCGGAGATGATAATAAGTCGGCTT TGTTCGGTAAGTACGATCTCGGTAAGCTCCTCGGTAGCG*GCGC*GTTTGCC AAAGTCTACCAAGCGGAGGA
6–14	TTGGTGGATCCCTTAAC*GCGC*TTCTTCTTCTTCTTTCGCGAGATAACCTA GAAACCCTTTTCCTTTCGTTCGCTTCTTCAATCCGCCATGGGTACGGGTT CTCGAGCTCTCTCTTTCTAGTCATTGGTCTATGTGTCTTCTTTCTCTCTCG ATTTCTCGATTAT*GCGC*TTACTACTTTTGTTGGTCGATCGGATCTTTTCTTC AATTTTTGTTGAATT
7–19	TCTCTCGGGTTACAGGAAAGCTTCCACTTATCAGTCCTCCGGTGAGTTTC AATTGCATTCATTAGTTGCCCACATAT
9–57	TAATGCCTATTGCTTTCTGATCAACTGGAATTTGAGCCAAGACATTTCC*G* *CGC*CCAAAAGGTGTTCGATGAAATGTCTGAACCACTAATTCCAGA
10–66	TTATTAAGGCAATAGCAATG*GCGC*TACCGGTCTACTCGATGAACTGCTTC TTACTTCCTACTTTAA
11–21	AGTATAAGACATAGAACCGCAACCGGATCATGAAAGCCTAAGTAGTGTTT CCTTGTTAGAAGATAGAAAGCCAAAGACTCATACGGACTTCGGCTACA CAATCAAAGCTATGAGAAGCAAGAAGAAGCTTTGTTAGATTTTTGTAGT CAAATATGACTAGATGTCATGTGTATGATTGAGTATAAGAACTAGAATCGC AACCGGATCTTAAAA

-CCGG-*: recognizing and cutting site of Hpa II.
-*GCGC*-**: recognizing and cutting site of Hha I.

followed by 40 cycles of 95°C for 5 s and 60°C for 30 s (CFX96 Real-Time PCR Detection System, Bio-Rad). The results were analyzed by the Bio-Rad CFX Manager software 6.541.1028. The primer sequences are listed in Table S2.

4. Results

4.1. A Differential-Methylation Subtractive Library Was Constructed. By the methylation-sensitive restriction enzymes digestion of genomic DNA, tester and driver preparation, suppression subtractive hybridization, and target cloning, we constructed a differential-methylation subtractive library consisting of about 8,000 clones (Figures S1–S5). To test our protocol, 426 clones were sent to sequence. In these clones, 363 (about 85.21% of total) were PCR2 primers positive. Among these primer-positive clones, 318 (about 87.60%) were -CCGG- or -GCGC- containing fragments (Table 2). The total efficiency was 74.64%.

4.2. Sequencing Results Analysis. 54 gene fragments were obtained from the 318 clones by BLAST searching the *Arabidopsis* genome database (Table 3). The distribution of the methylation site (-CCGG-/-GCGC-) was listed as follows: 11 in 5′ regions, 4 in 3′ regions, and 26 in the gene coding regions. We next investigated the relationship of methylation site with the gene expression. The result showed that DNA methylation, wherever in 5′ region, 3′ region of gene or in coding regions (including intron), suppresses gene expression and demethylation of these sites activates transcription (data not shown), which supported the recent reports [26].

4.3. DNA Methylation Analysis. To check the methylation status of the genome, a methylation-sensitive restriction endonuclease PCR (MS-RE PCR) was performed for 9 out of the 54 genes. The results showed that the PCR products can be found in plants grown in normal condition but not in plants treated with low temperature (4°C) or 5-Aza (50 μM) (Figure 1), suggesting that the -CCGG-/-GCGC- sites were methylated in plants grown under normal condition and were demethylated in plants treated with low temperature or 5-Aza.

Table 3: Analysis of the sequencing results of some clones from the differential-methylation subtractive library.

Clone	Size	Locus tag	Position	Gene identification
1–35	340	AT4G06700	5′	Pseudogene
1–69	227	ArthCp029	In gene	ATPB
2–10	128	ArthMp006	In gene	NAD5
2–26	188	AT4G30840	5′	Transducing/WD40 domain-containing protein
2–32	227	AT5G29041	5′	Pseudogene
2–37	307	AT2G04730	In gene	Pseudogene, F-box protein related
2–51	342	ArthCp064	In gene	RPL2
2–53	274	AT2G11720	In gene	Pseudogene
2–63	291	ArthCp079	In gene	NDHA
2–68	346	AT4G06477	3′	Pseudogene
2–71	278	AT5G34623	In gene	Pseudogene
3-4	129	AT2G06810	In gene	Pseudogene
3–23	394	AT1G42300	In gene	Transposable element gene
3–32	160	Arthct120	5′	trnN; tRNA-Asn
3–35	158	AT2G23720	In gene	Transposable element gene
3–43	315	AT3G30330	In gene	Pseudogene
3–48	275	AT3G30587	In gene	Pseudogene
3–64	315	AT2G07732	In gene	Ribulose-bisphosphate carboxylase
3–81	157	AT4G09380	In gene	Transposable element gene
3–83	247	ArthCp022	In gene	PSAA
3–85	158	AT4G28970	In gene	Transposable element gene
4–1	195	AT1G43624	5′	Unknown protein
4-5	235	AT3G33004	In gene	Pseudogene
4–16	261	AT3G43990	In gene	BAH domain-containing protein
4–32	438	ArthCp023	5′	YCF3
4–40	280	ArthCp069	In gene	RPS7
4–49	338	AT1G63360	In gene	Disease resistance protein (CC-NBS-LRR class), putative
4–62	218	AT1G16970	In gene	KU70
4–81	418	AT4G22150	5′	PUX3
5–16	186	AT5G38280	In gene	PR5K
5–38	378	AT1G22920	In gene	CSN5A
5–44	192	AT4G06678	3′	Pseudogene
5–53	229	ArthCp077	In gene	NDHG
5–58	364	ArthCp014	In gene	RPOB
5–76	311	ArthCt089	3′	trnK; tRNA-Lys
5–86	169	AT2G38490	In gene	CIPK22
5–88	288	AT3G30763	In gene	Transposable element gene
6–14	224	AT1G18070	In gene	G1 to S phase transition protein
6–15	676	ArthCr088	5′	16S ribosomal RNA
6–27	243	ArthCp062	5′	RPL22
6–28	258	AT1G23380	In gene	KNAT6
6–31	165	AT1G18370	In gene	HIK
6–87	105	ArthCp065	In gene	RPL23
7–19	386	AT4G33360	In gene	FLDH
7–44	411	ArthCp026	In gene	NDHK
9–57	213	AT4G06574	5′	Transposable element gene
9–91	273	AT1G38870	3′	Pseudogene
10–66	187	AT2G01840	In gene	Transposable element gene
11–21	212	AT1G38790	5′	Unknown protein
11–29	237	AT5G01080	In gene	Beta-galactosidase related protein
11–44	174	AT1G38630	3′	Unknown protein

Table 3: Continued.

Clone	Size	Locus tag	Position	Gene identification
11–92	407	AT3G29037	5′	Pseudogene of AT5G35760; beta-galactosidase
13–35	125	AT1G20190	In gene	EXPA11
13–56	213	ArthCp063	In gene	RPS19

4.4. Transcription Levels Analysis. The transcription levels of some genes mentioned above were examined. Comparing to the control, the plants treated with low temperature or 5-Aza showed higher expression level (Figure 2). It was notable that the genes expression levels of plants treated with low temperature were not the same as those from plants treated with 5-Aza, suggesting that demethylation and other mechanisms could play a combined role in regulating the gene expression in response to low temperature.

5. Discussion

In the present study, we described a protocol combining methylation-sensitive restriction endonuclease (MS-RE) digestion with suppression subtractive hybridization (SSH) to construct a differential-methylation subtractive library for finding genes upregulated by DNA demethylation.

We obtained a library consisting of about 8,000 clones in this study. To test the protocol, we sent some clones for sequencing. The sequencing results showed that about 85.21% of total samples were PCR2 primers positive and about 87.60% in the PCR2 primer-positive clones were -CCGG- or -GCGC- fragment containing (Table 2). The total efficiency was about 74.64%. DNA methylation status analysis indicated that DNA demethylation appeared in plants treated with low temperature but kept methylation in plants grown in normal conditions (Figure 1). These results suggest that this protocol enables efficient isolation of differentially methylated fragments from a genome and constructing the differential-methylation DNA library.

It has been reported that DNA methylation plays an important role in regulating gene expression [4, 27–29]. DNA hypomethylation leads to enhancing the gene expression [30–32]. We examined the transcription level of some genes. The results indicated that higher expression levels were observed in plants treated with low temperature or 5-Aza compared to those grown under normal conditions (Figure 2). Considering the methylation status of these genes, we could make a conclusion that the demethylation of some genes appeared in the low temperature treatment which subsequently activates gene expression. The results showed credibility of using this protocol to find genes regulated by methylation/demethylation mechanism.

A potential disadvantage of this protocol is that incomplete digestion of DNA by Hha I/Hpa II may lead to an unreliable library. To avoid this problem, we conducted Hha I/Hpa II double digestion twice with excess enzyme every time. Furthermore, high ratio of driver to tester (40 : 1 or higher) in SSH procedure is desirable [25, 33]. In this study, the ratio of driver to tester was about 60 : 1. This protocol can be modified to isolate genes downregulated by DNA hypermethylation as well.

Abbreviations

MS-RE: Methylation-sensitive restriction endonuclease
SSH: Suppression subtractive hybridization
MSAP: Methylation-sensitive amplified polymorphism.

Conflict of Interests

The authors declare that there is no conflict of interests regarding the publication of this paper.

Authors' Contribution

Wei Hu and Xiaolei Liang contributed equally to this work.

Acknowledgments

This work was supported by the National Natural Science Foundation of China (31170225; 31201145), the National High Technology Research and Development Program (2007AA021401), Major State Basic Research Development Program of China (973 Program) (2012CB026105), Foundation of Science and Technology Program of Gansu Province (1107RJYA005), Foundation of Study and Application Program of Biological Technology in Gansu Province (GNSW-2013-15), and Fundamental Research Funds for the Central Universities (lzujbky-2012-104).

References

[1] E. J. Richards, "DNA methylation and plant development," *Trends in Genetics*, vol. 13, no. 8, pp. 319–323, 1997.

[2] E. J. Finnegan, R. K. Genger, W. J. Peackock, and E. S. Dennis, "DNA methylation in plants," *Annual Review of Plant Physiology and Plant Molecular Biology*, vol. 49, pp. 223–247, 1998.

[3] S. Feng, S. J. Cokus, X. Zhang et al., "Conservation and divergence of methylation patterning in plants and animals," *Proceedings of the National Academy of Sciences of the United States of America*, vol. 107, pp. 8689–8694, 2010.

[4] T. Kakutani, J. A. Jeddeloh, S. K. Flowers, K. Munakata, and E. J. Richards, "Developmental abnormalities and epimutations associated with DNA hypomethylation mutations," *Proceedings of the National Academy of Sciences of the United States of America*, vol. 93, pp. 12406–12411, 1996.

[5] D. Leljak-Levanić, N. Bauer, S. Mihaljević, and S. Jelaska, "Changes in DNA methylation during somatic embryogenesis

in *Cucurbita pepo* L.," *Plant Cell Reports*, vol. 23, no. 3, pp. 120–127, 2004.

[6] J. Paszkowski and S. A. Whitham, "Gene silencing and DNA methylation processes," *Current Opinion in Plant Biology*, vol. 4, no. 2, pp. 123–129, 2001.

[7] J. P. Jost and H. P. Saluz, *DNA Methylation: Molecular Biology and Biological Significance*, Birkhauser, 1993.

[8] E. J. Finnegan, W. J. Peacock, and E. S. Dennis, "DNA methylation, a key regulator of plant development and other processes," *Current Opinion in Genetics and Development*, vol. 10, no. 2, pp. 217–223, 2000.

[9] I. A. Hafiz, M. A. Anjum, A. G. Grewal, and G. A. Chaudhary, "DNA methylation—an essential mechanism in plant molecular biology," *Acta Physiologiae Plantarum*, vol. 23, no. 4, pp. 491–499, 2001.

[10] R. A. Martienssen and V. Colot, "DNA methylation and epigenetic inheritance in plants and filamentous fungi," *Science*, vol. 293, no. 5532, pp. 1070–1074, 2001.

[11] R. Franco, O. Schoneveld, A. G. Georgakilas, and M. I. Panayiotidis, "Oxidative stress, DNA methylation and carcinogenesis," *Cancer Letters*, vol. 266, no. 1, pp. 6–11, 2008.

[12] W. Wang, Y. Pan, X. Zhao et al., "Drought-induced site-specific DNA methylation and its association with drought tolerance in rice (Oryza sativa L.)," *Journal of Experimental Botany*, vol. 62, no. 6, pp. 1951–1960, 2011.

[13] A. Kovařik, B. Koukalová, M. Bezděk, and Z. Opatrny, "Hypermethylation of tobacco heterochromatic loci in response to osmotic stress," *Theoretical and Applied Genetics*, vol. 95, pp. 301–306, 1997.

[14] I. R. Henderson and C. Dean, "Control of Arabidopsis flowering: the chill before the bloom," *Development*, vol. 131, no. 16, pp. 3829–3838, 2004.

[15] O. V. Dyachenko, N. S. Zakharchenko, T. V. Shevchuk, H. J. Bohnert, J. C. Cushman, and Y. I. Buryanov, "Effect of hypermethylation of CCWGG sequences in DNA of Mesembryanthemum crystallinum plants on their adaptation to salt stress," *Biochemistry*, vol. 71, no. 4, pp. 461–465, 2006.

[16] C. Choi and H. Sano, "Abiotic-stress induces demethylation and transcriptional activation of a gene encoding a glycerophosphodiesterase-like protein in tobacco plants," *Molecular Genetics and Genomics*, vol. 277, no. 5, pp. 589–600, 2007.

[17] M. Wang, L. Qin, C. Xie et al., "Induced and constitutive DNA methylation in a salinity tolerant wheat introgression line," *Plant and Cell Physiology*, 2014.

[18] L. Zhong, Y. H. Xu, and J. B. Wang, "The effect of 5-azacytidine on wheat seedlings responses to NaCl stress," *Biologia Plantarum*, vol. 54, no. 4, pp. 753–756, 2010.

[19] T. S. Smith, *DNA methylation and transgenerational stress memories in Arabidopsis thaliana [Ph.D. dissertation]*, University of York, 2013.

[20] G. E. Reyna-López, J. Simpson, and J. Ruiz-Herrera, "Differences in DNA methylation patterns are detectable during the dimorphic transition of fungi by amplification of restriction polymorphisms," *Molecular and General Genetics*, vol. 253, no. 6, pp. 703–710, 1997.

[21] T. Ushijima, K. Morimura, Y. Hosoya et al., "Establishment of methylation-sensitive-representational difference analysis and isolation of hypo- and hypermethylated genomic fragments in mouse liver tumors," *Proceedings of the National Academy of Sciences of the United States of America*, vol. 94, no. 6, pp. 2284–2289, 1997.

[22] M. Frommer, L. E. McDonald, D. S. Millar et al., "A genomic sequencing protocol that yields a positive display of 5-methylcytosine residues in individual DNA strands," *Proceedings of the National Academy of Sciences of the United States of America*, vol. 89, no. 5, pp. 1827–1831, 1992.

[23] P. S. Yan, C. M. Chen, H. Shi et al., "Dissecting complex epigenetic alterations in breast cancer using CpG island microarrays," *Cancer Research*, vol. 61, no. 23, pp. 8375–8380, 2001.

[24] M. G. Murray and W. F. Thompson, "Rapid isolation of high molecular weight plant DNA," *Nucleic Acids Research*, vol. 8, no. 19, pp. 4321–4326, 1980.

[25] L. Diatchenko, Y. C. Lau, A. P. Campbell et al., "Suppression subtractive hybridization: a method for generating differentially regulated or tissue-specific cDNA probes and libraries," *Proceedings of the National Academy of Sciences of the United States of America*, vol. 93, no. 12, pp. 6025–6030, 1996.

[26] M. Gehring and S. Henikoff, "DNA methylation dynamics in plant genomes," *Biochimica et Biophysica Acta*, vol. 1769, no. 5-6, pp. 276–286, 2007.

[27] R. Holliday and J. E. Pugh, "DNA modification mechanisms and gene activity during development. Developmental clocks may depend on the enzymic modification of specific bases in repeated DNA sequences," *Science*, vol. 187, no. 4173, pp. 226–232, 1975.

[28] J. B. Morel, P. Mourrain, C. Béclin, and H. Vaucheret, "DNA methylation and chromatin structure affect transcriptional and post-transcriptional transgene silencing in Arabidopsis," *Current Biology*, vol. 10, no. 24, pp. 1591–1594, 2000.

[29] L. Bartee, F. Malagnac, and J. Bender, "Arabidopsis cmt3 chromomethylase mutations block non-CG methylation and silencing of an endogenous gene," *Genes and Development*, vol. 15, no. 14, pp. 1753–1758, 2001.

[30] F. Agius, A. Kapoor, and J. Zhu, "Role of the Arabidopsis DNA glycosylase/lyase ROS1 in active DNA demethylation," *Proceedings of the National Academy of Sciences of the United States of America*, vol. 103, no. 31, pp. 11796–11801, 2006.

[31] Y. Kinoshita, H. Saze, T. Kinoshita et al., "Control of FWA gene silencing in *Arabidopsis thaliana* by SINE-related direct repeats," *Plant Journal*, vol. 49, no. 1, pp. 38–45, 2007.

[32] T.-F. Hsieh, C. A. Ibarra, P. Silva et al., "Genome-wide demethylation of *Arabidopsis* endosperm," *Science*, vol. 324, no. 5933, pp. 1451–1454, 2009.

[33] N. S. Akopyants, A. Fradkov, D. E. Berg et al., "PCR-based subtractive hybridization and differences in gene content among strains of *Helicobacter pylori*," *Proceedings of the National Academy of Sciences of the United States of America*, vol. 95, no. 22, pp. 13108–13113, 1998.

Hindawi Publishing Corporation
Journal of Chemistry
Volume 2014, Article ID 693573, 6 pages
http://dx.doi.org/10.1155/2014/693573

Research Article

Protective Effects of *Elaeagnus angustifolia* Leaf Extract against Myocardial Ischemia/Reperfusion Injury in Isolated Rat Heart

Binsheng Wang,[1] Hengyi Qu,[2] Jun Ma,[3] Xiling Sun,[1] Dong Wang,[4] Qiusheng Zheng,[1] and Du Xing[5]

[1] *Binzhou Medical University, Yantai 264000, China*
[2] *Affiliated Hospital of Binzhou Medical University, Yantai 264000, China*
[3] *Yantai University, Yantai 264005, China*
[4] *Shandong Provincial Qianfoshan Hospital, Jinan, Shandong 250014, China*
[5] *Yuhuangding Hospital of Yantai City, Yantai 264000, China*

Correspondence should be addressed to Dong Wang; wangdong9859@sina.com and Qiusheng Zheng; zqsyt@sohu.com

Received 10 April 2014; Accepted 18 June 2014; Published 8 July 2014

Academic Editor: Wang Chunming

The purpose of this study is to clarify the cardioprotective property of the aqueous extract of *Elaeagnus angustifolia* L. leaf (EA) against myocardial ischemia/reperfusion injury in isolated rat heart. The myocardial ischemia/reperfusion (I/R) injury model of isolated rat heart was set up by the use of improved Langendorff retrograde perfusion technology. Compared with the ischemia/reperfusion (I/R) group, the aqueous extract of *Elaeagnus angustifolia* L. leaf (0.5 mg/mL, 1.0 mg/mL) pretreatment markedly improved the coronary flow (CF) and raised left ventricular developed pressure (LVDP) and maximum rise/down velocity ($\pm dp/dt$max). The infarct size of the EA-treated hearts was smaller than that of I/R group. After treatment with EA, the superoxide dismutase (SOD) activity increased; malondialdehyde (MDA) and protein carbonyl content reduced more obviously ($P < 0.01$) than that of I/R injury myocardial tissue. *Conclusion*. Results from the present study showed that the aqueous extract of *Elaeagnus angustifolia* L. leaf has obvious protective effects on myocardial I/R injury, which may be related to the improvement of myocardial oxidative stress states.

1. Introduction

Cardiovascular disease is one of the main causes of mortality of people all over the world [1]; acute myocardial infarction (MI) is one of the leading causes of death in human cardiovascular disease, which is caused by thrombotic occlusion of the coronary artery induced by the death of myocardial cells. Quick return to normal blood supply is the only effective way to reduce heart injury. Paradoxically, reperfusion can cause myocardial injury and further lead to cardiac dysfunction, referred to as "reperfusion injury" [2–4]. Therefore, mitigating myocardial ischemia-reperfusion (I/R) injury is a very important way for the ischemic heart disease treatment [5].

I/R injury is a very complicated process which involves a lot of kinds of possible mechanisms. Oxidative stress damage plays an important role in the progression of I/R injury, which is one of the most important mechanisms involved in I/R injury [6, 7]. Some studies have shown that increased expression of antioxidant enzymes will protect against I/R injury. A lot of antioxidants, such as vitamin E, catalase (CAT), melatonin, and superoxide dismutase (SOD), have been reported to protect the heart from I/R injury; all the evidences confirm that reduced oxidative stress could decrease the injury induced by I/R [8, 9].

Elaeagnus angustifolia, used as a food ingredient or herbal drug for its reputed medicinal properties, commonly called wild olive, silver berry, Russian olive, or oleaster, is a species of *Elaeagnus*, native to western and central Asia, from southern Russia and Kazakhstan to Turkey and Iran [10]. It has been found that *Elaeagnus angustifolia* is used in traditional Turkish medicine as antipyretic, diuretic, tonic, and antidiarrheal and as a medication against kidney disorders (inflammatory or kidney stone) [11, 12] and in Iranian folk medicine for

its anti-inflammatory, antinociceptive, and analgesic effects. Also, decoction and infusion of its fruits are considered to be a good remedy for fever, jaundice, asthma, tetanus, and rheumatoid arthritis [13]; the aqueous and ethanolic extracts of its fruits induced a muscle relaxant effect in a dose dependent manner [14]. In the present study, we investigated the effects of aqueous extract from *Elaeagnus angustifolia* L. leaf on protecting rat heart against I/R injury.

2. Material and Methods

2.1. Plant Material. The mature leaves of *Elaeagnus angustifolia* L. were collected during the month of October from Shihezi, Xinjiang, China, and the authenticity of the material was verified by one of the authors and later confirmed by a botanist.

2.2. Chemicals. Triphenyltetrazolium chloride (TTC) was obtained from the Beijing Biodee Biotechnology Co., Ltd. (Beijing, China). The malondialdehyde (MDA), super oxide dismutase (SOD), and protein carbonyl analyzing reagent kits were obtained from Nanjing Jiancheng Bioengineering Institute (Nanjing, China). All of the other chemicals used in the study for the biochemical estimation were of analytical grade obtained commercially.

2.3. Preparation of Extract. Fresh *Elaeagnus angustifolia* L. leaves were washed in distilled water and air-dried in the shade. Thirty grams of leaves was cut into small pieces and extracted with 70°C distilled water (DW) (DW: material, 10 : 1, v/w) thrice in an incubator at 85°C for 3 h. The water extract was filtered through a 2 μm pore sterile filter paper. The combined filtrates were concentrated in a vacuum at 60°C, and the resulting filtrates were 50 mL (amount to 6×10^2 mg/mL crude drug).

2.4. Experimental Groups and Drug Delivery. Male Wistar rats (250–280 g) were obtained from Xinjiang Medicine University Medical Laboratory Animal Center (SDXK 2011-004). All experimental procedures complied with the Institutional Animal Care and Use Committee of National Institute Pharmaceutical Education and Research.

The rats were divided into four groups randomly: control group (Sham), I/R group, low concentration of aqueous extract of *Elaeagnus angustifolia* L. leaves (EA) treatment group, and high concentration of EA treatment group.

2.5. Preparation for Isolated Heart. The male Wistar rats (250–280 g) were anesthetized by an intraperitoneal injection of 60 mmol/L chloral hydrate (0.35 g/kg). To anticoagulate, 250 U/kg of heparin was sublingually venously injected into the rats. Thoracic surgery was performed to remove the heart [15], hearts were excised and mounted on Langendorff's apparatus quickly, and then the hearts were immersed in ice-cold Krebs-Henseleit buffer (1.2 mM KH_2PO_4, 1.2 mM $CaCl_2$, 25 mM sodium acetate, 120 mM NaCl, 1.2 mM $MgSO_4$, and 11 mM glucose; pH 7.4) piped with a gas mixture comprised of 95% O_2/5% CO_2; then the hearts were maintained in 37°C in a water-jacketed organ chamber [16]. The pressure recording was established by a water-filled latex balloon, coupled to a pressure transducer (Statham), which was inserted into the left ventricular cavity via the left auricle.

Control group hearts were stabilized by perfusion for 95 min and the I/R group hearts were stabilized for 30 min, and then, after 20 min global ischemia, the reperfusion was established for 45 min. Hearts in EA treatment group were stabilized for 20 min, instead of K-H buffer with EA (0.5 mg/mL, 1 mg/mL) for 10 min, and then global ischemia for 20 min and reperfusion for 45 min were established.

2.6. Measurement of Heart Hemodynamic Parameters. A computer-based data acquisition system was used to continuously monitor the hemodynamic parameters including the following functional parameters: left ventricular developed pressure (LVDP, LVDP = LVSP − LVEDP), left ventricular end-diastolic pressure (LVEDP), left ventricular systolic pressure (LVSP), maximum rise/down velocity of left intraventricular pressure ($\pm dp/dt$max), and heart rate (HR) were monitored continuously using 4S AD Instruments biology polygraph (Powerlab, Australia). The coronary flow (CF) was measured using a flowmeter with an in-line probe.

2.7. Evaluation of Myocardial Infarct Size. Frozen hearts were cut into 2 mm thick cross-sectional slices for evaluation of myocardial size. The slices were stained by putting them into the 1% triphenyltetrazolium chloride (TTC) solution for 10 minutes at 37°C. The stained slices were transferred to a formalin solution for 10 min after TTC staining; then we placed them into phosphate buffer (pH 7.4) [17]. The heart slices were then digitally imaged using a digital camera. The ischemic (white) and nonischemic (red) area were measured digitally using Image Pro Plus software. The infarct size was represented as percentage of the ischemic area.

2.8. Assay of Oxidative Stress. At the end of the perfusions, the hearts were kept at −70°C for later oxidative stress analysis. Liquid nitrogen-chilled tissue pulverizer was used to crush the frozen hearts to a powder. For tissue analyses, weighed amounts of the frozen tissues were homogenized in appropriate buffer using microcentrifuge tube homogenizer. Then, the SOD activity, malondialdehyde (MDA), and protein carbonyl content were analyzed spectrophotometrically according to the instruction of the assay kits (Nanjing Jiancheng Bioengineering Institute, Nanjing, China).

2.9. Statistical Analysis. Data were presented as mean ± standard deviation from at least six independent experiments. Differences in hemodynamic parameters, infarct size, MDA level, SOD activity, and carbonyl content level were analyzed using the one-way ANOVA with Student's t-test. Statistical significance was considered at the probability value of less than 0.05. Analyses were carried out using the Origin 8.0 software (Origin Lab Corporation, Northampton, MA, USA).

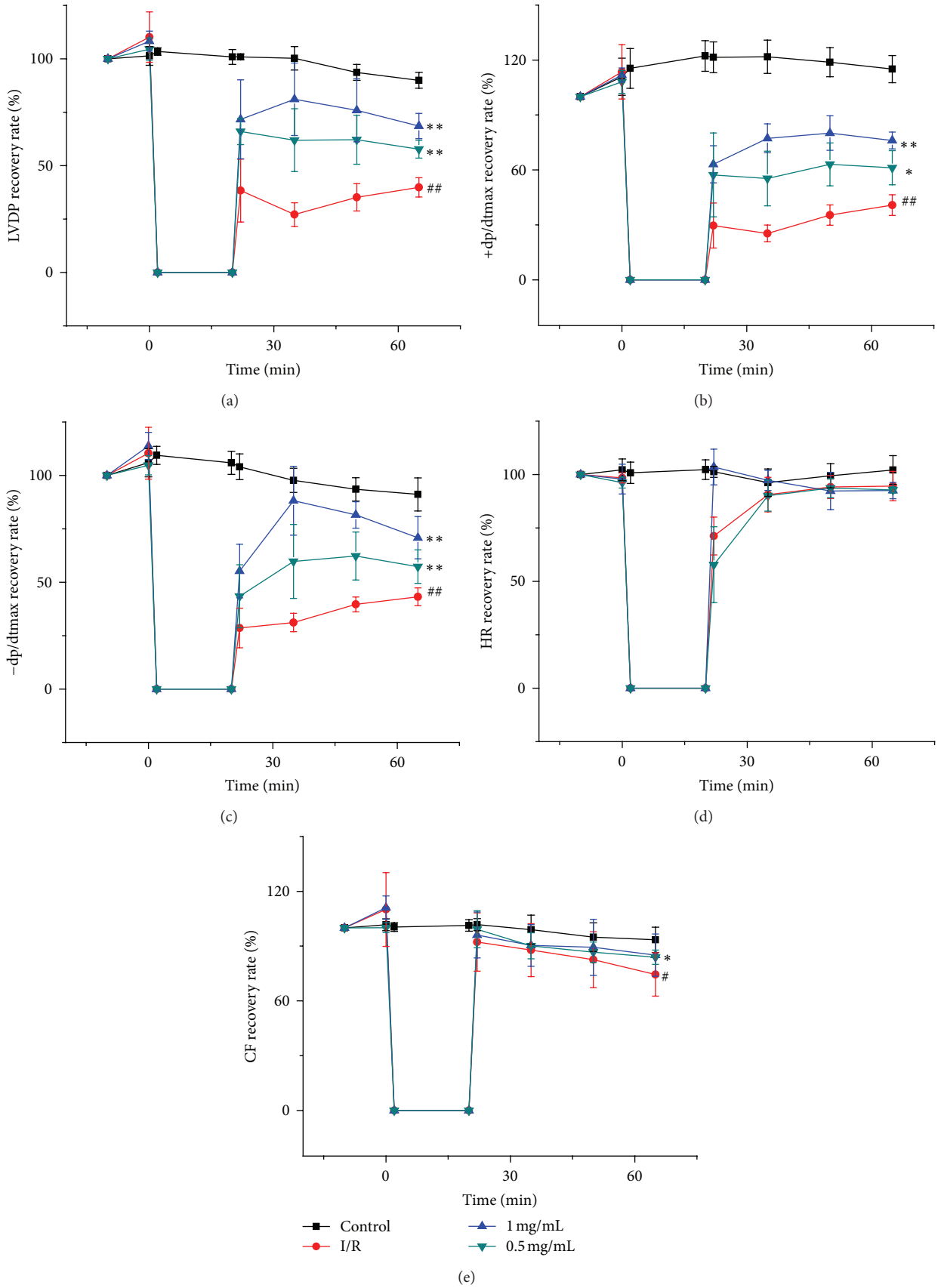

Figure 1: Effects of the aqueous extract of *Elaeagnus angustifolia* L. leaves upon hemodynamics in a model of ischemia-reperfusion using isolated rat heart. Data are the mean ± SD. Values marked with $^{\#\#}P < 0.01$ and $^{\#}P < 0.05$ are significantly different from control group. Values marked with $^{**}P < 0.01$ and $^{*}P < 0.05$ are significantly different from I/R group.

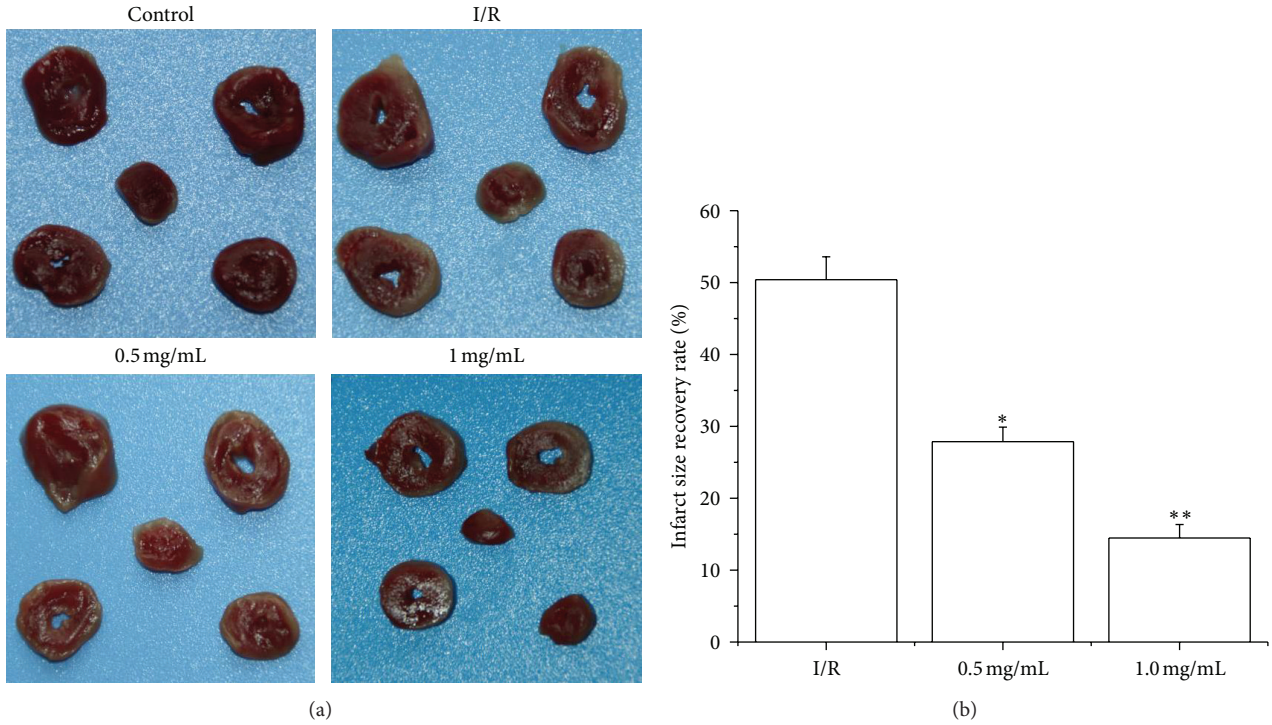

FIGURE 2: Effects of the aqueous extract of *Elaeagnus angustifolia* L. leaves upon myocardial infarct size. Data are the mean ± SD. Values marked with $^{**}P < 0.01$ and $^{*}P < 0.05$ are significantly different from I/R group.

3. Result

3.1. The Aqueous Extract of Elaeagnus angustifolia L. Leaves (EA) Enhanced Recovery of I/R Induced Changes in Cardiac Function. The cardiac function was monitored continuously using 4S AD Instruments biology polygraph. Compared to the sham I/R group, I/R injury caused a significant decrease in left ventricular developed pressure (LVDP), maximum rise/down velocity of left intraventricular pressure ($\pm dp/dt$max), and coronary flow (CF). As shown in Figure 1, the EA administration significantly blunted the reduction of LVDP (Figure 1(a)), $\pm dp/dt$max (Figures 1(b) and 1(c)), and CF (Figure 1(d)) caused by I/R injury. However, there were no significant changes in HR (Figure 1(e)) among all of the four groups.

3.2. The EA Reduced Myocardial Infarct Size following I/R Injury. At the end of reperfusion, myocardial infarct size was assessed using the TTC staining method. As illustrated in Figure 2, ischemia for 20 min followed by 45 min of reperfusion resulted in development of substantial myocardial infarcts, while the 0.5 mg/mL and 1.0 mg/mL EA preconditioning substantially decreased I/R induced percentage of myocardial infarct size.

3.3. The EA Improved Oxidative Stress State Induced by I/R. To identify the possible mechanisms of EA on cardioprotection, the SOD activity and MDA level were determined in myocardial tissue. The SOD activity significantly increased (Figure 3(a)), while MDA level (Figure 3(b)) was significantly decreased in EA pretreatment groups compared with that of I/R group. Protein carbonyls are formed through oxidation of proteins by a variety of mechanisms which are the sensitive markers of oxidative injury. As shown in Figure 2, the hearts subjected to global myocardial ischemia for 20 min followed by 45 min of reperfusion showed a significant increase of level of carbonyl content, while the EA preconditioning substantially decreased I/R induced rise of level of carbonyl content.

4. Discussion

The present work was aimed at studying the cardioprotective activity of the aqueous extract of *Elaeagnus angustifolia* L. leaf (EA) in ischemia/reperfusion (I/R) induced cardiotoxicity in isolated rat heart. The results of this study revealed that EA at the doses of 0.5 mg/mL and 1.0 mg/mL dependently and significantly ameliorated the cardiotoxicity by restoring cardiac function and myocardial biochemical parameters towards the normal values.

After reperfusion of the ischemic myocardium, significant myocardial dysfunction, including LVDP, $\pm dp/dt$max, CF and HR, and myocardial infarct, was induced by I/R. Reperfusion is a key role among a number of events leading to myocardial dysfunction associated with I/R injury. In the present study, we found that EA improved recovery of I/R-altered hemodynamic parameters (LVDP, $\pm dp/dt$ max, and CF and HR) and attenuated infarct size induced by I/R significantly.

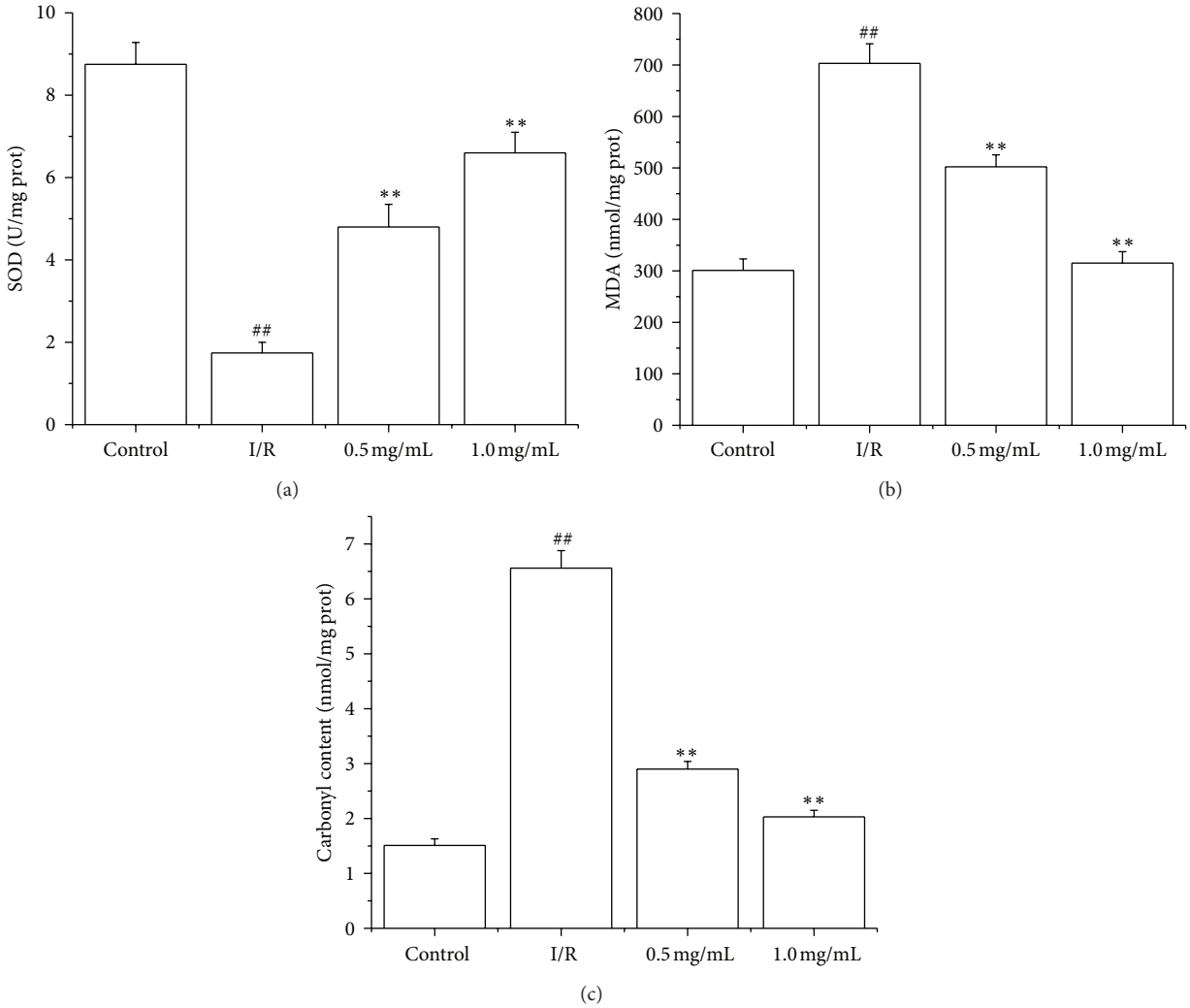

Figure 3: Effects of EA on SOD activity (a), MDA level (b), and carbonyl content level (c). Values are means with their standard deviation ($n = 8$); $^{\#\#}P < 0.01$ compared with control group; $^{**}P < 0.01$ compared with I/R group.

The generation of reactive oxygen species (ROS) plays an important role in the I/R induced myocardial injury [18, 19]. The ROS can be diminished by antioxidant systems that include antioxidant enzymes, such as SOD in the normal conditions [20]. However, when the amount of ROS is beyond the capacity of those enzymes and cannot be diminished during reperfusion, oxidative stress occurs. More and more evidence suggested that cardiomyocyte death and myocardial injury occurred during ischemia and reperfusion accompanied with oxidative stress [21–23]. Therefore, reduction of oxidative stress is one of the favorable strategies to alleviate myocardial injury induced by I/R. MDA is a maker of the peroxidation of cell membrane lipids caused by ROS. SOD is one of the most significant antioxidant enzymes, functioning as a superoxide anion scavenger, protein carbonyl is a sensitive biomarker of oxidative injury of proteins, and carbonyls are formed through oxidation of proteins. To further investigate the mechanism of cardioprotective effect of EA, an experiment was performed to examine whether EA affected the levels of MDA, protein carbonyls, and SOD activity induced by I/R. The present results illuminated that EA protected against myocardial I/R induced injury, accompanied by the attenuation of MDA production and protein carbonyls content and enhancement of SOD activity indicating that one of the mechanisms of the cardioprotection of EA was associated with its antioxidant effects.

In the present investigation, administration of EA significantly enhanced the recovery of I/R-altered cardiac function by blunting the reduction of left ventricular developed pressure (LVDP), maximum rise/down velocity of left intraventricular pressure ($\pm dp/dt$max), and coronary flow (CF) decreased by I/R injury. Also, EA treatment resulted in significant modulation of cardioprotection content, the SOD activity, and MDA level. Therefore, it can be concluded that the aqueous extract of *Elaeagnus angustifolia* L. leaf has obvious protective effects on myocardial I/R injury, which may be related to the improvement of myocardial oxidative stress states.

Conflict of Interests

The authors declare that there is no conflict of interests regarding the publication of this paper.

Authors' Contribution

Binsheng Wang and Hengyi Qu contribute equally to this work.

Acknowledgments

This study was supported by the Natural Science Foundation of Shandong Province (no. ZR2011HL013) to Dong Wang, the Xinjiang Production and Construction Corps Fund for Distinguished Young Scientists (2011CD006), and International Cooperation Project 2012BC001 to Qiusheng Zheng.

References

[1] G. Martínez-Sánchez, L. Delgado-Roche, A. Díaz-Batista et al., "Effects of ozone therapy on haemostatic and oxidative stress index in coronary artery disease," *European Journal of Pharmacology*, vol. 691, no. 1–3, pp. 156–162, 2012.

[2] P. A. Grace, "Ischaemia-reperfusion injury," *British Journal of Surgery*, vol. 81, no. 5, pp. 637–647, 1994.

[3] H. Inafuku, Y. Kuniyoshi, S. Yamashiro et al., "Determination of oxidative stress and cardiac dysfunction after ischemia/reperfusion injury in isolated rat hearts," *Annals of Thoracic and Cardiovascular Surgery*, vol. 19, no. 3, pp. 186–194, 2013.

[4] J. J. Ley, R. Prado, J. Q. Wei, N. H. Bishopric, D. A. Becker, and M. D. Ginsberg, "Neuroprotective antioxidant STAZN protects against myocardial ischemia/reperfusion injury," *Biochemical Pharmacology*, vol. 75, no. 2, pp. 448–456, 2008.

[5] E. Gao, Y. H. Lei, X. Shang et al., "A novel and efficient model of coronary artery ligation and myocardial infarction in the mouse," *Circulation Research*, vol. 107, no. 12, pp. 1445–1453, 2010.

[6] M. Khan, S. Varadharaj, L. P. Ganesan et al., "C-phycocyanin protects against ischemia-reperfusion injury of heart through involvement of p38 MAPK and ERK signaling," *The American Journal of Physiology—Heart and Circulatory Physiology*, vol. 290, no. 5, pp. H2136–H2145, 2006.

[7] E. Murphy and C. Steenbergen, "Mechanisms underlying acute protection from cardiac ischemia-reperfusion injury," *Physiological Reviews*, vol. 88, no. 2, pp. 581–609, 2008.

[8] D. K. Das and N. Maulik, "Antioxidant effectiveness in ischemia-reperfusion tissue injury," *Methods in Enzymology*, vol. 233, pp. 601–610, 1994.

[9] Z. Chen, T. D. Oberley, Y. S. Ho et al., "Overexpression of CuZnSOD in coronary vascular cells attenuates myocardial ischemia/reperfusion injury," *Free Radical Biology and Medicine*, vol. 29, no. 7, pp. 589–596, 2000.

[10] L. H. Bailey and E. Z. Bailey, *Hortus Third: A Concise Dictionary of Plants Cultivated in the United States and Canada*, Macmillan, New York, NY, USA, 1976.

[11] F. A. Ayaz and E. Bertoft, "Sugar and phenolic acid composition of stored commercial oleaster fruits," *Journal of Food Composition and Analysis*, vol. 14, no. 5, pp. 505–511, 2001.

[12] I. Gürbüz, O. Üstün, E. Yesilada, E. Sezik, and O. Kutsal, "Anti-ulcerogenic activity of some plants used as folk remedy in Turkey," *Journal of Ethnopharmacology*, vol. 88, no. 1, pp. 93–97, 2003.

[13] A. Ahmadiani, J. Hosseiny, S. Semnanian et al., "Antinociceptive and anti-inflammatory effects of *Elaeagnus angustifolia* fruit extract," *Journal of Ethnopharmacology*, vol. 72, no. 1-2, pp. 287–292, 2000.

[14] H. Hosseinzadeh, M. Ramezani, and N. Namjo, "Muscle relaxant activity of Elaeagnus angustifolia L. fruit seeds in mice," *Journal of Ethnopharmacology*, vol. 84, no. 2-3, pp. 275–278, 2003.

[15] N. Khandoudi, M. Laville, and A. Bril, "Protective effect of the sodium/hydrogen exchange inhibitors during global low-flow ischemia," *Journal of Cardiovascular Pharmacology*, vol. 28, no. 4, pp. 540–546, 1996.

[16] J. L. Zweier, J. Fertmann, and G. Wei, "Nitric oxide and peroxynitrite in postischemic myocardium," *Antioxidants and Redox Signaling*, vol. 3, no. 1, pp. 11–22, 2001.

[17] D. J. Bester, K. Kupai, T. Csont et al., "Dietary red palm oil supplementation reduces myocardial infarct size in an isolated perfused rat heart model," *Lipids in Health and Disease*, vol. 9, article 64, 2010.

[18] H. P. Grill, J. L. Zweier, P. Kuppusamy, M. L. Weisfeldt, and J. T. Flaherty, "Direct measurement of myocardial free radical generation in an in vivo model: effects of postischemic reperfusion and treatment with human recombinant superoxide dismutase," *Journal of the American College of Cardiology*, vol. 20, no. 7, pp. 1604–1611, 1992.

[19] M. Shen, R. Wu, L. Zhao et al., "Resveratrol attenuates ischemia/reperfusion injury in neonatal cardiomyocytes and its underlying mechanism," *PLoS ONE*, vol. 7, no. 12, Article ID e51223, 2012.

[20] X. Yuan, B. Yu, Y. Wang et al., "Involvement of endoplasmic reticulum stress in isoliquiritigenin-induced SKOV-3 cell apoptosis," *Recent Patents on Anti-Cancer Drug Discovery*, vol. 8, no. 2, pp. 191–199, 2013.

[21] J. M. McCord, "Oxygen-derived free radicals in postischemic tissue injury," *The New England Journal of Medicine*, vol. 312, no. 3, pp. 159–163, 1985.

[22] J. A. Thompson and M. L. Hess, "The oxygen free radical system: a fundamental mechanism in the production of myocardial necrosis," *Progress in Cardiovascular Diseases*, vol. 28, no. 6, pp. 449–462, 1986.

[23] S. W. Werns, M. J. Shea, and B. R. Lucchesi, "Free radicals and myocardial injury: pharmacologic implications," *Circulation*, vol. 74, no. 1, pp. 1–5, 1986.

Hindawi Publishing Corporation
Journal of Chemistry
Volume 2014, Article ID 368376, 6 pages
http://dx.doi.org/10.1155/2014/368376

Research Article

Cardioprotective Effect of the Aqueous Extract of Lavender Flower against Myocardial Ischemia/Reperfusion Injury

Dong Wang,[1] Xin Guo,[2] Mingjie Zhou,[1] Jichun Han,[3] Bo Han,[3] and Xiling Sun[4]

[1] *Shandong Provincial Qianfoshan Hospital, Jinan, Shandong 250014, China*
[2] *Affiliated Traditional Medical Hospital of Xinjiang Medical University, Urumqi 830000, China*
[3] *School of Pharmacy, Shihezi University, Shihezi 832002, China*
[4] *School of Integrated Traditional Chinese and Western Medicine, Binzhou Medical University, Yantai 264000, China*

Correspondence should be addressed to Xiling Sun; sunxiling@sohu.com

Received 6 April 2014; Revised 31 May 2014; Accepted 1 June 2014; Published 29 June 2014

Academic Editor: Wang Chunming

This study was conducted to evaluate the cardioprotective property of the aqueous extract of lavender flower (LFAE). The myocardial ischemia/reperfusion (I/R) injury of rat was prepared by Langendorff retrograde perfusion technology. The heart was preperfused with K-H solution containing LFAE for 10 min before 20 minutes global ischemia, and then the reperfusion with K-H solution was conducted for 45 min. The left ventricular developed pressure (LVDP) and the maximum up/downrate of left ventricular pressure ($\pm dp/dt_{max}$) were recorded by physiological recorder as the myocardial function and the myocardial infarct size was detected by TTC staining. Lactate dehydrogenase (LDH) and creatine kinase (CK) activities in the effluent were measured to determine the myocardial injury degree. The superoxide anion dismutase (SOD) and malondialdehyde (MDA) in myocardial tissue were detected to determine the oxidative stress degree. The results showed that the pretreatment with LFAE significantly decreased the myocardial infarct size and also decreased the LDH, CK activities, and MDA level, while it increased the LVDP, $\pm dp/dt_{max}$, SOD activities, and the coronary artery flow. Our findings indicated that LFAE could provide protection for heart against the I/R injury which may be related to the improvement of myocardial oxidative stress states.

1. Introduction

Cardiovascular disease is common and results in much of mortality of people throughout the world. Acute myocardial infarction is particularly formidable in cardiovascular disease cases, coronary artery stenosis is the initial factor that sets off a chain reaction, and the consequence is myocardial necrosis caused by conditions of acute continuous ischemia and hypoxia. Timely and effective recovery of demand of blood supply is an effective method that is able to minimize the heart injuries. Paradoxically, reperfusion itself can cause myocardial injury and cardiac dysfunction, referred to as "reperfusion injury" [1–3]. As a consequence, relieving the ischemic reperfusion injury can be seen as an additional method to secure the heart against cardiovascular disease [4].

Ischemia-reperfusion injury refers to reducing organ of blood donation for a period of time, there will be damage during reperfusion. Doctors gradually found that the main factors that cause damage to an organ, not ischemia itself, but reperfusion. In the process of reperfusion, tissue cells produce oxygen free radicals in excess. Oxidative stress is an important way involved in I/R injury [5, 6]. Several studies have shown that increased expression of antioxidant enzymes will protect against postischemic injury. It has been reported that antioxidants vitamin E, catalase (CAT), melatonin, and superoxide dismutase (SOD) defend the heart against I/R injury. From another aspect, it confirms that the oxidative stress has been involved in ischemia/reperfusion process [7, 8].

Lavender as a traditional botanical medicine has been applied for many years [9]; people in many countries and regions from ancient times employed lavender as an effective medicine to treat diseases; it has many beneficial effects consisting of anti-inflammatory [10], antioxidant [11],

antibacterial [12], antisenile dementia [13], and anxiolytic, which is particularly evident [14]. The purpose of our study was to detect the protective effect of aqueous extract of lavender flowers on the heart.

2. Material and Methods

2.1. Plant Material. The flowers of *Lavandula angustifolia* Mill were collected in Yili, Xinjiang, China, and the material authenticity was established by one of the authors and later confirmed by a botanist.

2.2. Preparation of Extract. Dried flowers of *Lavandula angustifolia* Mill were washed in distilled water and air-dried in the shade; flowers were extracted with warm distilled water (DW) (DW: material, 10 : 1, v/w) twice in an incubator at 80°C for 1.5 h. The hot-water extract was filtered through a 2 μm pore sterile filter paper. The combined filtrates were concentrated in a vacuum at 60°C, and the resulting filtrates were amounted to 5×10^2 mg/mL crude drug.

2.3. Animals and Experimental Groups. Male Wistar rats (250–280 g) were obtained from Xinjiang Medicine University Medical Laboratory Animal Center (SDXK (new) 2011-004). All experimental procedures were approved by the Institutional Animal Care and Use Committee of National Institute Pharmaceutical Education and Research.

The rats were randomly divided into three groups: control group (Sham), I/R group, and aqueous extract of lavender flower (LFAE) treatment group. Hearts in control group were uninterruptedly perfused with K-H buffer purely for the 95 min. I/R group hearts were perfused firstly for 30 min and then we Suspended the infusion for 20 min and reperfusion for 45 min. Hearts in treatment groups were perfused firstly for 20 min instead of K-H buffer with LFEA (1 mg/mL) for 10 min and then we Suspended the infusion for 20 min and reperfusion for 45 min.

2.4. Isolated Rat Heart Preparation. The male Wistar rats (250–280 g) were anesthetized by an intraperitoneal injection of 60 mmol/L chloral hydrate (0.35 g/kg). To anticoagulate, 250 U/kg of heparin was given as a sublingual venous injection to the rats. After a few minutes, we performed the thoracic surgery on rat to remove heart. we cut the ribs and opened the chest, Then cut off the blood vessels and obtained the heart and then put the heart into pre-cooling K-H solution, squeezed out the blood gently. After that, the heart was excised quickly and immediately mounted on Langendorff's apparatus. The hearts were immersed in ice-cold K-H buffer (120 mM NaCl, 1.2 mM KH_2PO_4, 1.2 mM $CaCl_2$, 1.2 mM $MgSO_4$, 25 mM sodium acetate, and 11 mM glucose, pH7.4) equilibrated with a gas mixture comprised of 95% O_2/5% CO_2. Immediately, the heart was connected to the Langendorff apparatus which was maintained at 37°C [15], and then we cut the left atrial appendage and inserted the latex balloon filled with water into the left ventricle through the left atrial appendage. Hemodynamic parameters will be displayed on the recorder screen, finally.

Table 1: Effect of the aqueous extract of lavender flower (LFAE) on levels of CK and LDH in coronary flow of ischemia/reperfusion injury ($\overline{x} \pm s$, $n = 8$).

Groups	Before ischemia	Reperfusion	
		20 min	45 min
CK (U/L)			
Control	15.59 ± 1.35	17.01 ± 1.37	18.57 ± 1.31
I/R	14.98 ± 1.09	45.25 ± 3.59**	50.36 ± 2.63**
LFAE	15.67 ± 1.05	21.26 ± 2.00$^{\#\#}$	30.63 ± 2.28$^{\#\#}$
LDH (U/L)			
Control	12.34 ± 1.13	13.23 ± 1.80	14.48 ± 1.07
I/R	12.63 ± 1.17	30.91 ± 2.62**	37.68 ± 2.01**
LFAE	13.06 ± 0.83	21.39 ± 1.33$^{\#\#}$	27.60 ± 1.55$^{\#\#}$

$^{**}P < 0.01$, compared with control group; $^{\#\#}P < 0.01$, compared with I/R group.

Table 2: Effects of LFAE on SOD activity and MDA level. Values are means with their standard deviation ($\overline{x} \pm s$, $n = 8$).

Group	Dosage (mg·mL^{-1})	After reperfusion	
		SOD (U/mgPr)	MDA (μmol/mgPr)
Control	—	9.29 ± 0.66	190.78 ± 11.93
I/R	—	3.60 ± 0.28**	433.66 ± 29.16**
LFAE	1	7.46 ± 0.51$^{\#\#}$	231.41 ± 18.93$^{\#\#}$

$^{**}P < 0.01$, compared with control group; $^{\#\#}P < 0.01$, compared with I/R group.

2.5. Measurement of Heart Hemodynamic Parameters. The hemodynamic parameters were accurately detected by a signal collecting system (PC Power lab with Chart 5 software, 4S AD instruments). The following functional parameters were measured: left ventricular systolic pressure (LVSP), left ventricular end-diastolic pressure (LVEDP, LVDP = LVSP − LVEDP), $\pm dp/dt_{\max}$ (reflecting the important indicators of left ventricular systolic function and diastolic function), and heart rate (HR) were detected uninterruptedly using 4S AD instruments biology polygraph (Power lab, Australia). The coronary flow (CF) was detected using a flow meter with an in-line probe (model T106, Transonic).

2.6. Enzymes Activities Assays. To determine creatine kinase (CK) and lactate dehydrogenase (LDH) activity in the perfusate, samples were collected from the coronary effluent before 20 min ischemia and after 20 min and 45 min of reperfusion. LDH and CK were assayed spectrophotometrically using LDH and CK kits (Nanjing Jiancheng Bioengineering Institute, Nanjing, China).

2.7. Evaluation of Myocardial Infarct Size. In the wake of frozen, the hearts were cut into five slices along the transverse direction, and every piece was 2 mm thick. We put the sliced hearts in TTC with the concentration of 1% to be incubated for 15 minutes and we turned over the hearts once in this process. When the TTC staining was over, the heart slices were dried with filter paper, and then these slices were covered in formalin solution for 15 minutes, Finally, these

Table 3: Supplemental data for Figure 1.

Group	Reperfusion		
	15 min	30 min	45 min
LVDP			
Control	92.88 ± 4.76	88.13 ± 4.01	85.63 ± 4.81
I/R	46.38 ± 3.20**	52.67 ± 2.83**	44.22 ± 3.60**
LFAE	72.37 ± 3.16##	69.38 ± 2.83##	58.88 ± 3.06##
$+dp/dt_{max}$			
Control	94.63 ± 4.69	89.63 ± 3.96	83.62 ± 3.93
I/R	48.25 ± 2.71**	46.13 ± 2.70**	43.50 ± 2.62**
LFAE	66.75 ± 3.54##	63.38 ± 2.87##	60.63 ± 3.02##
$-dp/dt_{min}$			
Control	91.25 ± 4.10	89.50 ± 3.77	86.13 ± 4.40
I/R	45.75 ± 3.03**	42.38 ± 2.50**	37.38 ± 3.12**
LFAE	64.63 ± 3.29##	61.88 ± 3.27##	58.75 ± 2.66##
CF			
Control	85.75 ± 3.83	83.13 ± 3.87	76.50 ± 2.78
I/R	58.88 ± 3.56**	52.50 ± 2.45**	51.63 ± 3.66**
LFAE	73.75 ± 3.80##	68.38 ± 4.15##	64.63 ± 3.28##
HR			
Control	97.75 ± 4.06	92.63 ± 4.69	90.13 ± 4.64
I/R	81.75 ± 3.37**	74.75 ± 4.71**	73.50 ± 3.25**
LFAE	88.38 ± 4.44#	84.88 ± 4.67#	80.88 ± 5.00#

** $P < 0.01$, compared with control group; ## $P < 0.01$, # $P < 0.05$, compared with I/R group.

slices were immersed in phosphate buffer at 4°C (pH 7.4) [16]. Heart slices were digitally imaged using a Canon camera. The area of infarcted part (pale) and viable part (red) was measured digitally using Image Pro Plus software. Infarct size was represented as percentage of the area of ischemia [17].

2.8. Assay of Oxidative Stress. When the perfusions finished, we froze the hearts under the condition of −70°C to prepare for further testing. The frozen ventricles were crushed to powder by liquid nitrogen-chilled tissue pulverizer. For tissue analyses, weighed amounts of the frozen tissues were homogenized in appropriate buffer using microcentrifuge tube homogenizer. Then the SOD and malondialdehyde (MDA) were analyzed spectrophotometrically according to the instruction of the assay kits (Nanjing Jiancheng Bioengineering Institute, Nanjing, China).

2.9. Statistical Analysis. The results were expressed as mean ± S.D. and analyzed by one-way analysis of variance (ANOVA). The values with $P < 0.05$ were considered statistically significant. $P < 0.01$ was considered very statistically significant. The analyses were carried out using the Origin 8.0 software (Origin Lab Corporation, Northampton, MA, USA).

3. Result and Discussion

3.1. The Aqueous Extract of Lavender Flower Improves Resumer of I/R-Induced Cardiac Function. The effects of treatment on LVDP, $\pm dp/dt_{max}$, CF, and HR during reperfusion in control group, I/R group, and treated hearts were shown in Figure 1. The datum was recovery ratio between the value after 15, 30, and 45 min of reperfusion and one minute before stopping irrigation in Table 3. When compared with the unprotected I/R hearts, exposure of 1 mg/mL extract during early reperfusion significantly improved functional recovery. The hearts underwent 20 minutes of ischemia time followed by 45 min of reperfusion and showed a remarkable reduction in the resumer of LVDP, $+dp/dt_{max}$, $-dp/dt_{max}$, CF, and HR. The resumer of LVDP, $\pm dp/dt_{max}$, CF, and HR after 45 min of reperfusion was higher ($^{*}P < 0.05$) in hearts perfused with aqueous extract of lavender flower 10 minutes before ischemia.

3.2. The Aqueous Extract of Lavender Flower (LFAE) Attenuates I/R-Induced Enzyme Release in Rat Heart. Before ischemia, CK and LDH levels in the effluent from control group, I/R group, and LFAE (1 mg/mL) group are fundamentally the same. As shown in Table 1, after 20 min of ischemia followed by 20 min and 45 min of reperfusion, the leakage of CK and LDH markedly increased compared to that of control. The LFAE pretreatment significantly reduced the I/R-induced increase in LDH and CK release in rat heart.

3.3. The Aqueous Extract of Lavender Flower Reduced Myocardial Infarct Size following I/R Injure. At the end of reperfusion,myocardial infarct size was assessed using the TTC staining method. As illustrated in Figure 2(a), there was only a small piece of infarction in control group (Sham) and ischemia for 20 min followed by 45 min of reperfusion resulted in development of substantial myocardial infarcts,

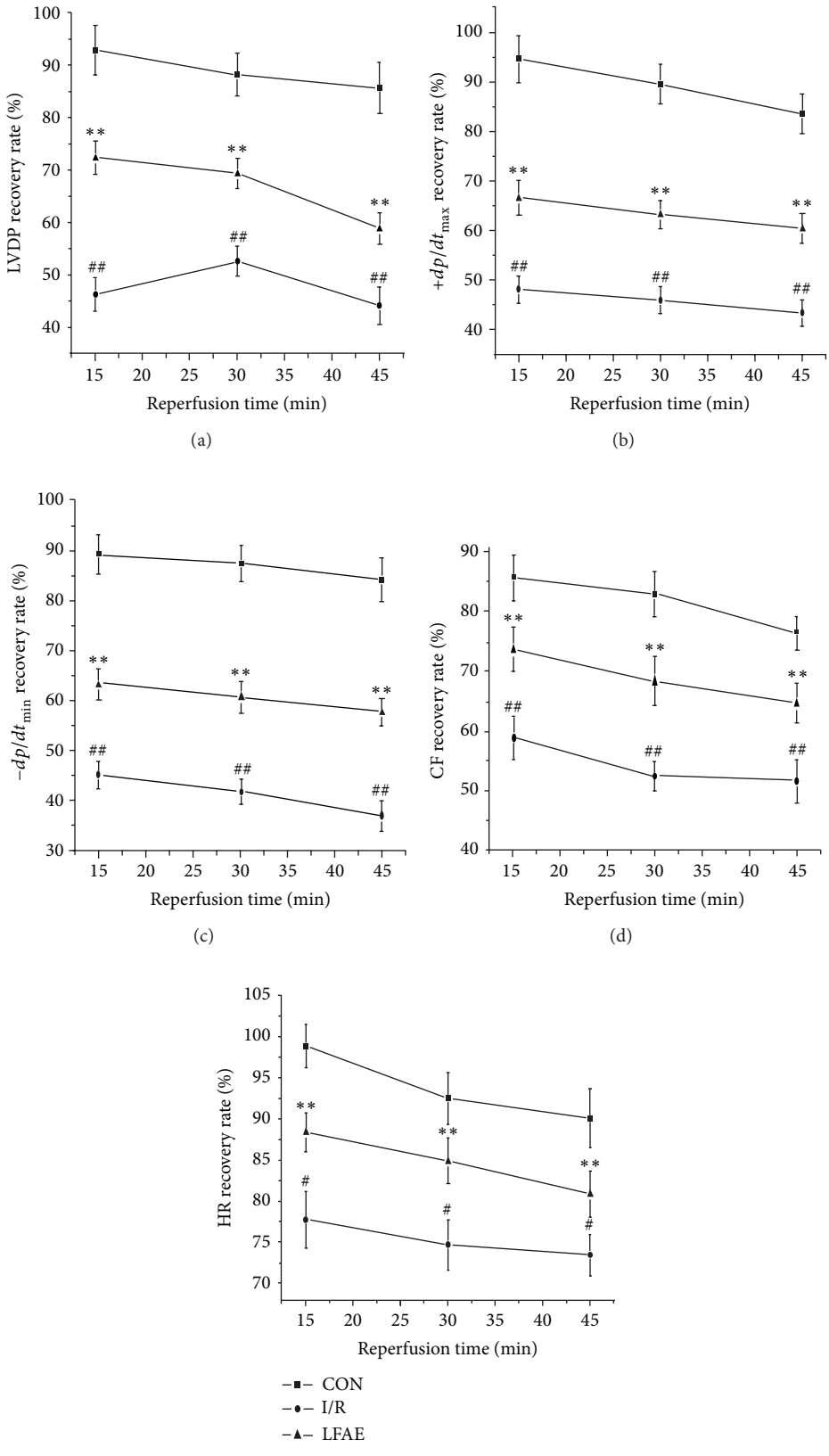

Figure 1: Effect of LFAE on cardiac function (LVDP, $+dp/dt_{max}$, $-dp/dt_{min}$, CF, HR) in rats subjected to I/R ($\overline{x} \pm s$, %, $n = 8$). $^{**}P < 0.01$, compared with control group; $^{\#\#}P < 0.01$, compared with I/R group. CON: control group (Sham), I/R: I/R group, and LFAE: aqueous extract of lavender flower treatment group.

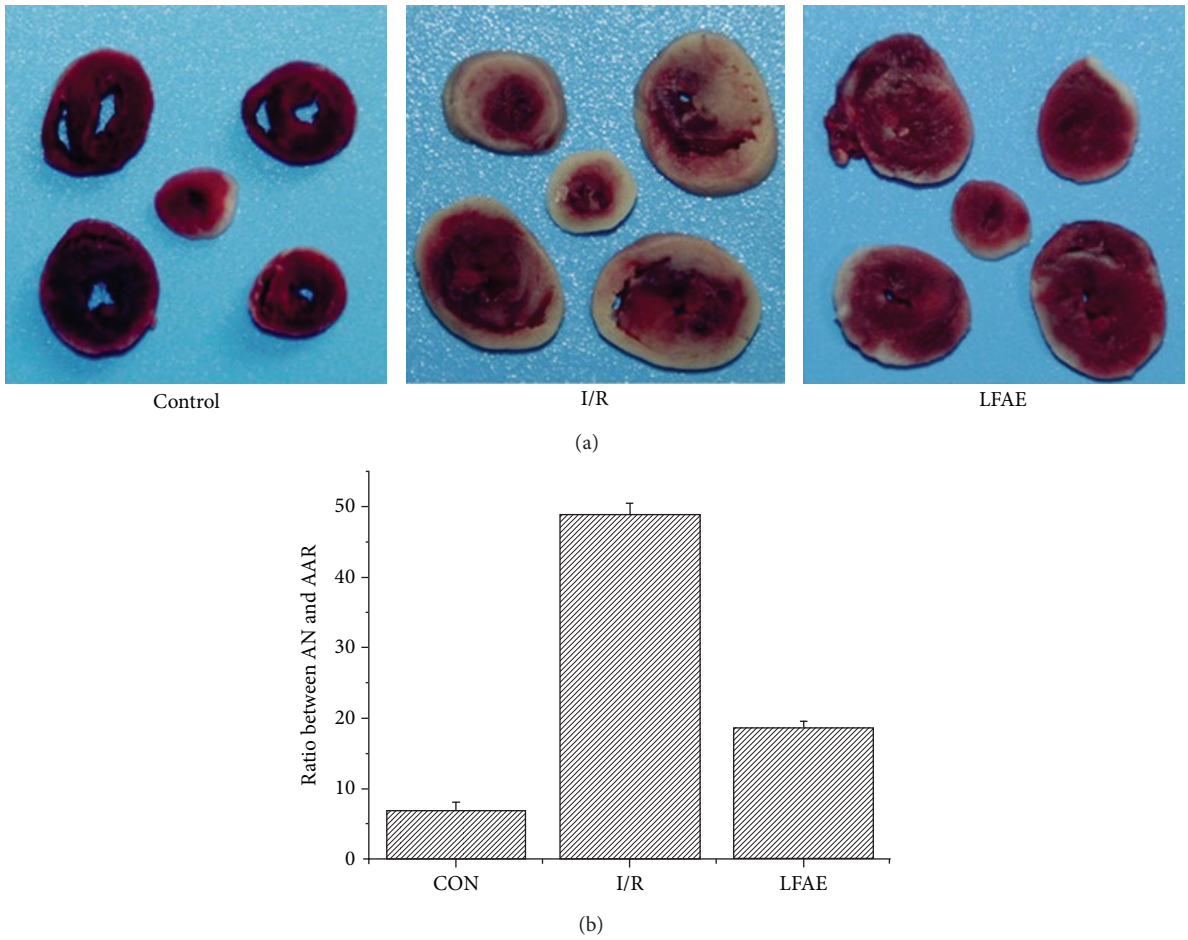

Figure 2: The aqueous extract of lavender flower (LFAE) reduces I/R-induced infarct size. (a) Photos of myocardial tissue sections of control, LFAE and I/R group, respectively, showing infarct (white) zones after TTC staining. (b) Ratio between the AN and AAR, AN is ischemic necrosis area; AAR is ischemic area. Values are means with their standard deviation ($\overline{x} \pm s$, $n = 8$), $^{**}P < 0.01$ compare with I/R group. CON: control group (Sham), I/R: I/R group, and LFAE: aqueous extract of lavender flower treatment group.

while the 1.0 mg/mL LFAE preconditioning substantially decreased I/R induced percentage of myocardial infarct size. In Figure 2(b), the Ratio between the ischemic necrosis area (AN) and the ischemic area (AAR) is 7% approximately in control group (Sham), the Ratio between the AN and AAR is 49% approximately in I/R group, the Ratio between the AN and AAR is 19% approximately in LFAE group.

3.4. The LFAE Improved Oxidative Stress State Induced by I/R. To identify the possible mechanisms of LFAE on cardioprotection, the SOD activity and MDA level were determined in myocardial tissue. As shown in Table 2, the SOD activity significantly increased, while MDA level was significantly decreased in LFAE (1 mg/mL) pretreatment groups compared with that of I/R group.

The present work was aimed at studing the cardioprotective activity of the aqueous extract of lavender flower (LFAE) in ischemia/reperfusion induced cardiotoxicity in isolated heart. The results of this study revealed that LFAE at the doses of 1.0 mg/mL dependently and significantly ameliorated the cardiotoxicity by restoring cardiac function and myocardial biochemical parameters towards the normal values.

I/R injury leads to heart dysfunction, which is one of the most significant etiological factors [18]. In the present study, we observed significant myocardial dysfunction, including changed hemodynamic parameters (LVDP, $\pm dp/dt_{max}$, CF and HR) and induced myocardial infarct after reperfusion of the ischemic myocardium. This is in agreement with numerous reports, indicating reperfusion as a key trigger of a number of events leading to myocardial dysfunction associated with I/R injury. LFAE markedly improved recovery of I/R-altered hemodynamic parameters (LVDP, $\pm dp/dt_{max}$, CF, and HR) and attenuated infarct size induced by I/R.

Reactive oxygen species (ROS) generation is identified as the major factors of I/R injury [19, 20]. Under normal circumstances, the ROS can be eliminated by antioxidant systems that include antioxidant enzymes, such as SOD [21]. Several studies demonstrated that oxidative stress in the heart caused by ischemia and reperfusion leads to cardiomyocyte death and myocardial injury. To further investigate the mechanism of cardioprotective effect of LFAE, an experiment was

performed to examine whether LFAE affected the changes in MDA level and SOD activity induced by I/R. The present results illuminated that LFAE protected against myocardial I/R-induced injury, accompanied by the attenuation of MDA production and enhancement of SOD activity indicating that one of the mechanisms of the cardioprotection of LFAE was associated with its antioxidant effects.

4. Conclusions

In the present investigation, administration of LFAE significantly enhanced the resumer of I/R-altered cardiac function by blunting the reduction of left ventricular developed pressure (LVDP), maximum up/down rate of left ventricular pressure ($\pm dp/dt_{max}$), and coronary flow (CF) decreased by I/R injury. Also, LFAE treatment resulted in significant modulation of cardioprotection content, the SOD activity and MDA level. Therefore, it can be concluded that the aqueous extract of lavender flower possesses obvious protective effects on myocardial I/R injury, which may be concerned with the improvement of myocardial oxidative stress states.

Conflict of Interests

No conflicts of interests are declared by the authors.

Acknowledgments

This study was supported by the Natural Science Foundation of Shandong Province (no. ZR2011HL013) to Dong Wang and the Xinjiang Production and Construction Corps Fund for Distinguished Young Scientists (2011CD006).

References

[1] P. A. Grace, "Ischaemia-reperfusion injury," *British Journal of Surgery*, vol. 81, no. 5, pp. 637–647, 1994.

[2] H. Inafuku, Y. Kuniyoshi, S. Yamashiro et al., "Determination of oxidative stress and cardiac dysfunction after ischemia/reperfusion injury in isolated rat hearts," *Annals of Thoracic and Cardiovascular Surgery*, vol. 19, no. 3, pp. 186–194, 2013.

[3] J. J. Ley, R. Prado, J. Q. Wei, N. H. Bishopric, D. A. Becker, and M. D. Ginsberg, "Neuroprotective antioxidant STAZN protects against myocardial ischemia/reperfusion injury," *Biochemical Pharmacology*, vol. 75, no. 2, pp. 448–456, 2008.

[4] Q. Yang, K. Yang, and A. Li, "microRNA-21 protects against ischemia-reperfusion and hypoxia-reperfusion-induced cardiocyte apoptosis via the phosphatase and tensin homolog/Akt-dependent mechanism," *Molecular Medicine Reports*, vol. 9, no. 6, pp. 2213–2220, 2014.

[5] M. Khan, S. Varadharaj, L. P. Ganesan et al., "C-phycocyanin protects against ischemia-reperfusion injury of heart through involvement of p38 MAPK and ERK signaling," *The American Journal of Physiology—Heart and Circulatory Physiology*, vol. 290, no. 5, pp. H2136–H2145, 2006.

[6] J. J. Martindale and J. M. Metzger, " Uncoupling of increased cellular oxidative stress and myocardial ischemia reperfusion injury by directed sarcolemma stabilization," *Journal of Molecular and Cellular Cardiology*, vol. 67, pp. 26–37, 2014.

[7] D. K. Das and N. Maulik, "Antioxidant effectiveness in ischemia-reperfusion tissue injury," *Methods in Enzymology*, vol. 233, pp. 601–610, 1994.

[8] G. Chang, P. Zhang, L. Ye et al., "Protective effects of sitagliptin on myocardial injury and cardiac function in an ischemia/reperfusion rat model," *European Journal of Pharmacology*, vol. 718, no. 1–3, pp. 105–113, 2013.

[9] G. Woronuk, Z. Demissie, M. Rheault, and S. Mahmoud, "Biosynthesis and therapeutic properties of oil constituents," *Planta Medica*, vol. 77, no. 1, pp. 7–15, 2011.

[10] S. Sosa, G. Altinier, M. Politi, A. Braca, I. Morelli, and R. Della Loggia, "Extracts and constituents of Lavandulamultifida with topical anti-inflammatory activity," *Phytomedicine*, vol. 12, no. 4, pp. 271–277, 2005.

[11] B. Blažeković, S. Vladimir-Knežević, A. Brantner, and M. B. Štefan, "Evaluation of antioxidant potential of Lavandula x intermedia Emeric ex Loisel. "Budrovka": a comparative study with L. angustifolia Mill," *Molecules*, vol. 15, no. 9, pp. 5971–5987, 2010.

[12] M. Adaszyńska, M. Swarcewicz, M. Dzięcioł, and A. Dobrowolska, "Comparison of chemical composition and antibacterial activity of lavender varieties from Poland," *Natural Product Research: Formerly Natural Product Letters*, vol. 27, no. 16, pp. 1497–1501, 2013.

[13] M. Hancianu, O. Cioanca, M. Mihasan, and L. Hritcu, "Neuroprotective effects of inhaled lavender oil on scopolamine-induced dementia via anti-oxidative activities in rats," *Phytomedicine*, vol. 20, no. 5, pp. 446–452, 2013.

[14] L. R. Chioca, M. M. Ferro, I. P. Baretta et al., "Anxiolytic-like effect of lavender essential oil inhalation in mice: participation of serotonergic but not GABAA/benzodiazepine neurotransmission," *Journal of Ethnopharmacology*, vol. 147, no. 2, pp. 412–418, 2013.

[15] J. L. Zweier, J. Fertmann, and G. Wei, "Nitric oxide and peroxynitrite in postischemic myocardium," *Antioxidants & Redox Signaling*, vol. 3, no. 1, pp. 11–22, 2001.

[16] D. J. Bester, K. Kupai, T. Csont et al., "Dietary red palm oil supplementation reduces myocardial infarct size in an isolated perfused rat heart model," *Lipids in Health and Disease*, vol. 9, article 64, 2010.

[17] R. Ferrera, S. Benhabbouche, J. C. Bopassa, B. Li, and M. Ovize, "One hour reperfusion is enough to assess function and infarct size with ttc staining in langendorff rat model," *Cardiovascular Drugs and Therapy*, vol. 23, no. 4, pp. 327–331, 2009.

[18] A. Z. Xia, Z. Xue, W. Wang et al., "Naloxone postconditioning alleviates rat myocardial ischemia-reperfusion injury by inhibiting JNK activity," *The Korean Journal of Physiology and Pharmacology*, vol. 18, pp. 67–72, 2014.

[19] H. Lee, E. H. Ko, M. Lai et al., "Delineating the relationships among the formation of oxygen species, cell membrane instability and innate autoimmunity in intestinal reperfusion," *Molecular Immunology*, vol. 58, no. 2, pp. 151–159, 2014.

[20] S. Ma, Z. Zhang, F. Yi et al., "Protective effects of low-frequency magnetic fields on cardiomyocytesfrom ischemia reperfusion injury via ROS and NO/$ONOO^-$," *Oxidative Medicine and Cellular Longevity*, vol. 2013, Article ID 529173, 9 pages, 2013.

[21] J. M. McCord, "Oxygen-derived free radicals in postischemic tissue injury," *The New England Journal of Medicine*, vol. 312, no. 3, pp. 159–163, 1985.

Hindawi Publishing Corporation
Journal of Chemistry
Volume 2014, Article ID 373872, 9 pages
http://dx.doi.org/10.1155/2014/373872

Research Article

Neuroprotective Activity of Water Soluble Extract from *Chorispora bungeana* against Focal Cerebral Ischemic/Reperfusion Injury in Mice

Ya-Xuan Sun,[1,2] Ting Liu,[3] Xue-Ling Dai,[1] Ya-Bo Li,[4] Yu-Yao Li,[4] Hua Zhang,[4] and Li-Zhe An[4]

[1] *Beijing Key Laboratory of Bioactive Substances and Functional Foods, Beijing Union University, Beijing 100191, China*
[2] *Cold and Arid Regions Environmental and Engineering Research Institute, Chinese Academy of Sciences, Lanzhou 730000, China*
[3] *School of Pharmacy, Shihezi University, Shihezi 832002, China*
[4] *Key Laboratory of Arid and Grassland Agroecology (Ministry Education), School of Life Sciences, Lanzhou University, Lanzhou 730000, China*

Correspondence should be addressed to Li-Zhe An; lizhean@lzu.edu.cn

Received 4 April 2014; Revised 3 June 2014; Accepted 4 June 2014; Published 23 June 2014

Academic Editor: Qiusheng Zheng

The purpose of the present study was to clarify whether the water extract of *Chorispora bungeana* was an antioxidant agent against cerebral ischemia/reperfusion (I/R). Our results showed that water extract of *Chorispora bungeana* treatment significantly reduced neurological deficit scores, infarct size, MDA and carbonyl contents, and GSH/GSSG ratio compared with the model control group. After being treated by *Chorispora bungeana*, SOD, CAT, and GSH-Px activities remarkably increased. *Chorispora bungeana* treatment also improved 8-OHdG expression and cell apoptosis. Our findings indicated that the water extract of *Chorispora bungeana* possesses neuroprotective effect which is most likely achieved by antioxidant and antiapoptotic activities.

1. Introduction

Stroke is one of the leading causes of disability and death with astronomical financial repercussions on health systems, and about 16 million strokes take place and cause a total of 5.7 million deaths in the world ever year. The global mortality is supposed to rise to 6.5 million in 2015 and to 7.8 million in 2030 [1, 2]. It is therefore urgent to develop effective therapies for stroke.

Cerebral ischemia is the most common type of stroke accounting for 88% of cases and it is reported that cerebral ischemia results in a cascade of cellular and molecular events including oxidative stress, excitotoxicity, calcium overlord, neuroinflammation, and apoptosis [3]. Reperfusion is a good measure for dealing with ischemia, but the beneficial effects of reperfusion may be in part reversed by the occurrence of reperfusion injury [4].

Oxidative stress was suggested to be implicating in the pathogenesis of cerebral ischemia/reperfusion (I/R) injury. Formation of reactive oxygen species (ROS) mainly includes the arachidonic acid pathway, the mitochondrial chain respiratory chain, the oxidation of xanthine, and hypoxanthine by xanthine oxidase and NADPH-oxidases [5, 6]. The brain is sensitive to oxidative stress because of relative low level of antioxidant enzyme and abundance of oxidizable substrates and transition metals [7].

Oxidative stress also induces neuronal apoptosis which is a feature found in cerebral ischemia/reperfusion [8–10]. Chen et al. [11] found that hydrogen peroxide, a major oxidant generated when oxidative stress occurs, leads to neuronal apoptosis in a concentration- and time-dependent manner. Wang et al. [12] suggested that hydrogen peroxide and nitric oxide synergistically induced neuronal apoptosis involving activation of p38 mitogen-activated protein kinase

and caspase-3. However, recovery of blood supply is necessary to remedy the compromised ischemic brain tissue. Antioxidants may reduce reperfusion-induced injury and extend the therapeutic window for thrombolysis [13–16].

Chorispora bungeana Fisch. And C.A. Mey (C. bungeana) is a rare alpine subnival plant species that inhabits periglacial regions in a severe low-temperature environment [17, 18]. The plant is a perennial herb belonging to the Brassicaceae-family [19]. Liu et al. [20] concluded that brassinosteroids could play the positive roles in alleviating chilling-induced oxidative damage by enhancing antioxidant defense system in suspension cultured cells of *Chorispora bungeana*. Guo et al. [21] found that a sequential and synergetic action between antioxidant enzymes such as superoxide dismutase, dehydroascorbate reductase, ascorbate peroxidase, and glutathione reductase, leading to a low antioxidation rate which contributes to retard lipid peroxidation and plays an important role in the resistance of suspension cultured cells of *Chorispora bungeana* to freezing temperatures. We presume that *Chorispora bungeana* may reduce oxidative stress induced by cerebral ischemia/reperfusion.

The present study was undertaken to evaluate the neuroprotection of water extract of *Chorispora bungeana* in cerebral ischemia/reperfusion with use of middle cerebral artery occlusion (MCAO) model and a series of oxidative stress markers.

2. Materials and Methods

2.1. Chemicals and Reagents. 2,3,5-Triphenyltetrazolium chloride, hypoxanthine, xanthine oxidase, catalase, 5,5′-dithiobis(2-nitrobenzoic acid), oxidized disulfide, and reduced glutathione were purchased from Sigma Chemical Co. (St. Louis, MO). 1,1,3,3-Tetramethoxypropane has been obtained from Fluka Chemical Co. (Ronkonkoma, NY). All other chemicals and reagents were of analytical grade.

2.2. Animals. Male ICR (26 ± 2 g) were obtained from Vital River Laboratories (Peking, China) for this study. Animals were housed in a room at a temperature of 24 ± 1°C and 12-h dark and light cycle with free access to standard food and water. The experimental protocol was approved by the Institutional Animal Care and Use Committee of National Institute Pharmaceutical Education and Research.

2.3. Chorispora bungeana Water Extract Preparation. A wild species of *Chorispora bungeana* was obtained by the method described by Fu et al. [22].

Freshly collected *Chorispora bungeana* whole plant was dried under shade and the dried material was milled to obtain a coarse powder. The powder was immersed in water for 1 h and then was extracted at boiling temperature for 1.5 h and repeated twice. The whole water extract was freeze-dried and redissolved in water at a concentration of 0.5 g/mL.

2.4. Drug Administration. Mice were randomly divided into six groups, each consisting of eight animals. Water extract of *Chorispora bungeana*, diluted with distilled water was fed by oral gavage every day at a fixed time for 5 d in 5, 2.5, and 1.25 g/kg (equivalent to the amount of crude drug) three different doses. The model control group and sham group were treated with vehicle orally for 5 d. Edaravone group was treated with Edaravone at a dose of 3 mg/kg for 5 d and served as positive control. On day 5, 1 h after the above treatments, the mice were subjected to the middle cerebral artery occlusion.

2.5. Transient Focal Cerebral Ischemic/Reperfusion Model. All mice were subjected to 2 h transient focal cerebral ischemia followed by 22 h reperfusion, using an intraluminal suture technique described by Longa et al. [23] and Ha et al. [24] with little modification. In brief, mice were anesthetized with chloral hydrate (400 mg/kg, i. p.). Midline incision was made on ventral side of mouse neck. The left common carotid artery (CCA), the external carotid artery (ECA), and the internal carotid artery (ICA) were carefully exposed and dissected away from adjacent muscles and nerves. Microvascular aneurysm clips were applied to the left CCA and the ICA. A coated filament was introduced into an arteriotomy hole, fed distally into the ICA and advanced about 12 mm from the carotid bifurcation. The ICA clamp was removed and focal cerebral ischemia started. After occlusion for 2 h, the filament was gently pulled out. The collar suture at the base of the ECA stump was tightened. The skin was closed, anesthesia discontinued, and the animals were returned to the prewarmed cages. Body temperature was maintained at 37 ± 0.5°C by lamp during the whole surgical procedures. Animals in sham control group underwent a neck dissection and coagulation of the external carotid artery, but no occlusion of middle cerebral artery.

2.6. Neurological Deficit Scores. After 22 h of reperfusion, an observer who was unaware of the identity of the groups evaluated the neurological deficits by using the method described by Longa et al. [23]. 0: no neurological deficit; 1: failure to extend the right forepaw fully; 2: circling to the right; 3: falling to the right; 4: no spontaneous walking with a depressed level of consciousness.

2.7. Infarct Size. Mice were decapitated after 22 h of reperfusion and these brains were quickly removed and sectioned coronally into five 1.5-mm-thick coronal sections. The sections were stained with 0.5% TTC at 37°C for 20 min. The stained brain sections were postfixed in 10% formalin solution and photographed with a digital camera and the infarct areas of each section were determined with the analysis of pixel counting by a computer program of Photoshop 6.0.

2.8. Biochemical Assays

2.8.1. Tissue Preparation. To measure of the contents of MDA and carbonyl, the activities of SOD, CAT, and GSH-Px, the ratio of GSH/GSSG, these mouse brains were weighed

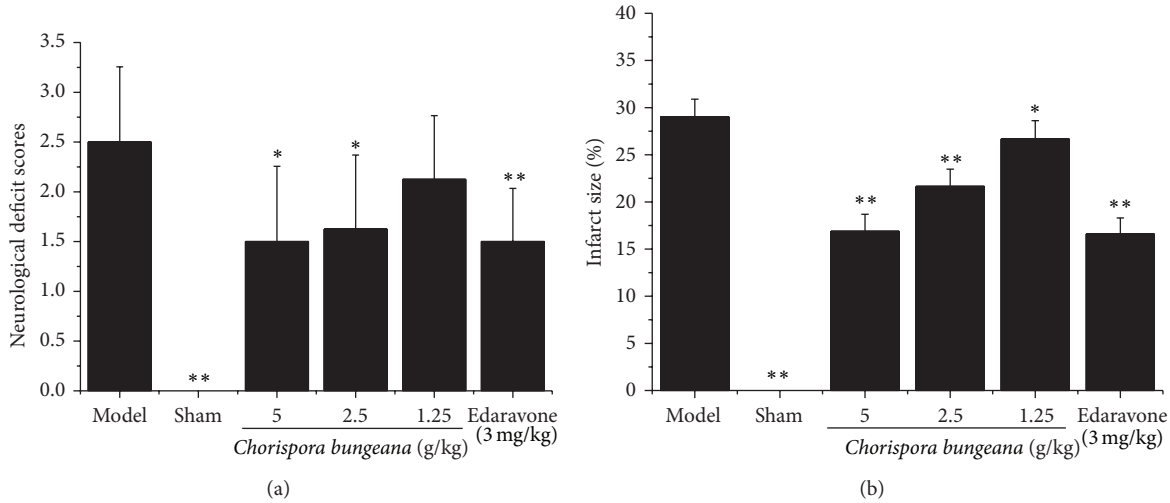

Figure 1: Effect of *Chorispora bungeana* water extract on neurological deficit scores (a) and infarct size (b) in mice subjected to cerebral ischemia/reperfusion. Data were expressed as mean ± S.M.E. Differences were considered significant at $P < 0.05$. $^{*}P < 0.05$ versus model group. $^{**}P < 0.01$ versus model group.

and homogenized with ice-cold normal saline and then centrifuged at 4624 ×g for 15 min at 4°C. The supernatant was used for bioassays. Protein content of the supernatant was determined by the method of Bradford [25] using bovine serum albumin as the protein standard.

2.8.2. GSH/GSSG Ratio. The ratio of GSH/GSSG was determined by a previously described method [26]. Briefly, T-GSH was determined basing on the 5,5-dithiobis (2-nitrobenzoic) acid (DTNB)-GSSG reductase recycling. GSSG was assayed by measuring 5-thio-2-nitrobenzoic acid (TNB) which was produced from the reaction of reduced GSH with DTNB. GSH level in brain tissue was calculated as the difference between T-GSH and GSSG.

2.8.3. Measurement of MDA Content. The MDA content was assayed in the brain tissue using a method as described by Cao et al. [27]. 1,1,3,3-Tetramethoxypropane was used as standard and the content of MDA was expressed as nmol/mg protein.

2.8.4. Measurement of Carbonyl Content. Carbonyl content was evaluated using the method according to Levine et al. [28]. The content of carbonyl was calculated by using the extinction coefficient of 22000 $M^{-1}cm^{-1}$/mg protein and expressed as nmol/mg protein.

2.8.5. Measurement of Antioxidant Enzyme Activities. SOD activity was measured as described by Jung et al. [29]. One unit of SOD activity was defined as the amount that shows 50% inhibition. SOD activity was expressed as U/mg protein.

CAT activity was evaluated according to the method of Campo et al. [30]. One unit of CAT activity was defined as the amount of CAT required to decompose 1 μmol/L of hydrogen peroxide in min. CAT activity was expressed as U/mg protein.

GSH-Px activity was determined by the method of Jagetia et al. [31]. One unit of GSH-Px activity was defined as the GSH-Px in 1 mg protein that led to the decrease of 1 μmol/L GSH in the reactive system per minute. GSH-Px activity was expressed as U/mg protein.

2.9. Immunohistochemistry Assay. Animals were overdosed with anesthetic and perfused with 4% paraformaldehyde in 0.1 M phosphate buffer solution (PBS, pH = 7.4) after 22 h of reperfusion. Brains were removed and further fixed in 4% paraformaldehyde at 4°C for 24 h and then cut into equally spaced blocks. Paraffin-embedded blocks were cut into a series of 5-μm-thick slices.

8-Hydroxyl-deoxyguanosine (8-OHdG) immunohistochemistry was used to identify oxidized DNA and performed by the method of Wang et al. [32]. In brief, deparaffinized brain sections were immunostained with 5 μg/mL mouse anti-8-OHdG antibody followed by 0.5% goat anti-mouse IgG labeled with horseradish peroxidase.

Cell apoptosis was observed by the terminal deoxynucleotidyl transferase-mediated Dutp-biotin nick end labeling (TUNEL) assay. In brief, brain sections were deparaffinized and rehydrated followed by incubating with 20 μg/mL proteinase K in 0.01 M Tris-HCl (pH = 7.4) and permeabilized in a solution which contains 0.1% Triton-X 100 and 0.1% sodium citrate. Then these sections were incubated in TUNEL-reaction mixture containing terminal deoxynucleotidy transferase.

2.10. Statistical Analysis. Data were expressed as mean ± S.M.E. Statistical analysis was evaluated with one way

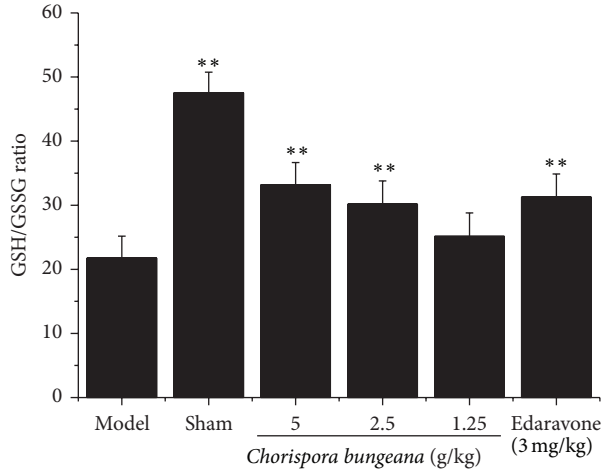

Figure 2: Effect of *Chorispora bungeana* water extract on GSH/GSSG ratio in mice subjected to cerebral ischemia/reperfusion. Data were expressed as mean ± S.M.E. Differences were considered significant at $P < 0.05$. $^{*}P < 0.05$ versus model group. $^{**}P < 0.01$ versus model group.

analysis of variance (ANOVA) and followed by a Student-Newman-Keuls (SNK) test for multiple comparisons. $P < 0.05$ was regarded as statistically significant.

3. Results

3.1. Effect of Chorispora bungeana Water Extract on Neurological Deficit Scores and Infarct Size. After 22 h of reperfusion, neurological deficit scores and infarct size in ischemic/reperfusion mice were obviously higher than those of the sham control mice, indicating that we had successfully established the cerebral ischemic/reperfusion model. Treatment with *Chorispora bungeana* water extract significantly decreased neurological deficit scores and infarct size as compared to the model control group (Figures 1(a) and 1(b)).

3.2. Effect of Chorispora bungeana Water Extract on GSH/GSSG. The GSH/GSSG ratio in the mouse brain tissue, a typically of oxidative stress, was markedly lower in the model control group as compared to the sham control group. As shown in Figure 2, there was a significant increase in the ratio of GSH/GSSG in the *Chorispora bungeana* water extract treatment groups (5 and 2.5 g/kg) compared with the model control group ($P < 0.01$).

3.3. Effect of Chorispora bungeana Water Extract on MDA and Carbonyl Contents. MDA and carbonyl are the two main products of oxidative damage. Figure 3 showed that MDA and carbonyl contents were much higher in the model control group than those in the sham control group. The treatment with *Chorispora bungeana* water extract evidently reduced the contents of MDA and carbonyl in brain tissue compared with the model control group.

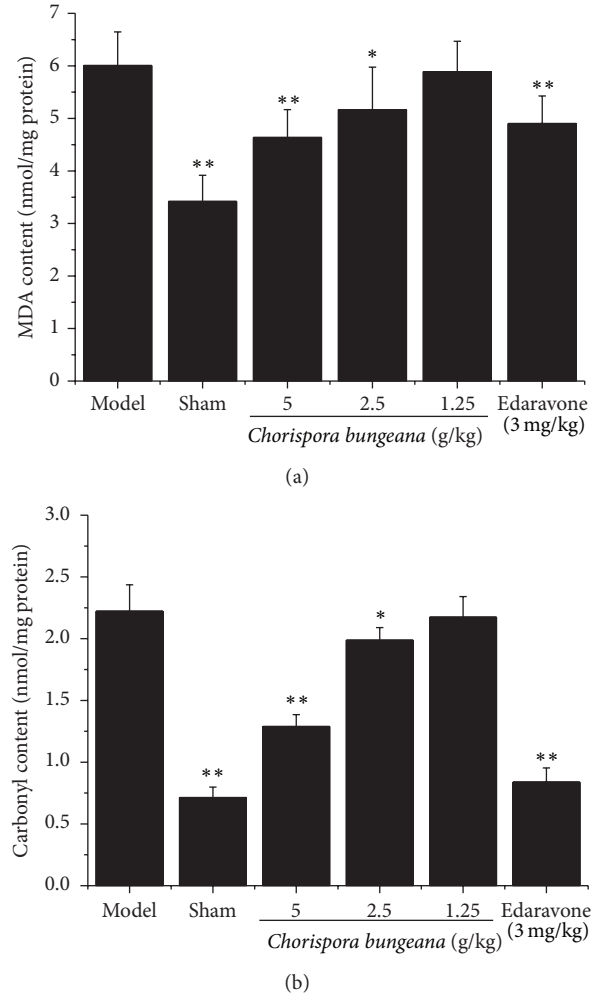

Figure 3: Effect of *Chorispora bungeana* water extract on MDA (a) and carbonyl (b) in mice subjected to cerebral ischemia/reperfusion. Data were expressed as mean ± S.M.E. Differences were considered significant at $P < 0.05$. $^{*}P < 0.05$ versus model group. $^{**}P < 0.01$ versus model group.

3.4. Effect of Chorispora bungeana Water Extract on Antioxidant Enzyme Activities. Table 1 showed that the activities of SOD, CAT, and GSH-Px were obviously decreased in model control group as compared to the sham control group and attenuated significantly by treatment of *Chorispora bungeana* water extract (5 and 2.5 g/kg) compared with the control group ($P < 0.05$).

3.5. Effect of Chorispora bungeana Water Extract on 8-OHdG Expression. The expression of 8-OHdG obviously increased in the model control group as compared to the sham control group. Treatment of *Chorispora bungeana* water extract markedly weakened 8-OHdG compared with the model control group (Figure 4, Table 2).

3.6. Effect of Chorispora bungeana Water Extract on Apoptosis. Very few TUNEL positive cells were found in normal mouse brain tissue and the number of TUNEL positive cells was

Table 1: Effect of *Chorispora bungeana* water extract on antioxidant enzyme activities in mice subjected to cerebral ischemia/reperfusion.

Group	Dose (g/kg)	SOD (U/mg protein)	CAT (U/mg protein)	GSH-Px (U/mg protein)
Model	/	62.95 ± 6.72	6.11 ± 0.61	684.53 ± 83.57
Sham	/	81.83 ± 4.09**	8.32 ± 0.47**	1054.06 ± 49.03**
Chorispora bungeana	5	79.04 ± 6.84**	7.39 ± 0.60**	961.56 ± 67.77**
Chorispora bungeana	2.5	71.51 ± 5.36*	6.95 ± 0.53*	798.45 ± 78.41*
Chorispora bungeana	1.25	63.41 ± 6.97	6.73 ± 0.58	724.03 ± 60.32
Edaravone	0.003	78.88 ± 5.23**	7.88 ± 0.57**	912.43 ± 61.37**

Data were expressed as mean ± S.M.E. Differences were considered significant at $P < 0.05$. *$P < 0.05$ versus model group. **$P < 0.01$ versus model group.

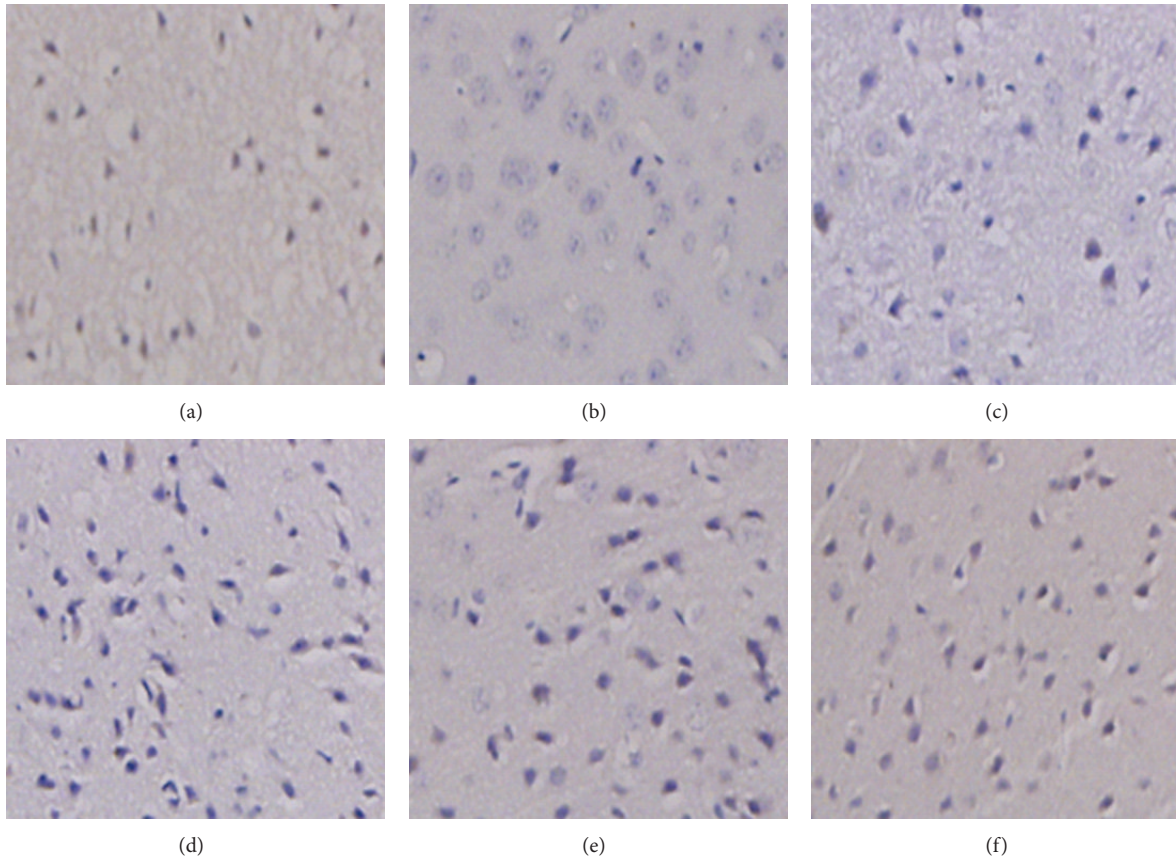

Figure 4: Effect of *Chorispora bungeana* water extract on 8-OHdG expression in mice subjected to cerebral ischemia/reperfusion. The nucleus of positive expressed cell is brown colored. (a) Model group; (b) Sham group; (c) Edaravone-treatment group (3 mg/kg); (d) *Chorispora bungeana*-treatment group (5 g/kg); (e) *Chorispora bungeana*-treatment group (2.5 g/kg); (f) *Chorispora bungeana*-treatment group (1.25 g/kg).

significantly increased by ischemia/reperfusion. Administration of *Chorispora bungeana* water extract markedly reduced TUNEL positive cells as compared to the model control group (Figure 5, Table 2).

4. Discussion

The present study reported the neuroprotective effect of *Chorispora bungeana* water extract in terms of oxidative stress markers and apoptosis in cerebral ischemic/reperfusion mouse brain for the first time. We found that water extract of *Chorispora bungeana* prevents brain from ischemic/reperfusion damage, as indicated by the improved recovery of neurological function, decreases in infarct size and oxidative stress, and increases in antioxidant enzyme activities and reduction in apoptosis.

We set up cerebral ischemic/reperfusion model with intraluminal thread insertion method in mice and tested

Table 2: Effect of *Chorispora bungeana* water extract on 8-OHdG expression and cell apoptosis in mice subjected to cerebral ischemia/reperfusion.

Group	Dose (g/kg)	8-OHdG positive cells	TUNEL positive cells
Model	/	20.88 ± 3.31	21.63 ± 4.21
Sham	/	2.13 ± 1.25**	2.25 ± 1.04**
Chorispora bungeana	5	16.25 ± 2.60**	17.13 ± 3.40*
Chorispora bungeana	2.5	17.13 ± 3.17*	18.25 ± 3.99
Chorispora bungeana	1.25	19.88 ± 3.83	19.50 ± 4.41
Edaravone	0.003	15.38 ± 3.42**	17.25 ± 3.24*

Data were expressed as mean ± S.M.E. Differences were considered significant at $P < 0.05$. *$P < 0.05$ versus model group. **$P < 0.01$ versus model group.

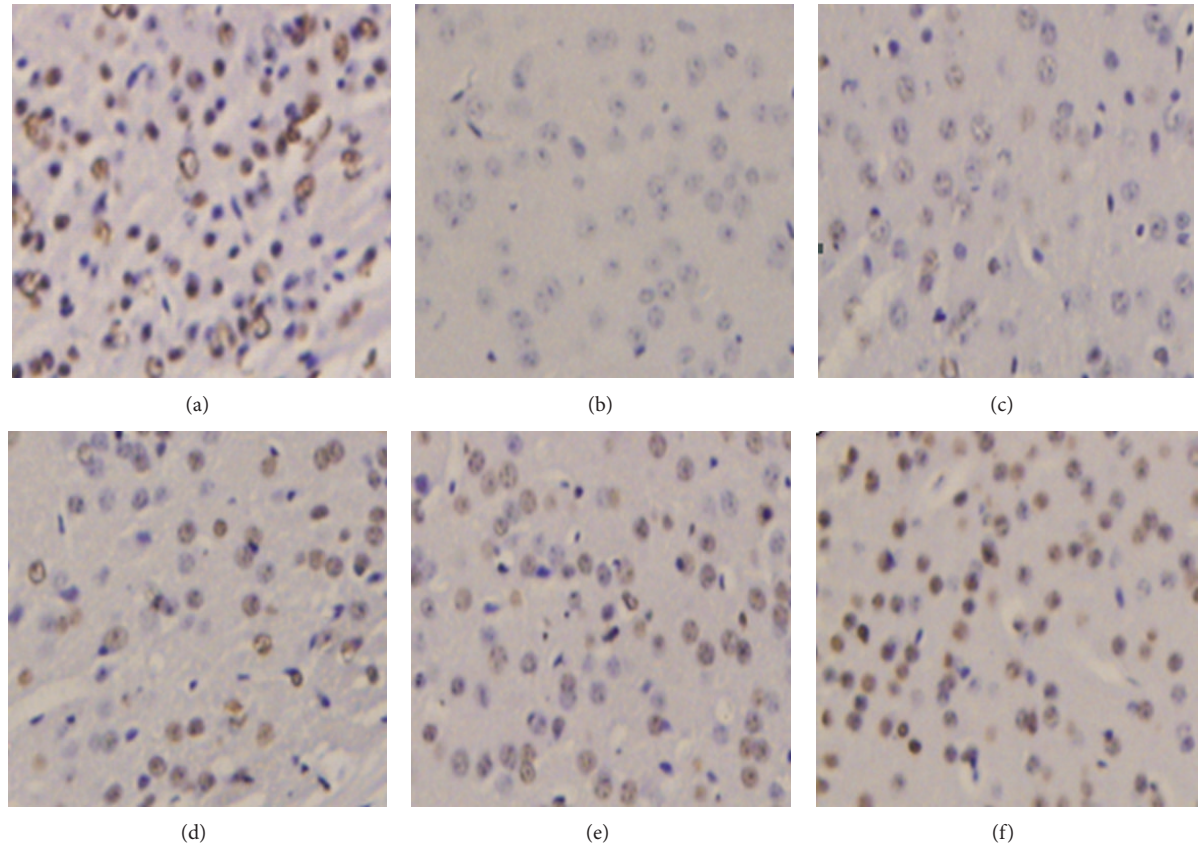

Figure 5: Effect of *Chorispora bungeana* water extract on cell apoptosis in mice subjected to cerebral ischemia/reperfusion. Nucleus has brown granules were positive cell. (a) Model group; (b) sham group; (c) Edaravone-treatment group (3 mg/kg); (d) *Chorispora bungeana*-treatment group (5 g/kg); (e) *Chorispora bungeana*-treatment group (2.5 g/kg); (f) *Chorispora bungeana*-treatment group (1.25 g/kg).

whether the model was successfully established by means of assaying the neurological deficit scores and infarct size. The mice showed visible neurological deficits and brain infarction in model control group. Treatment of *Chorispora bungeana* water extract reducing the neurological deficit scores and infarct size in a dose-dependent manner demonstrated that water extract of *Chorispora bungeana* was provided with neuroprotective activity against cerebral ischemic/reperfusion injury.

Then we determined whether brain was in oxidative stress status after 22 h of reperfusion. The ratio of GSH/GSSG is proposed to be a sensitive index of oxidative stress [33, 34]. Our data showed that the ratio of GSH/GSSG was decreased in model control group, but the decrease was attenuated by treatment of *Chorispora bungeana* water extract. That indicated that *Chorispora bungeana* water extract could release oxidative stress in ischemic/reperfusion brain tissue.

Reactive oxygen species (ROS) contain one or more unpaired electrons in their outer orbit and are highly reactive play key roles in organism physiology and pathophysiology [35–38]. Excessive production of ROS may depress cell membrane properties and cause oxidative damage to lipids, proteins, and DNA that may make them nonfunctional because of brain tissue contains large amount of unsaturated fatty

acids and catecholamines after cerebral ischemia and particularly reperfusion [6, 39, 40]. Malondialdehyde (MDA), carbonyl, and 8-hydroxy-2′-deoxyguanosine (8-OHdG) are representative markers of oxidative damage of brain [39]. We measured the MDA and carbonyl contents by using of a spectrocolorimetric assay and detected the 8-OHdG expression by immunohistochemistry. The water extract of *Chorispora bungeana* effectively reduced the content of MDA and carbonyl; the expression of 8-OHdG revealed that it could lighten oxidative damage induced by cerebral ischemia/reperfusion.

The ROS is maintained in an appropriate level by the endogenous antioxidant enzymes such as superoxide dismutase (SOD), catalase (CAT), and glutathione peroxidase (GSH-Px) under normal physiological conditions [6, 41]. SOD catalyzes the dismutation of superoxide anions to hydrogen peroxide and molecular oxygen and CAT together with GSH-Px eliminates hydrogen and molecular oxygen [42]. But these antioxidant enzyme activities were reported to decrease during cerebral ischemia/reperfusion [43, 44]. The present study showed that the reduced activities of SOD, CAT, and GSH-Px in ischemic/reperfusion mice were significantly attenuated in *Chorispora bungeana* water extract-treated group when compared with the model control group.

Broughton et al. [45] pointed out that cerebral ischemia triggers two main pathways of apoptosis. One originates from mitochondrial release of cytochrome c and another originates from the activation of cell surface death receptors. Fujimura et al. [46] agreed that ROS mediated the mitochondrial signaling pathway that may result in apoptosis following cerebral ischemia. In order to determine the antiapoptotic activity of *Chorispora bungeana* water extract, we evaluated the apoptosis with terminal deoxynucleotidyl transferase mediated d UTP-biotin nick end labeling (TUNEL). *Chorispora bungeana* water extract was proved to be able to inhibit cell apoptosis in our study.

In summary, our study demonstrated that the water extractof *Chorispora bungeana* could effectively attenuate brain injury in focal cerebral ischemia/reperfusion. The neuroprotective activity was associated with inhibiting oxidative stress and apoptosis. Chorispora bungeana may have the potential to cure nervous system diseases as an unusual alpine subnival plant and more pharmacodynamics research work needs to be done.

Conflict of Interests

The authors declare that there is no conflict of interests regarding the publication of this paper.

Acknowledgments

This study was supported by the National Outstanding Youth Foundation of China (30625008), the National High Technology Research and Development Program (863 Program, 2007AA021401), National Basic Research Program of China (973, 2007CB108902), International Cooperation Program of the Ministry of Science and Technology of China (2009DFA61060), the Major Project of Cultivating New Varieties of Transgenic Organisms (2008ZX08009-003), and the National Natural Science Foundation (30900172). This work was supported by Grants the National Basic Research Program of China (973 Program 2013CB429904); the Key Program of National Nature Science Foundation of China (31230014); the Funding Project for Academic Human Resources Development in Institutions of Higher Learning Under the Jurisdiction of Beijing Municipality [PHR201107150, PHR201108422].

References

[1] K. Strong, C. Mathers, and R. Bonita, "Preventing stroke: saving lives around the world," *The Lancet Neurology*, vol. 6, no. 2, pp. 182–187, 2007.

[2] C. L. Allen and U. Bayraktutan, "Oxidative stress and its role in the pathogenesis of ischaemic stroke," *International Journal of Stroke*, vol. 4, no. 6, pp. 461–470, 2009.

[3] E. Candelario-Jalil, "Injury and repair mechanisms in ischemic stroke: considerations for the development of novel neurotherapeutics," *Current Opinion in Investigational Drugs*, vol. 10, no. 7, pp. 644–654, 2009.

[4] N. Tapuria, Y. Kumar, M. M. Habib, M. A. Amara, A. M. Seifalian, and B. R. Davidson, "Remote ischemic preconditioning: a novel protective method from ischemia reperfusion injury," *Journal of Surgical Research*, vol. 150, no. 2, pp. 304–330, 2008.

[5] G. Fiskum, A. N. Murphy, and M. F. Beal, "Mitochondria in neurodegeneration: acute ischemia and chronic neurodegenerative diseases," *Journal of Cerebral Blood Flow and Metabolism*, vol. 19, no. 4, pp. 351–369, 1999.

[6] I. Margaill, M. Plotkine, and D. Lerouet, "Antioxidant strategies in the treatment of stroke," *Free Radical Biology and Medicine*, vol. 39, no. 4, pp. 429–443, 2005.

[7] J. Lehotský, R. Murín, A. Strapková, A. Uríková, Z. Tatarková, and P. Kaplán, "Time course of ischemia/reperfusion-induced oxidative modification of neural proteins in rat forebrain," *General Physiology and Biophysics*, vol. 23, no. 4, pp. 401–415, 2004.

[8] C. Cheng, S. Su, N. Tang, T. Ho, S. Chiang, and C. Hsieh, "Ferulic acid provides neuroprotection against oxidative stress-related apoptosis after cerebral ischemia/reperfusion injury by inhibiting ICAM-1 mRNA expression in rats," *Brain Research*, vol. 1209, pp. 136–150, 2008.

[9] C. Pekcetin, M. Kiray, B. U. Ergur et al., "Carnosine attenuates oxidative stress and apoptosis in transient cerebral ischemia in rats," *Acta Biologica Hungarica*, vol. 60, no. 2, pp. 137–148, 2009.

[10] K. Niizuma, H. Yoshioka, H. Chen et al., "Mitochondrial and apoptotic neuronal death signaling pathways in cerebral ischemia," *Biochimica et Biophysica Acta*, vol. 1802, no. 1, pp. 92–99, 2010.

[11] L. Chen, L. Liu, J. Yin, Y. Luo, and S. Huang, "Hydrogen peroxide-induced neuronal apoptosis is associated with inhibition of protein phosphatase 2A and 5, leading to activation of MAPK pathway," *International Journal of Biochemistry and Cell Biology*, vol. 41, no. 6, pp. 1284–1295, 2009.

[12] J. Wang, A. Y. C. Shum, and Y. Ho, "Oxidative neurotoxicity in rat cerebral cortex neurons: synergistic effects of H_2O_2 and NO on apoptosis involving activation of p38 mitogen-activated

protein kinase and caspase-3," *Journal of Neuroscience Research*, vol. 72, no. 4, pp. 508–519, 2003.

[13] Y. Gürsoy-Özdemir, A. Can, and T. Dalkara, "Reperfusion-induced oxidative/nitrativie injury to neurovascular unit after focal cerebral ischemia," *Stroke*, vol. 35, no. 6, pp. 1449–1453, 2004.

[14] V. M. Chandrashekhar, V. L. Ranpariya, S. Ganapaty, A. Parashar, and A. A. Muchandi, "Neuroprotective activity of Matricaria recutita Linn against global model of ischemia in rats," *Journal of Ethnopharmacology*, vol. 127, no. 3, pp. 645–651, 2010.

[15] T. Yu, Q. Chen, Z. Chen, Z. Xiong, and M. Ye, "Protective effects of total flavones of rhododendra against global cerebral ischemia reperfusion injury," *The American Journal of Chinese Medicine*, vol. 37, no. 5, pp. 877–887, 2009.

[16] C. Elango, K. S. Jayachandaran, and S. Niranjali Devaraj, "Hawthorn extract reduces infarct volume and improves neurological score by reducing oxidative stress in rat brain following middle cerebral artery occlusion," *International Journal of Developmental Neuroscience*, vol. 27, no. 8, pp. 799–803, 2009.

[17] J. Wu, T. Qu, S. Chen, Z. Zhao, and L. An, "Molecular cloning and characterization of a γ-glutamylcysteine synthetase gene from Chorispora bungeana," *Protoplasma*, vol. 235, no. 1–4, pp. 27–36, 2009.

[18] Y. Shi, L. An, M. Zhang, C. Huang, H. Zhang, and S. Xu, "Regulation of the plasma membrane during exposure to low temperatures in suspension-cultured cells from a cryophyte (*Chorispora bungeana*)," *Protoplasma*, vol. 232, no. 3-4, pp. 173–181, 2008.

[19] J. Wang, L. An, R. Wang et al., "Plant regeneration of *Chorispora bungeana* via somatic embryogenesis," *Plant*, vol. 42, no. 2, pp. 148–151, 2006.

[20] Y. Liu, Z. Zhao, J. Si, C. Di, J. Han, and L. An, "Brassinosteroids alleviate chilling-induced oxidative damage by enhancing antioxidant defense system in suspension cultured cells of *Chorispora bungeana*," *Plant Growth Regulation*, vol. 59, no. 3, pp. 207–214, 2009.

[21] F. Guo, M. Zhang, Y. Chen et al., "Relation of several antioxidant enzymes to rapid freezing resistance in suspension cultured cells from alpine Chorispora bungeana," *Cryobiology*, vol. 52, no. 2, pp. 241–250, 2006.

[22] X. Fu, J. Chang, L. An et al., "Association of the cold-hardiness of *Chorispora bungeana* with the distribution and accumulation of calcium in the cells and tissues," *Environmental and Experimental Botany*, vol. 55, no. 3, pp. 282–293, 2006.

[23] E. Z. Longa, P. R. Weinstein, S. Carlson, and R. Cummins, "Reversible middle cerebral artery occlusion without craniectomy in rats," *Stroke*, vol. 20, no. 1, pp. 84–91, 1989.

[24] S. K. Ha, P. Lee, J. A. Park et al., "Apigenin inhibits the production of NO and PGE2 in microglia and inhibits neuronal cell death in a middle cerebral artery occlusion-induced focal ischemia mice model," *Neurochemistry International*, vol. 52, no. 4-5, pp. 878–886, 2008.

[25] M. M. Bradford, "A rapid and sensitive method for the quantitation of microgram quantities of protein utilizing the principle of protein dye binding," *Analytical Biochemistry*, vol. 72, no. 1-2, pp. 248–254, 1976.

[26] E. Candelario-Jalil, N. H. Mhadu, S. M. Al-Dalain, G. Martínez, and O. S. León, "Time course of oxidative damage in different brain regions following transient cerebral ischemia in gerbils," *Neuroscience Research*, vol. 41, no. 3, pp. 233–241, 2001.

[27] D. Cao, J. Xu, R. Xue, W. Zheng, and Z. Liu, "Protective effect of chronic ethyl docosahexaenoate administration on brain injury in ischemic gerbils," *Pharmacology Biochemistry and Behavior*, vol. 79, no. 4, pp. 651–659, 2004.

[28] R. L. Levine, D. Garland, C. N. Oliver et al., "Determination of carbonyl content in oxidatively modified proteins," *Methods in Enzymology*, vol. 186, pp. 464–478, 1990.

[29] H. Jung, J. H. Nam, J. Choi, K. Lee, and H. Park, "Antiinflammatory effects of chiisanoside and chiisanogenin obtained from the leaves of *Acanthopanax chiisanensi*s in the carrageenan- and Freund's complete adjuvant-induced rats," *Journal of Ethnopharmacology*, vol. 97, no. 2, pp. 359–367, 2005.

[30] G. M. Campo, A. Avenoso, S. Campo et al., "Hyaluronic acid and chondroitin-4-sulphate treatment reduces damage in carbon tetrachloride-induced acute rat liver injury," *Life Sciences*, vol. 74, no. 10, pp. 1289–1305, 2004.

[31] G. C. Jagetia, G. K. Rajanikant, S. K. Rao, and M. Shrinath Baliga, "Alteration in the glutathione, glutathione peroxidase, superoxide dismutase and lipid peroxidation by ascorbic acid in the skin of mice exposed to fractionated γ radiation," *Clinica Chimica Acta*, vol. 332, no. 1-2, pp. 111–121, 2003.

[32] Q. Wang, A. Y. Sun, A. Simonyi et al., "Oral administration of grape polyphenol extract ameliorates cerebral ischemia/reperfusion-induced neuronal damage and behavioral deficits in gerbils: comparison of pre- and post-ischemic administration," *Journal of Nutritional Biochemistry*, vol. 20, no. 5, pp. 369–377, 2009.

[33] D. P. Jones, "Redefining oxidative stress," *Antioxidants and Redox Signaling*, vol. 8, no. 9-10, pp. 1865–1879, 2006.

[34] D. P. Jones, "Redox potential of GSH/GSSG couple: assay and biological significance," *Methods in Enzymology*, vol. 348, pp. 93–112, 2002.

[35] N. Tuteja and R. Tuteja, "Unraveling DNA repair in human: molecular mechanisms and consequences of repair defect," *Critical Reviews in Biochemistry and Molecular Biology*, vol. 36, no. 3, pp. 261–290, 2001.

[36] M. Valko, D. Leibfritz, J. Moncol, M. T. D. Cronin, M. Mazur, and J. Telser, "Free radicals and antioxidants in normal physiological functions and human disease," *International Journal of Biochemistry and Cell Biology*, vol. 39, no. 1, pp. 44–84, 2007.

[37] C. Kohchi, H. Inagawa, T. Nishizawa, and G. Soma, "ROS and innate immunity," *Anticancer Research*, vol. 29, no. 3, pp. 817–822, 2009.

[38] M. Hultqvist, L. M. Olsson, K. A. Gelderman, and R. Holmdahl, "The protective role of ROS in autoimmune disease," *Trends in Immunology*, vol. 30, no. 5, pp. 201–208, 2009.

[39] A. Cherubini, C. Ruggiero, M. C. Polidori, and P. Mecocci, "Potential markers of oxidative stress in stroke," *Free Radical Biology and Medicine*, vol. 39, no. 7, pp. 841–852, 2005.

[40] N. Ogawa, "Free radicals and neural cell damage," *Rinshō Shinkeigaku*, vol. 34, no. 12, pp. 1266–1268, 1994.

[41] C. D. Kamat, S. Gadal, M. Mhatre, K. S. Williamson, Q. N. Pye, and K. Hensley, "Antioxidants in central nervous system diseases: preclinical promise and translational challenges," *Journal of Alzheimer's Disease*, vol. 15, no. 3, pp. 473–493, 2008.

[42] N. S. Dhalla, A. B. Elmoselhi, T. Hata, and N. Makino, "Status of myocardial antioxidants in ischemia-reperfusion injury," *Cardiovascular Research*, vol. 47, no. 3, pp. 446–456, 2000.

[43] S. Yousuf, S. Salim, M. Ahmad, A. S. Ahmed, M. A. Ansari, and F. Islam, "Protective effect of Khamira Abresham Uood Mastagiwala against free radical induced damage in focal cerebral ischemia," *Journal of Ethnopharmacology*, vol. 99, no. 2, pp. 179–184, 2005.

[44] M. M. Khan, A. Ahmad, T. Ishrat et al., "Rutin protects the neural damage induced by transient focal ischemia in rats," *Brain Research*, vol. 1292, pp. 123–135, 2009.

[45] B. R. S. Broughton, D. C. Reutens, and C. G. Sobey, "Apoptotic mechanisms after cerebral ischemia," *Stroke*, vol. 40, no. 5, pp. 331–339, 2009.

[46] M. Fujimura, T. Tominaga, and P. H. Chan, "Neuroprotective effect of an antioxidant in ischemic brain injury: involvement of neuronal apoptosis," *Neurocritical Care*, vol. 2, no. 1, pp. 59–66, 2005.

Hindawi Publishing Corporation
Journal of Chemistry
Volume 2014, Article ID 749047, 6 pages
http://dx.doi.org/10.1155/2014/749047

Research Article

Changes in Antioxidant Enzyme Activity and Transcript Levels of Related Genes in *Limonium sinense* Kuntze Seedlings under NaCl Stress

Xia Zhang, HaiBo Yin, ShiHua Chen, Jun He, and ShanLi Guo

Key Laboratory of Plant Molecular & Developmental Biology, College of Life Sciences, Yantai University, Yantai, Shandong 264005, China

Correspondence should be addressed to ShanLi Guo; gsl@ytu.edu.cn

Received 11 April 2014; Accepted 9 June 2014; Published 19 June 2014

Academic Editor: Wang Zhenhua

The halophyte *Limonium sinense* Kuntze is used in traditional Chinese medicine for clearing heat and for detoxification. To examine the detoxification and salt-tolerance mechanisms of this plant, we analyzed antioxidant enzyme activities and transcript levels of genes encoding antioxidant enzymes in *L. sinense* seedlings under salt stress (500 mmol/L NaCl). Catalase showed the largest increase in activity, peaking on day 4 of the 7-day NaCl treatment. Peroxidase and superoxide dismutase activities also increased, peaking on days 2 and 3 of the NaCl treatment, respectively. The activities of antioxidant enzymes decreased as the duration of the NaCl treatment extended. The transcript levels of genes encoding antioxidant enzymes were upregulated under NaCl stress. The peak in the *LsCAT* transcript level was earlier than the peaks in *LsAPX* and *LsGPX* transcript levels. The malondialdehyde content only slightly increased in *L. sinense* seedlings under NaCl stress. This was indicative of a low level of lipid peroxidation, consistent with the increased antioxidant enzyme activities and gene transcript levels. These results show that, under NaCl stress, the antioxidant system of *L. sinense* is activated and effectively scavenges reactive oxygen species. This reduces oxidative damage and allows the plant to maintain growth under NaCl stress.

1. Introduction

Salt in soils is the main environmental factor restricting the growth and productivity of agricultural crops [1]. Salt tolerance in plants is a complex process that involves changes in the structures of numerous tissues and organs and many physiological and biochemical processes [2]. In plants, salt stress results in increased generation of reactive oxygen species (ROS). These highly reactive substances can alter normal cellular metabolism via oxidative damage to membranes, proteins, and nucleic acids. They can also cause lipid peroxidation, denature proteins, and mutate DNA [3, 4].

Plants have developed a complex ROS-scavenging system to prevent sensitive cellular components from ROS-induced damage. This system comprises enzymatic and nonenzymatic antioxidants. The sum of the activities of all of the enzymes that make up the enzymatic antioxidant system represents the antioxidant capacity of plants. Catalase (CAT), peroxidase (POD), and superoxide dismutase (SOD) are important antioxidant enzymes that play key roles in eliminating superoxide (O_2^-) and hydrogen peroxide (H_2O_2).

Limonium sinense Kuntze is a perennial herb with strong tolerance to salt, aridity, and drought. This salt-secreting halophyte is used in traditional Chinese medicine for clearing heat and dampness, for hemostasis, and for detoxification. Its close relative, *Limonium gmelinii* (Wildl.) Kuntze, grows in salt meadows and has abundant salt glands on the adaxial and abaxial sides of the leaf [5]. The salt-tolerance mechanisms of *L. sinense* include its salt-secreting glands and its ability to compartmentalize ions in cells and regulate osmotic status. Early studies on this species focused on the structure of its salt glands and on methods for its tissue culture, rapid propagation, and artificial cultivation [6, 7]. Less attention has been paid to the physiological mechanisms of stress resistance in *L. sinense*. The aim of this study was to investigate ROS scavenging and the protective effects of the antioxidant

enzyme system in *L. sinense* seedlings by detecting changes in CAT, POD, and SOD activities and in the transcript levels of the genes encoding these enzymes, under NaCl stress.

2. Materials and Methods

2.1. Plant Material and Growth Conditions. Seeds of *L. sinense* were obtained from the halophyte garden of Dongying City, Shandong Province. Seeds were germinated in a growth chamber at 20°C. After 20 days of growth, seedlings were transplanted into soil in pots (5 seedlings/pot) and then grown in a greenhouse for 50 days under the following conditions: 12 h light/12 h dark photoperiod, 25°C, and 65% relative humidity.

2.2. Experimental Design. In each pot, seedlings were treated with 50 mL 500 mmol/L NaCl solution for 0, 1, 2, 3, 4, 5, 6, and 7 days. On each sampling day, the leaves of three seedlings in each group were harvested, weighed to determine fresh weight, frozen in liquid nitrogen, and then used for enzyme activity assays and gene expression analyses. All assays and measurements were conducted in triplicate.

2.3. Determination of Enzyme Activity and Isoenzyme Composition. The activities of CAT, POD, and SOD were assayed as described by Gao et al. [8]. Malondialdehyde (MDA) content was determined using the thiobarbituric acid reaction [9]. All values shown are the mean values of three assays. Differences between mean values of NaCl-treated samples and untreated controls were considered significant at $P < 0.05$. The isoform composition of CAT, POD, and SOD was determined as described by El-Mashad and Mohamed [10].

2.4. Determination of Gene Expression Level. RNA isolation, reverse transcription, and real-time quantitative PCR (qPCR) were conducted as described by Zhang et al. [11]. Sequence information was based on sequences in the *Limonium sinense* plasmid cDNA library. The qPCR primers used to amplify genes encoding catalase (*LsCAT*), ascorbate peroxidase (*LsAPX*), glutathione peroxidase (*LsGPX*), and actin (*LsActin*) were designed using Primers3 (http://bioinfo.ut.ee/primer3-0.4.0/). The sequences were as follows (F for forward, R for reverse).

The primers for *LsCAT* (BXC35):

F: 5′-CACATCCTCCTGTTGTTTCGGGTAG-3′;

R: 5′-ACAGGCTCAACGTCAGACCAACC-3′;

The primers for *LsAPX* (BXC1267):

F: 5′-TCCAAGGACCCTCAAAGCCAG-3′;

R: 5′-CCCTGACGCAAAGAAAGGAAATG-3′;

The primers for *LsGPX* (BXC0933):

F: 5′-ATGAAGGAAAGCAACGGGAAGAC-3′;

R: 5′-AGTAGCCAAGCCAAACAGATCAGAC-3′;

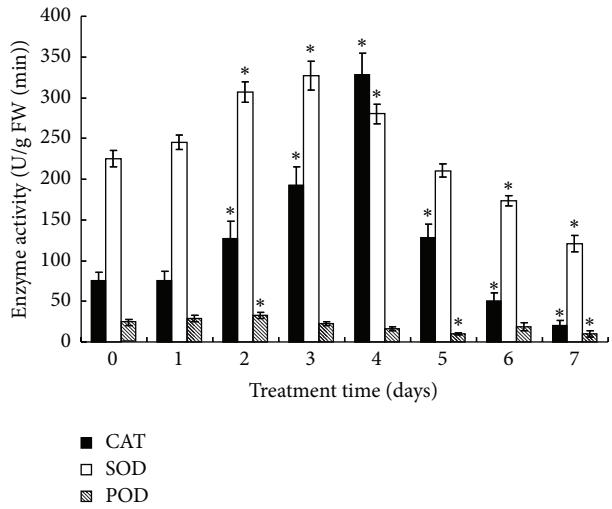

Figure 1: Activities of CAT, SOD, and POD in tissues of *L. sinense* under 500 mmol/L NaCl treatment. Values are means ± SD ($n = 3$). *Significant difference between untreated (day 0) and NaCl-treated sample ($P < 0.05$).

The primers for *LsActin*:

F: 5′-CAGTTTTCCCGAGTGTTGTTGGTAGG-3′;

R: 5′-ACCTCTTTTGGATTGTGCTTCGTCA-3′

To confirm specificity, primers and amplicons for each gene were compared with sequences in GenBank/NCBI. The gene *LsActin* was used as the reference gene. Relative expression of genes was calculated using the $2^{-\Delta\Delta Ct}$ method [12]. The experiments were repeated twice with three replicates.

2.5. Data Analysis. All data were analyzed using a one-way ANOVA with entries and sampling dates as factors. Mean separation processes were performed using a Fisher's protected LSD test at the $P < 0.05$ level of probability. For RT-qPCR, the $2^{-\Delta\Delta Ct}$ method is used to determine the changes of target gene expression based on normalization with the reference gene and one-way ANOVA was used to analyze differences between treatments' dates. The Pearson correlation analysis was made by SPSS software.

3. Results and Discussion

3.1. Antioxidant Enzymes' Activities and Isoenzymes of Seedlings. We measured the activities of antioxidant enzymes to evaluate the mechanisms of salt tolerance in *L. sinense*. The activity of CAT differed significantly between salt-stressed and untreated (day 0) seedlings. As shown in Figure 1, CAT activity showed the largest increase among all the antioxidant enzymes assayed. Compared with that on day 0, CAT activity increased by 0.7%, 68.7%, 154.6%, 336.2%, and 70.5% after 1, 2, 3, 4, and 5 days, respectively, of the 7-day NaCl treatment. The activity of CAT peaked on day 4 and then decreased as the duration of the NaCl treatment extended. The activity of SOD also showed a large increase under NaCl stress and peaked on

Figure 2: The phenotype of *L. sinense* seedlings under 500 mmol/L NaCl treatment.

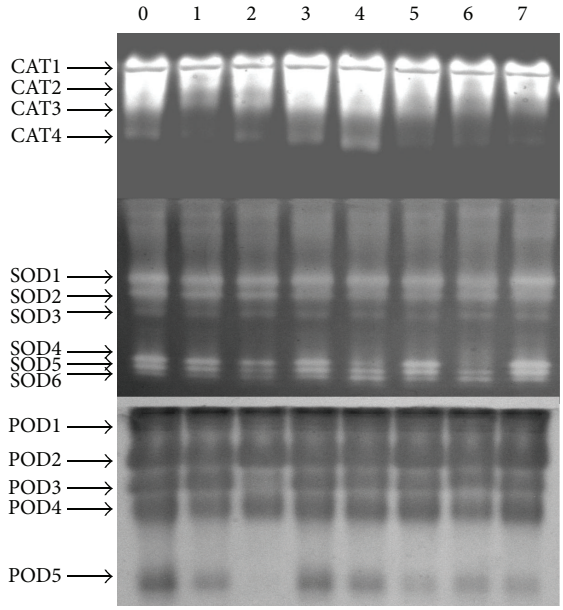

Figure 3: Identification of different isoenzymes (A-CAT, B-SOD, and C-POD) in *L. sinense* seedlings under NaCl stress. Each lane contains 45 μg protein. Arrows indicate different CAT, SOD, and POD isoenzymes.

day 3 of the 7-day salt treatment. Its activity decreased as the treatment time extended. Similarly, POD activity peaked on day 2 of the 7-day NaCl treatment (38.8% higher activity than that on day 0) and then decreased. The phenotype of *L. sinense* seedlings under NaCl stress was shown in Figure 2, which was in general accord with the activities of antioxidant enzymes.

As shown in Figure 3, the isoenzyme analysis revealed four CAT isoenzymes, six SOD isoenzymes, and five POD isoenzymes in *L. sinense*. The number of CAT, SOD, and POD isoenzymes changed under salt stress. The largest number of isoforms was on days 3-4 of the NaCl treatment for CAT, on day 2 for SOD, and on days 6-7 for POD. These results were consistent with the patterns of antioxidant enzyme activity during the NaCl treatment.

In plants, the activity of one or more antioxidant enzymes generally increases under stress conditions. This increase in antioxidant enzyme activity correlates with increased stress tolerance [13]. Antioxidant enzymes cooperate to remove excess ROS, thereby protecting the structures and functions of cellular components. SOD, which catalyzes the dismutation of superoxide into oxygen and hydrogen peroxide, is an essential component of the antioxidant defense system in plants [14]. Several studies reported that SOD activity increased in response to excess salt in potato, switchgrass, and *Brassica juncea* [15–17], consistent with our results.

Our results suggested that the H_2O_2 produced via SOD activity was effectively consumed by CAT and/or POD. CAT, which is located in peroxisomes, catalyzes the dismutation of excess H_2O_2 into oxygen and water and maintains H_2O_2 at a low level. At low concentrations, H_2O_2 is mainly cleared by POD [14]. POD is widely distributed in plant tissues and is involved in diverse growth, development, and senescence processes in plants. Our findings suggested that the increased POD activity in *L. sinense* under salt stress might be sufficient to protect proteins and lipids against ROS. Induction of CAT and POD activities under salt stress has also been reported in tomato, sugar beet, and *Plantago* [18]. Our results showed that the activities of these antioxidant enzymes decreased as the duration of the salt stress treatment extended, even to levels below that in untreated samples. A similar result was reported for potato under salt stress [15].

3.2. Changes of Related Genes Expression of Seedlings. To investigate the molecular mechanism of salt tolerance in *L. sinense*, we used real-time qPCR to evaluate changes in the transcript levels of three genes: *LsCAT*, *LsAPX*, and *LsGPX*. The relative transcript levels of these three genes changed significantly under NaCl stress (Figure 4). After 3 days of NaCl stress, the transcript level of *LsCAT* was 100-fold than in the untreated control (Figure 4(a)). This gene was induced more strongly than the other two genes analyzed. The transcript levels of *LsAPX* also increased markedly under NaCl stress, to a maximum of 20.9 times than in the control after 5 days of NaCl stress. After 7 days of NaCl stress, the transcript level of *LsAPX* decreased to below the control level (Figure 4(b)). The transcript levels of *LsGPX* peaked at 6.13 times than in the control after 4 days of NaCl stress and then decreased to the control level or even lower as the duration of the NaCl treatment extended (Figure 4(c)).

To protect plant cells from oxidative injury caused by abiotic stresses such as salt stress, several genes encoding antioxidant enzymes including CAT, APX, and GPX are upregulated [19]. Therefore, analyses of the transcript levels of antioxidant defense genes can reflect the contributions of their products to the salt stress response in plants [20]. Our results showed that the peak in *LsCAT* transcript levels on day 3 was earlier than the peaks in the transcript levels of *LsAPX* and *LsGPX* (days 4-5). Additionally, the *LsCAT* transcript level was higher in NaCl-treated samples than in untreated samples throughout the treatment period. Induction of *CAT* gene expression under other abiotic stress conditions has been reported for other plant species [21]. We also observed that the upregulated transcript level of *LsCAT* was consistent

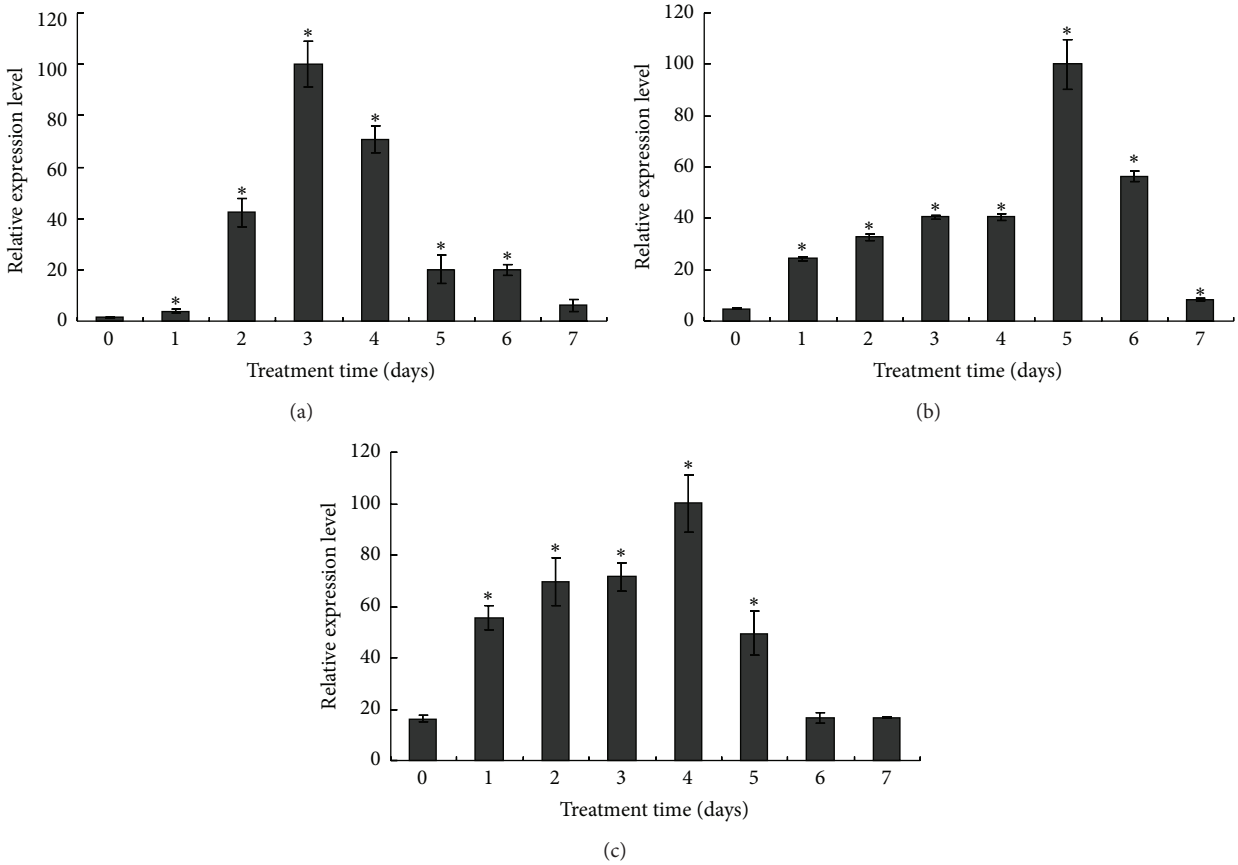

Figure 4: Relative transcript levels of *LsCAT* (a), *LsAPX* (b), and *LsGPX* (c) in *L. sinense* under 500 mM NaCl treatment. Transcript level of each gene was normalized to that of *LsActin*. Values are average relative expression level from three biological replicates. *Significant difference between NaCl-treated and untreated sample ($P < 0.05$).

with the increase in CAT enzyme activity, suggesting that CAT might play a key role in scavenging excessive ROS in NaCl-treated *L. sinense*.

Like CAT, APX has a high affinity for H_2O_2. In other studies, APX activity was shown to increase in response to a number of stress conditions, including salt stress [22, 23]. The transcript levels of *LsAPX* increased during the NaCl treatment, reaching peak levels on day 5 and then declining thereafter. Compared with transcription of *LsCAT*, that of *LsAPX* responded more slowly to salt stress. Similar results have been reported for other APX genes, for example, *Ec-apx1* from *Eleusine coracana*, in response to drought-induced oxidative stress [23].

The *LsGPX* transcript levels were higher in NaCl-treated seedlings than in untreated seedlings at most sampling times. Increased GPX activity could protect plant cells against the H_2O_2 released from the reaction catalyzed by SOD. In another study, it was reported that the transcript levels of *GPX* in *Panax ginseng* increased alongside an increase in GPX activity during abiotic stress [21].

3.3. MDA Content of Seedlings. The MDA content in leaves of *L. sinense* seedlings increased slightly throughout the duration of the NaCl treatment (Figure 5). The change in MDA content was not visible at the early stage (day 2), but

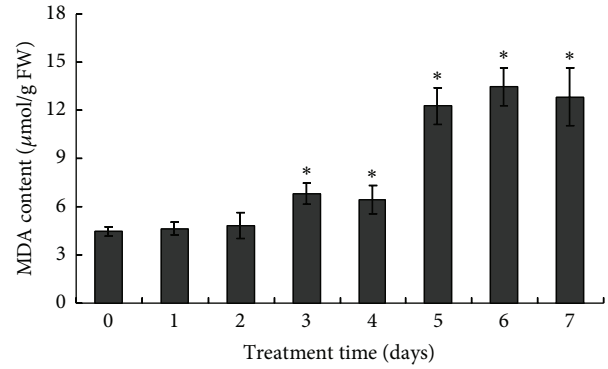

Figure 5: Effect of NaCl on MDA content of *L. sinense* seedlings. Values are means ± SD ($n = 3$). *Significant difference between NaCl-treated and untreated sample ($P < 0.05$).

after 3 days of salt treatment, it had increased to a level slightly higher than that in the control. The highest MDA content (twice that in the control) occurred after 6 days of NaCl stress. A significant negative correlation was observed between MDA content and SOD and POD activity ($R = -0.733$, $R = -0.791$, resp., $P < 0.05$), while no significant correlation was observed between MDA content and CAT activity ($R = -0.349$, $P > 0.05$).

Increased levels of lipid peroxides are indicative of enhanced ROS production [24]. MDA is a major cytotoxic product of lipid peroxidation, and therefore MDA content is another index to evaluate the extent of injury in plants under stress. It has been used as an indicator of free radical production in other studies [11]. The MDA content in seedlings of *L. sinense* only slightly increased under salt stress, suggesting that there was a low level of lipid peroxidation in these seedlings under salt stress. This might be because of the protective function of antioxidant enzymes in *L. sinense* seedlings, especially during the early phase of the salt stress response. These results indicate that the synergistic effect of various ROS-scavenging enzymes can effectively improve the antioxidant capacity of plants, thereby reducing the degree of oxidative injury.

4. Conclusion

The findings of this study indicate that the ability of *L. sinense* to cope with salt stress depends on antioxidant stress defense mechanisms. An increase in antioxidant enzyme activity and the resulting increase in ROS-scavenging capacity can improve the salt tolerance of plants [25]. This relationship between salt tolerance and increased activities of antioxidant enzymes has been demonstrated in pea [26], *Arabidopsis*, and rice [27]. Our results show that there were increases in antioxidant enzyme activity and in the transcript levels of genes encoding these enzymes under salt stress. These findings suggest that the response of *L. sinense* to salt stress involves CAT, SOD, APX, POD, and GPX. These results increase our understanding of how *L. sinense* responds to salt stress and provide evidence for the effectiveness of its detoxification mechanisms. At present, we are cloning and functionally analyzing *CAT* and *GPX* genes of *L. sinense* to investigate their regulation patterns in this salt-tolerant plant.

Conflict of Interests

The authors declare that they have no financial and personal relationships with other people or organizations that can inappropriately influence their work; there is no professional or other personal interests of any nature or kind in any product, service, and/or company that could be construed as influencing the position presented in, or the review of, this paper.

Acknowledgments

This work was supported by National Natural Science Foundation of China (no. 31000128), by the Promotive Research Fund for Excellent Young and Middle-aged Scientists of Shandong Province (BS2010SW036), by Shandong Provincial Natural Science Foundation of China (no. ZR2011CQ013), and by the Key Technologies R&D Program of Shandong Province of China (no. 2010GNC10937).

References

[1] A. Hediye Sekmen, I. Türkan, and S. Takio, "Differential responses of antioxidative enzymes and lipid peroxidation to salt stress in salt-tolerant *Plantago maritima* and salt-sensitive *Plantago media*," *Physiologia Plantarum*, vol. 131, no. 3, pp. 399–411, 2007.

[2] H. J. Bohnert, R. G. Jensen, T. J. Flowers, and A. R. Yeo, "Metabolic engineering for increased salt tolerance—the next step," *Australian Journal of Plant Physiology*, vol. 23, no. 5, pp. 661–667, 1996.

[3] J. A. Imlay, "Pathways of Oxidative Damage," *Annual Review of Microbiology*, vol. 57, pp. 395–418, 2003.

[4] M. Melchiorre, G. Robert, V. Trippi, R. Racca, and H. R. Lascano, "Superoxide dismutase and glutathione reductase overexpression in wheat protoplast: photooxidative stress tolerance and changes in cellular redox state," *Plant Growth Regulation*, vol. 57, no. 1, pp. 57–68, 2009.

[5] X.-F. Fan, Y.-L. Yang, and L.-X. Liu, "Tissue culture and rapid propagation of *Limonium gmelinii* (Willd.) Kuntze," *Plant Physiology Communications*, vol. 44, no. 3, p. 509, 2008.

[6] F. Ding and B. S. Wang, "Effect of NaCl on salt gland development and salt-secretion rate of the leaves of *Limonium sinense*," *Acta Botanica Boreali-Occidentalia Sinica*, vol. 26, pp. 1593–1599, 2006 (Chinese).

[7] L. L. Zhou, P. Liu, and J. H. Lu, "A SEM observation of the salt-secreting structure of leaves in four species of *Limonium*," *Bulletin of Botanical Research*, vol. 26, pp. 667–671, 2006 (Chinese).

[8] S. Gao, R. Yan, M. Cao, W. Yang, S. Wang, and F. Chen, "Effects of copper on growth, antioxidant enzymes and phenylalanine ammonia-lyase activities in *Jatropha curcas* L. seedling," *Plant, Soil and Environment*, vol. 54, no. 3, pp. 117–122, 2008.

[9] R. L. Heath and L. Packer, "Photoperoxidation in isolated chloroplasts. I. Kinetics and stoichiometry of fatty acid peroxidation," *Archives of Biochemistry and Biophysics*, vol. 125, no. 1, pp. 189–198, 1968.

[10] A. A. A. El-Mashad and H. I. Mohamed, "Brassinolide alleviates salt stress and increases antioxidant activity of cowpea plants (Vigna sinensis)," *Protoplasma*, vol. 249, no. 3, pp. 625–635, 2012.

[11] X. Zhang, S. Zhou, Y. Fu, Z. Su, X. Wang, and C. Sun, "Identification of a drought tolerant introgression line derived from Dongxiang common wild rice (*O. rufipogon* Griff.)," *Plant Molecular Biology*, vol. 62, no. 1-2, pp. 247–259, 2006.

[12] K. J. Livak and T. D. Schmittgen, "Analysis of relative gene expression data using real-time quantitative PCR and the $2^{-\Delta\Delta}$CT method," *Methods*, vol. 25, no. 4, pp. 402–408, 2001.

[13] M. Pilon, S. E. Abdel-Ghany, C. M. Cohu, K. A. Gogolin, and H. Ye, "Copper cofactor delivery in plant cells," *Current Opinion in Plant Biology*, vol. 9, no. 3, pp. 256–263, 2006.

[14] R. Mittler, "Oxidative stress, antioxidants and stress tolerance," *Trends in Plant Science*, vol. 7, no. 9, pp. 405–410, 2002.

[15] K. Aghaei, A. A. Ehsanpour, and S. Komatsu, "Potato responds to salt stress by increased activity of antioxidant enzymes," *Journal of Integrative Plant Biology*, vol. 51, no. 12, pp. 1095–1103, 2009.

[16] Q. Wang, C. Wu, B. Xie et al., "Model analysing the antioxidant responses of leaves and roots of switchgrass to NaCl-salinity stress," *Plant Physiology and Biochemistry*, vol. 58, pp. 288–296, 2012.

[17] S. Mittal, N. Kumari, and V. Sharma, "Differential response of salt stress on *Brassica juncea*: photosynthetic performance, pigment, proline, D1 and antioxidant enzymes," *Plant Physiology and Biochemistry*, vol. 54, pp. 17–26, 2012.

[18] T. Demiral and İ. Türkan, "Comparative lipid peroxidation, antioxidant systems and proline content in roots of two rice cultivars differing in salt tolerance," *Environmental and Experimental Botany*, vol. 53, no. 3, pp. 247–257, 2005.

[19] Z. Lu, D. Liu, and S. Liu, "Two rice cytosolic ascorbate peroxidases differentially improve salt tolerance in transgenic *Arabidopsis*," *Plant Cell Reports*, vol. 26, no. 10, pp. 1909–1917, 2007.

[20] K. de Carvalho, M. K. F. de Campos, D. S. Domingues, L. F. P. Pereira, and L. G. E. Vieira, "The accumulation of endogenous proline induces changes in gene expression of several antioxidant enzymes in leaves of transgenic *Swingle citrumelo*," *Molecular Biology Reports*, vol. 40, no. 4, pp. 3269–3279, 2013.

[21] C. A. Meyer, G. Sathiyaraj, O. R. Lee et al., "Transcript profiling of antioxidant genes during biotic and abiotic stresses in *Panax ginseng*," *Molecular Biology Reports*, vol. 38, no. 4, pp. 2761–2769, 2011.

[22] K. Asada, "Ascorbate peroxidase, a H_2O_2 scavenging enzyme in plants," *Physiologia Plantarum*, vol. 85, pp. 235–241, 1992.

[23] D. Bhatt, S. C. Saxena, S. Jain, A. K. Dobriyal, M. Majee, and S. Arora, "Cloning, expression and functional validation of drought inducible ascorbate peroxidase (*Ec-apx*1) from *Eleusine coracana*," *Molecular Biology Reports*, vol. 40, no. 2, pp. 1155–1165, 2013.

[24] J. Liu, Z. Xiong, T. Li, and H. Huang, "Bioaccumulation and ecophysiological responses to copper stress in two populations of *Rumex dentatus* L. from Cu contaminated and non-contaminated sites," *Environmental and Experimental Botany*, vol. 52, no. 1, pp. 43–51, 2004.

[25] R. G. Alscher, J. L. Donahue, and C. L. Cramer, "Reactive oxygen species and antioxidants: relationships in green cells," *Physiologia Plantarum*, vol. 100, no. 2, pp. 224–233, 1997.

[26] J. A. Hernández, A. Jiménez, P. Mullineaux, and F. Sevilla, "Tolerance of pea (*Pisum sativum* L.) to long-term salt stress is associated with induction of antioxidant defences," *Plant, Cell and Environment*, vol. 23, no. 8, pp. 853–862, 2000.

[27] M. L. Dionisio-Sese and S. Tobita, "Antioxidant responses of rice seedlings to salinity stress," *Plant Science*, vol. 135, no. 1, pp. 1–9, 1998.

Hindawi Publishing Corporation
Journal of Chemistry
Volume 2014, Article ID 848571, 6 pages
http://dx.doi.org/10.1155/2014/848571

Research Article

Preparation of Ginsenoside Rg3 and Protection against H_2O_2-Induced Oxidative Stress in Human Neuroblastoma SK-N-SH Cells

Gang Li,[1] Xiao-xiao Zhang,[1] Lin Lin,[1] Xiao-ning Liu,[1] Cheng-jun Ma,[1] Ji Li,[1] and Chi-bo Wang[2]

[1] *Life School of Yantai University, Yantai, Shandong 264005, China*
[2] *Department of Neurosurgery, Yantaishan Hospital, Yantai, Shandong 264000, China*

Correspondence should be addressed to Chi-bo Wang; wangcbyt@sohu.com

Received 16 May 2014; Accepted 30 May 2014; Published 18 June 2014

Academic Editor: Wang Chunming

The aim of this study is to evaluate the protection of ginsenoside Rg3 against oxidative stress in human neuroblastoma SK-N-SH cells. 20(R)-ginsenoside Rg3 (20(R)-Rg3) and 20(S)-ginsenoside Rg3 (20(S)-Rg3) were prepared by the method of chemical degradation and column chromatography, and the structure of the two compounds was characterized by ^{1}H-NMR and ^{13}C-NMR spectroscopy. MTT assay and LDH leakage assay were used to determine the cell viability and the oxidative stress cellular model was established by means of H_2O_2 (600 μM for 4 h). We also investigated the changes of intracellular MDA content, SOD activity, and ROS formation after the treatment of ginsenoside Rg3 for 20 h. The results indicated that both 20 (R)-Rg3 and 20 (S)-Rg3 had obvious protection against H_2O_2-induced oxidative stress in SK-N-SH cells. Moreover, 20(R)-Rg3 exhibited better antioxidant activity than 20(S)-Rg3 *in vitro*. These findings are expected to provide some implication for further research and application of ginsenoside Rg3 in neuroprotection.

1. Introduction

Panax ginseng is known to have various pharmacological activities [1]. Among several products of ginseng, ginsenosides are the main components and have been proved to possess many bioactivities, which mostly including antioxidation, neuroprotection, and anticancer [2].

Ginsenoside Rg3, a saponin extracted from ginseng, had been recently reported to protect the neuronal cells and animals with neurological injuries [3–6]. Ginsenoside Rg3 exists as stereoisomer of 20(R)- or 20(S)-form (Figure 1) and with different bioactivity [7, 8]. The two compounds can be biotransformed by human intestinal bacteria [9, 10]. In recent years, researchers have found the protection of different Rg3 isomer on nervous system. Tian et al. have investigated the neuroprotective effects of 20(S)-Rg3 on focal cerebral ischemia in rats and found that 20(S)-Rg3 could inhibit the opening of mitochondrial permeability transition pore by free radical scavenging action in the rats brain [11, 12]. He et al. have investigated the neuroprotective effect of 20(R)-Rg3 against transient focal cerebral ischemia in male Sprague-Dawley rats and finally indicated its neuroprotective effect may be involved in the downregulation of calpain I and caspase-3 [13]. However, rare reports have been found on the comparison study of 20(R)-Rg3 and 20(S)-Rg3, especially in the study of antioxidant and neural protection.

In the present study, we prepared the stereoisomer of 20(R)-Rg3 and 20(S)-Rg3 by chemical conversion method and characterized the structure by ^{1}H-NMR and ^{13}C-NMR spectroscopy. Human neuroblastoma SK-N-SH cells are often used as *in vitro* models of neuronal function and differentiation [14, 15]. Here, we established the oxidative stress model by using SK-N-SH cells exposed to H_2O_2, and the protection of ginsenoside Rg3 against H_2O_2-induced oxidative stress was evaluated by the measurement of lactate dehydrogenase (LDH) release, malondialdehyde (MDA) content, superoxide dismutase (SOD) activity, and intracellular reactive oxygen species (ROS) level. Some implication is

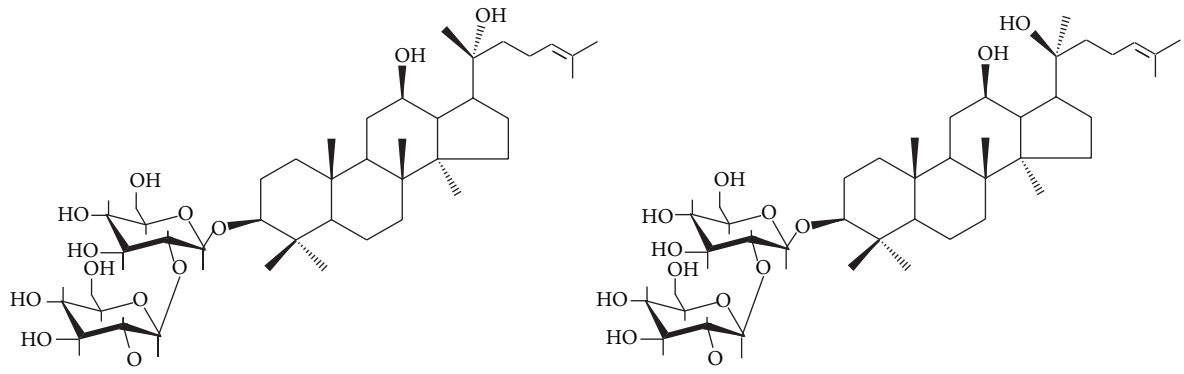

Figure 1: Structural formulas of 20(R)-Rg3 and 20(S)-Rg3.

expected to be provided for the further research and application of ginsenoside Rg3 in neuroprotection through this study.

2. Materials and Methods

2.1. Cells and Chemicals. Human neuroblastoma SK-N-SH cells were obtained from the cell bank of the Institute of Biochemistry and Cell Biology in Shanghai, China. Phosphate buffered saline (PBS), MEM medium, fetal bovine serum (FBS), penicillin-streptomycin solution, and Trypsin-EDTA solution were purchased from GIBCO Corporation (Beijing Representative Office, China). Ginseng stem-leave saponins (GSLS) were bought from Hongjiu Biological Technology Co., Ltd, in Jilin, China. Other chemical reagents were analytically pure and were purchased from Sinopharm Chemical Reagent Co., Ltd, Shanghai, China.

2.2. Preparation of Ginsenoside Rg3. 20 g of GSLS was dissolved with 500 mL of acetic acid water (30 : 70) and extracted under reflux at 90°C for 1 h. The extraction mixture was then filtered. The residue was washed using ethanol and recrystallized from methanol water. Finally, 1.48 g target compound was obtained. The structure of the compound was confirmed by ^{1}H-NMR and ^{13}C-NMR as 20(R)-ginsenoside Rg3 (20(R)-Rg3), 20(R)-protopanaxadiol-3-O-beta-D-glucopyranosyl(1 → 2)-beta-D-glucopyranoside.

20 g of GSLS was mixed with 1000 mL of glycerin and 100 g of sodium hydroxide and reacted at 210°C for 2 h. As the solution cooled, pH was adjusted to 7.4. Then the precipitation was concentrated to dryness in vacuum and 7.7 g of gray degradation was obtained. Then, the degradation underwent silica gel column chromatography and was eluted with ethyl acetate : methanol (8 : 2). The resulting eluate was combined into two fractions (Fr1 and Fr2) based on the silica gel TLC profiles of each tube. The Fr2 was then purified again with chloroform : methanol (7 : 3). The final compound was recrystallized with methanol and confirmed by ^{1}H-NMR and ^{13}C-NMR as 20(S)-ginsenoside Rg3 (20(S)-Rg3), 20(S)-protopanaxadiol-3-O-beta-D-glucopyranosyl(1 → 2)-beta-D-glucopyranoside.

2.3. Cell Culture. Human neuroblastoma SK-N-SH cells were cultured in MEM medium that contained 10% FBS, 100 U/mL penicillin, and 100 μg/mL streptomycin at 37°C in a humidified atmosphere containing 5% CO_2. Cells were seeded on Petri dishes (10 cm) and the medium was replaced every other day.

2.4. Cell Viability Assay. The cytotoxicity of ginsenoside Rg3 was detected by MTT assay. The oxidative damage of H_2O_2 to SK-N-SH cells was confirmed by measuring the release of the cytosolic enzyme LDH to the culture medium. And the protective effect of ginsenoside Rg3 against toxicity of H_2O_2 was also confirmed by both MTT assay and LDH assay.

2.4.1. MTT Assay. The cytotoxicity of ginsenoside Rg3 was determined by the MTT assay as described [16]. SK-N-SH cells were plated in triplicate at a density of 1×10^4 cells/well in 96-well plates for 24 h. The culture media were aspirated and replaced with fresh culture media containing various concentrations of 20(R)-Rg3 or 20(S)-Rg3 (1.5~200 μg/mL) for 20 h. Then, 10 μL MTT solution (5 mg/mL) was added into each well for further 4 h at 37°C. And 150 μL of DMSO was added in order to dissolve the formazan crystals. The UV absorbance of the solubilized formazan crystals was measured by microplate reader (Spectra MR, Dynex) at 490 nm. Cell viability (%) was calculated.

2.4.2. LDH Assay. The leakage of LDH was measured by using a colorimetric LDH assay kit (Nanjing Jiancheng Bioengineering Institute, Nanjing, China) according to the manufacturer's instructions. Briefly, 1×10^4 cells/well were cultured in 96 well plates overnight. Then, the cells were treated with various concentration of H_2O_2 (200, 400, 600, 800, 1000, and 1200 μM) for different time (2 h, 4 h, and 6 h). Then, 20 μL of cell medium was added into basic solution to measure extracellular LDH activity, which could catalyze the conversion of lactate to pyruvate and react with 2,4-dinitrophenylhydrazine to give the brownish red color [17]. The absorbance was measured at 450 nm by automatic microplate reader.

As for the protective effect of ginsenoside Rg3, SK-N-SH cells were preincubated with 20(R)-Rg3 or 20(S)-Rg3

(10, 20 μg/mL) for 24 h before H_2O_2 oxidative damage, and the detection of LDH released into the culture medium was completed with the same process.

2.5. Oxidative Stress Analysis. After pretreatment with 20(R)-Rg3 or 20(S)-Rg3 for 24 h and subsequent treatment with 600 μM H_2O_2 for 4 h, H_2O_2-induced oxidative stress and the protection of ginsenoside Rg3 were analyzed by cytosolic superoxide dismutase (SOD) assay, extracellular malondialdehyde (MDA) assay, and intracellular reactive oxygen species (ROS) detection.

2.5.1. SOD and MDA Determination. After treatment with ginsenoside Rg3 and H_2O_2, the culture supernatant was collected, and MDA contents were measured using a spectrometer at 586 nm according to the manufacturer of the assay kit (Nanjing Jiancheng Bioengineering Institute, Nanjing, China). Then, the cells were detached with 0.25% trypsin and centrifuged at 1200 rpm. SOD activities were analyzed according to the instruction of the assay kits (Nanjing Jiancheng Bioengineering Institute, Nanjing, China) at 550 nm.

2.5.2. Detection of Intracellular ROS. ROS production in SK-N-SH cells was measured using the redox-sensitive fluorescent dye DCFH-DA (Jiamei Biotechnology Co., Ltd., Beijing, China). After treatment with ginsenoside Rg3 and H_2O_2, cells were incubated with 25 μM DCFH-DA for 20 min. The cells were detached with 0.25% trypsin and centrifuged at 1200 rpm. Then, the cells were rinsed twice with phenol-red-free MEM containing 1% FBS, and fluorescence was detected on automatic microplate reader (488 nm excitation and 520 nm emission). The mean fluorescent signals for 10,000 cells were recorded and the relative intracellular ROS level (%) was calculated.

2.6. Statistical Analyses. Data were expressed as mean ± S.D., and differences were evaluated using unpaired Student's t-tests or ANOVA by SPSS 18.0 software. The level of statistical significance was set at $P < 0.05$.

3. Results and Discussion

3.1. Chemical Structure Identification. The structural identification of ginsenoside Rg3 was carried out by electrospray ionization mass spectrometry (ESI-MS), ^{1}H NMR, and ^{13}C NMR spectra as follows.

20(R)-Rg3: ^{1}H-NMR (400 Hz, C_5D_5N), δ: 0.83 (3H, S, CH_3-29), 1.01 (3H, S, CH_3-30), 0.96 (3H, S, CH_3-19), 1.12 (3H, S, CH_3-18), 1.30 (3H, S, CH_3-28), 1.66 (3H, S, CH_3-27), 1.70 (3H, S, CH_3-26), 4.63 (1H, d, J = 7.4 Hz), 5.31 (1H, d, J = 7.4 Hz); ^{13}C-NMR (400 Hz, C_5D_5N), δ: 39.1 (C-1), 26.7 (C-2), 88.9 (C-3), 39.9 (C-4), 56.3 (C-5), 18.4 (C-6), 35.1 (C-7), 36.9 (C-8), 50.6 (C-9), 39.7 (C-10), 32.2 (C-11), 70.9 (C-12), 49.2 (C-13), 51.7 (C-14), 31.4 (C-15), 28.1 (C-16), 50.4 (C-17), 16.6 (C-18), 72.9 (C-19), 22.8 (C-20), 43.3 (C-21), 22.6 (C-22), 126.0 (C-23), 130.8 (C-24), 25.8 (C-25), 17.7 (C-26), 26.6 (C-27), 15.8 (C-28), 17.3 (C-29), 105.1 (C-30), 83.5 (C-31), 71.6 (C-32), 77.9 (C-33), 62.6 (C-34), 106.1 (C-35), 77.1 (C-36), 78.3 (C-37), 71.6 (C-38), 78.1 (C-39), 62.8 (C-40).

20(S)-Rg3: ^{1}H-NMR (400 Hz, C_5D_5N), δ: 0.80 (3H, S, CH_3-29), 0.95 (3H, S, CH_3-30), 0.96 (3H, S, CH_3-19), 1.11 (3H, S, CH_3-18), 1.30 (3H, S, CH_3-28), 1.61 (3H, S, CH_3-27), 1.65 (3H, S, CH_3-26), 4.83 (1H, d, J = 7.6 Hz), 5.29 (1H, d, J = 7.2 Hz); ^{13}C-NMR (400 Hz, C_5D_5N), δ: 39.1 (C-1), 27.0 (C-2), 88.9 (C-3), 39.9 (C-4), 56.3 (C-5), 18.4 (C-6), 35.8 (C-7), 36.9 (C-8), 32.0 (C-9), 71.6 (C-10), 48.5 (C-11), 51.7 (C-12), 39.7 (C-13), 32.0 (C-14), 71.6 (C-15), 48.5 (C-16), 51.7 (C-17), 32.0 (C-18), 26.8 (C-19), 35.1 (C-20), 23.0 (C-21), 126.3 (C-22), 130.7 (C-23), 25.8 (C-24), 17.6 (C-25), 28.1 (C-26), 16.3 (C-27), 17.0 (C-28), 105.1 (C-29), 83.4 (C-30), 78.3 (C-31), 71.6 (C-32), 77.2 (C-33), 62.7 (C-34), 105.1 (C-35), 77.1 (C-36), 78.3 (C-37), 72.8 (C-38), 77.9 (C-39), 62.8 (C-40).

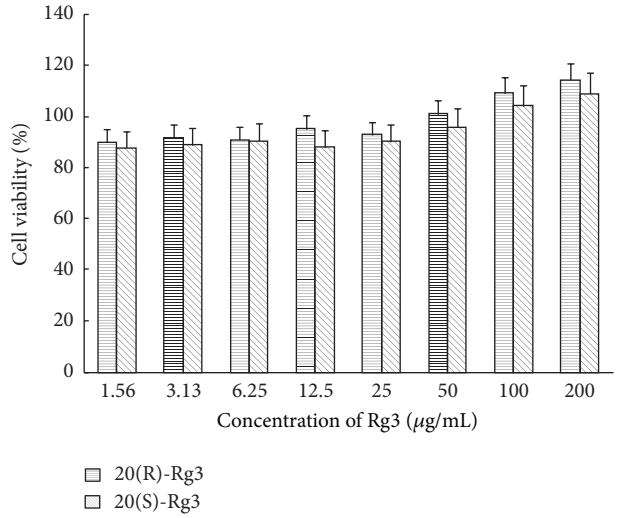

Figure 2: Cytotoxicity effects of ginsenoside Rg3 on SK-N-SH cells.

3.2. Cell Viability Assay. As showed in Figure 2, both 20(R)-Rg3 and 20(S)-Rg3 had no obvious cytotoxicity on SK-N-SH cells when the concentration was 1.5~200 μg/mL. Intracellular LDH assay has proved that H_2O_2 could significantly lead to cell damage along with the extension of the time and with the increase of the concentration (Figure 3). After incubated with H_2O_2, SK-N-SH cells were also found with different changes in shape through inverted microscope observation. Some cells were swelled, shrunken, and unevenly distributed. The cellular edge became unclear and even fell off when the damage was serious.

3.3. Protection of Rg3 against H_2O_2-Induced Oxidative Stress. The results from MTT assay and intracellular LDH analysis had suggested that H_2O_2-induced oxidative stress could lead to significant cell death. And previous ginsenoside Rg3 treatment was able to increase the cell survival rate and vitality with a dose-dependent manner (shown in Figures 4 and 5). Furthermore, the protective activity of 20(R)-Rg3 was significantly better than that of 20(S)-Rg3 ($P < 0.05$).

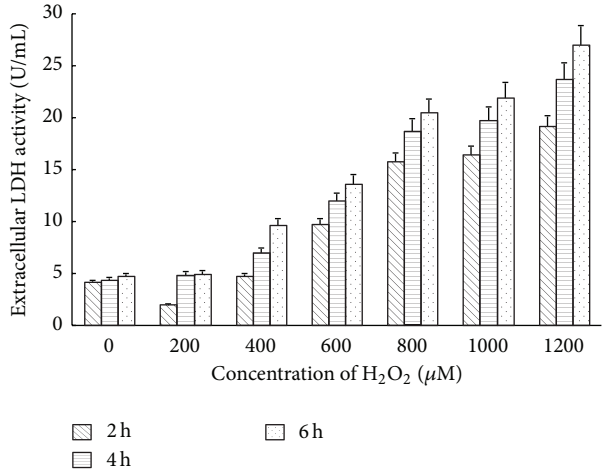

Figure 3: Effect of H_2O_2 on leakage of LDH in SK-N-SH cells.

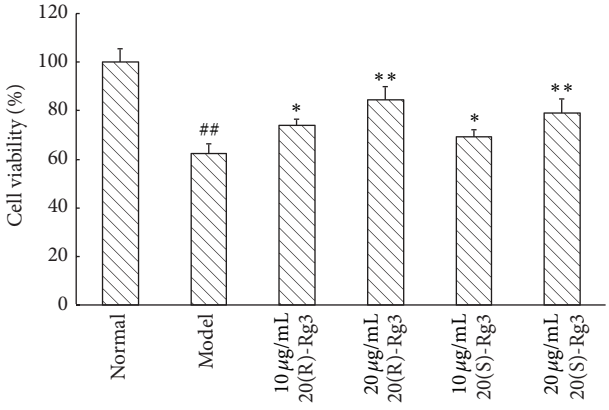

Figure 4: Protective effect of ginsenoside Rg3 on SK-N-SH cells by MTT assay. $^{\#\#}P < 0.01$ versus normal group, $^{*}P < 0.05$, and $^{**}P < 0.01$ versus model group.

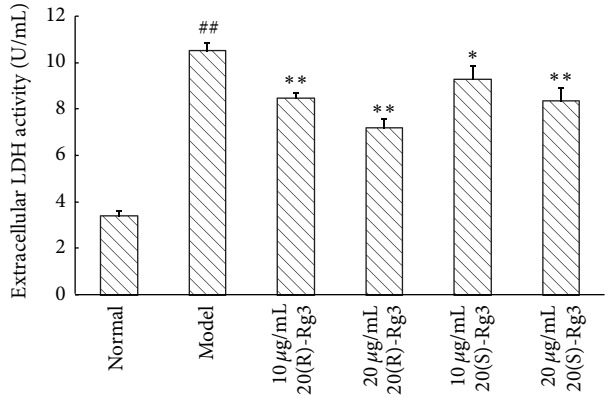

Figure 5: Protective effect of ginsenoside Rg3 on SK-N-SH cells by extracellular LDH assay. $^{\#\#}P < 0.01$ versus normal group, $^{*}P < 0.05$, and $^{**}P < 0.01$ versus model group.

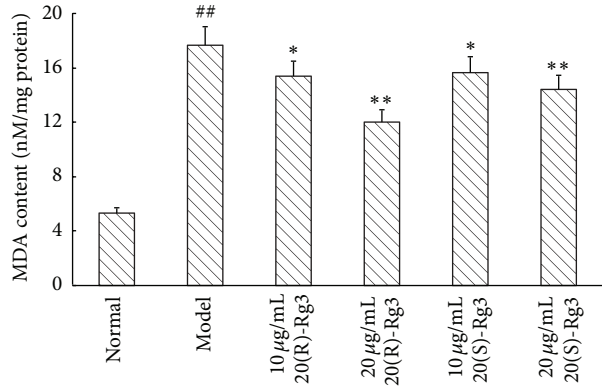

Figure 6: Ginsenoside Rg3 inhibited the MDA production in SK-N-SH cells. $^{\#\#}P < 0.01$ versus normal group, $^{*}P < 0.05$, and $^{**}P < 0.01$ versus model group.

MDA produced in cytoplasm was determined as a common indicator of lipid peroxidation [18]. H_2O_2 (600 μM for 4 h) could significantly increase the production of MDA generated in SK-N-SH cells. However, 20(R)-Rg3 and 20(S)-Rg3 could effectively reduce the content of MDA as showed in Figure 6.

SOD is an effective defense enzyme that catalyses the dismutation of superoxide anions into hydrogen peroxide [19]. Our results in the present study showed that the antioxidantive activity of intracellular SOD was significantly decreased in H_2O_2 toxic groups compared with the normal cells ($P < 0.01$), which implied increased oxidative damage to the cells. On the contrary, SOD levels were significantly elevated by incubation of 20(R)-Rg3 and 20(S)-Rg3. These results demonstrated that the antioxidant ability of ginsenoside Rg3 was very critical for its protection on SK-N-SH cells. In addition, the protective effects of 20(R)-Rg3 were remarkable and powerful than that of 20(S)-Rg3 at the concentration of 20 μg/mL ($P < 0.05$) (Figure 7).

Oxidative stress reflects an imbalance between the systemic manifestation of ROS and the ability to repair the resulting damage by the biological system or the intake of exogenous antioxidants [20]. Given oxidative stress, the intracellular ROS levels would sharply increase which had been confirmed by the H_2O_2 exposure in the present study (Figure 8). Ginsenoside Rg3 could obviously scavenge the ROS produced by H_2O_2. We investigated the intracellular ROS formation by fluorescent probe DCFH-DA. The results showed that compared with the H_2O_2 damaged group, 10 and 20 μg/mL of 20(R)-Rg3 could decrease the ROS formation by 44.1% and 64.7%, respectively, meanwhile 10 and 20 μg/mL of 20(S)-Rg3 could decrease the ROS level by 29.2% and 51.3%, respectively.

4. Conclusions

H_2O_2 exposure (600 μM for 4 h) to human neuroblastoma SK-N-SH cells could significantly cause oxidative stress by reducing the intracellular SOD activity and promoting the MDA production and lead to further damage to cells. Ginsenoside Rg3, no matter 20(R)-Rg3 or 20(S)-Rg3, possesses

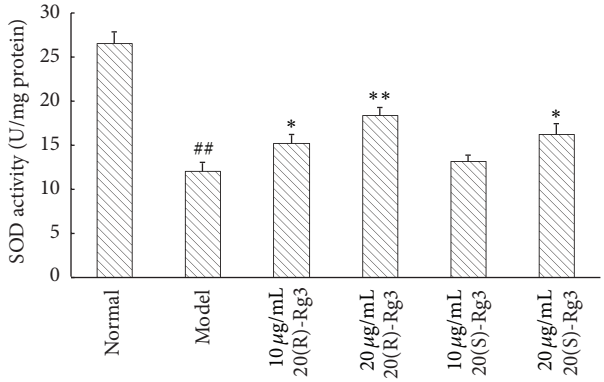

Figure 7: Ginsenoside Rg3 increased the SOD activity in SK-N-SH cells. $^{\#\#}P < 0.01$ versus normal group, $^{*}P < 0.05$, and $^{**}P < 0.01$ versus model group.

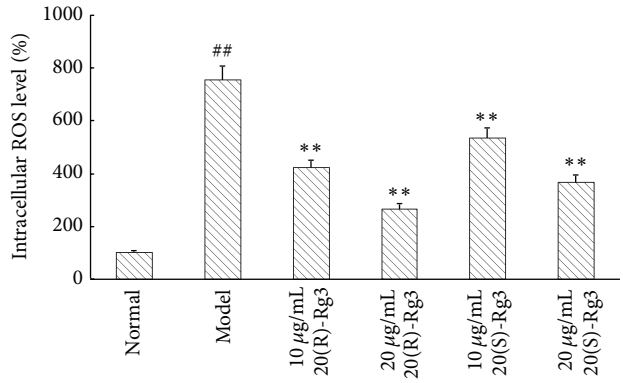

Figure 8: Ginsenoside Rg3 reduced the intracellular ROS formation in SK-N-SH cells. $^{\#\#}P < 0.01$ versus normal group and $^{**}P < 0.01$ versus model group.

powerful ability of scavenging free radicals produced by H_2O_2. Thus, they exhibited the strong protective effects on SK-N-SH cells. In addition, we also found in the present study that 20(R)-Rg3 displayed better antioxidant activity than 20(S)-Rg3 *in vitro*. These findings will benefit further research and application of ginsenoside Rg3 in neuroprotection.

Conflict of Interests

The authors declare that there is no conflict of interests regarding the publication of this paper.

Acknowledgments

This study was supported by the Natural Science Foundation of China (21372190) and the Excellent Young Scientists Award of Shandong Province, China (BS2012YY039).

References

[1] P. Y. K. Yue, N. K. Mak, Y. K. Cheng et al., "Pharmacogenomics and the Yin/Yang actions of ginseng: anti-tumor, angiomodulating and steroid-like activities of ginsenosides," *Chinese Medicine*, vol. 2, article 6, 2007.

[2] L. P. Christensen, "Ginsenosides: chemistry, biosynthesis, analysis, and potential health effects," *Advances in Food and Nutrition Research*, vol. 55, no. 1, pp. 1–99, 2008.

[3] Y. C. Kim, S. R. Kim, G. J. Markelonis, and T. H. Oh, "Ginsenosides Rb1 and Rg3 protect cultured rat cortical cells from glutamate-induced neurodegeneration," *Journal of Neuroscience Research*, vol. 53, no. 4, pp. 426–432, 1998.

[4] M. V. N. López, M. P. G.-S. Cuadrado, O. M. P. Ruiz-Poveda, A. M. V. Del Fresno, and M. E. C. Accame, "Neuroprotective effect of individual ginsenosides on astrocytes primary culture," *Biochimica et Biophysica Acta—General Subjects*, vol. 1770, no. 9, pp. 1308–1316, 2007.

[5] J.-H. Kim, S. Y. Cho, J.-H. Lee et al., "Neuroprotective effects of ginsenoside Rg3 against homocysteine-induced excitotoxicity in rat hippocampus," *Brain Research*, vol. 1136, no. 1, pp. 190–199, 2007.

[6] S. Y. Nah, "Ginseng ginsenoside pharmacology in the nervous system: involvement in the regulation of ion channels and receptors," *Frontiers in Physiology*, vol. 5, article 98, 2014.

[7] M. Mochizuki, Y. C. Yoo, K. Matsuzawa et al., "Inhibitory effect of tumor metastasis in mice by saponins, ginsenoside- Rb2, 20(R)- and 20(S)-ginsenoside-Rg3, of red ginseng," *Biological and Pharmaceutical Bulletin*, vol. 18, no. 9, pp. 1197–1202, 1995.

[8] H.-H. Kwok, G.-L. Guo, J. K.-C. Lau et al., "Stereoisomers ginsenosides-20(S)-Rg3 and -20(R)-Rg3 differentially induce angiogenesis through peroxisome proliferator-activated receptor-gamma," *Biochemical Pharmacology*, vol. 83, no. 7, pp. 893–902, 2012.

[9] E.-A. Bae, M. J. Han, M.-K. Choo, S.-Y. Park, and D.-H. Kim, "Metabolism of 20(S)- and 20(R)-ginsenoside Rg3 by human intestinal bacteria and its relation to in vitro biological activities," *Biological & Pharmaceutical Bulletin*, vol. 25, no. 1, pp. 58–63, 2002.

[10] Y. Wang, W. Zhao, X. Wu, and Y. Zhang, "Studies on the biotransformation of ginsenoside Rg3 by an active microorganism isolated from ginseng root soils in Changbai Mountain," *Journal of Traditional Medicines*, vol. 3, no. 5, 2008.

[11] J. Tian, F. Fu, M. Geng et al., "Neuroprotective effect of 20(S)-ginsenoside Rg3 on cerebral ischemia in rats," *Neuroscience Letters*, vol. 374, no. 2, pp. 92–97, 2005.

[12] J. Tian, S. Zhang, G. Li, Z. Liu, and B. Xu, "20(S)-Ginsenoside Rg3, a neuroprotective agent, inhibits mitochondrial permeability transition pores in rat brain," *Phytotherapy Research*, vol. 23, no. 4, pp. 486–491, 2009.

[13] B. He, P. Chen, J. Yang et al., "Neuroprotective effect of 20(R)-ginsenoside Rg3 against transient focal cerebral ischemia in rats," *Neuroscience Letters*, vol. 526, no. 2, pp. 106–111, 2012.

[14] J. W. Simpkins, P. S. Green, K. E. Gridley, M. Singh, N. C. De Fiebre, and G. Rajakumar, "Role of estrogen replacement therapy in memory enhancement and the prevention of neuronal loss associated with Alzheimer's disease," *The American Journal of Medicine*, vol. 103, no. 3, pp. 19–25, 1997.

[15] F. Ba, P. K. T. Pang, S. T. Davidge, and C. G. Benishin, "The neuroprotective effects of estrogen in SK-N-SH neuroblastoma cell cultures," *Neurochemistry International*, vol. 44, no. 6, pp. 401–411, 2004.

[16] P. Moongkarndi, C. Srisawat, P. Saetun et al., "Protective effect of mangosteen extract against β-amyloid-induced cytotoxicity, oxidative stress and altered proteome in SK-N-SH cells," *Journal of Proteome Research*, vol. 9, no. 5, pp. 2076–2086, 2010.

[17] G. Fotakis and J. A. Timbrell, "In vitro cytotoxicity assays: comparison of LDH, neutral red, MTT and protein assay in

hepatoma cell lines following exposure to cadmium chloride," *Toxicology Letters*, vol. 160, no. 2, pp. 171–177, 2006.

[18] T. P. A. Devasagayam, K. K. Boloor, and T. Ramasarma, "Methods for estimating lipid peroxidation: an analysis of merits and demerits," *Indian Journal of Biochemistry & Biophysics*, vol. 40, no. 5, pp. 300–308, 2003.

[19] J. M. Matés, "Effects of antioxidant enzymes in the molecular control of reactive oxygen species toxicology," *Toxicology*, vol. 153, no. 1–3, pp. 83–104, 2000.

[20] E. Birben, U. M. Sahiner, C. Sackesen, S. Erzurum, and O. Kalayci, "Oxidative stress and antioxidant defense," *The World Allergy Organization Journal*, vol. 5, no. 1, pp. 9–19, 2012.

Hindawi Publishing Corporation
Journal of Chemistry
Volume 2014, Article ID 646537, 5 pages
http://dx.doi.org/10.1155/2014/646537

Research Article

Antioxidant and Antimicrobial Activity of Ophiurasaponin Extracted from *Ophiopholis mirabilis*

Rongzhen Wang, Xiaoyu Xue, Jingrong Zhen, and Chenghua Guo

School of Life Sciences, Yantai University, Yantai 264005, China

Correspondence should be addressed to Chenghua Guo; gch@ytu.edu.cn

Received 1 April 2014; Revised 15 May 2014; Accepted 19 May 2014; Published 4 June 2014

Academic Editor: Wang Chunming

The aim of this study was to analyze antioxidant and antimicrobial activity of ophiurasaponin extracted from *Ophiopholis mirabilis* (overall). Ophiurasaponin was extracted with solvent extraction and purified through AB-8 macroporous resin, silica gel column chromatography, Sephadex LH-20 gel column chromatography, and C18 ODS column chromatography. The antioxidant activity of ophiurasaponin was detected by the chemiluminescence assay. The paper filtering method and the modified agar dilution method were used to determine antimicrobial activity. The results showed that the content of crude ophiurasaponin and the refined ophiurasaponin was 46.75% and 96.72%, respectively. The values of the IC_{50} of hydroxyl-radicals, superoxide anions, and peroxide were 25.54 mg/mL, 9.98 mg/mL, and 1.37 mg/mL, respectively. The refined ophiurasaponin had a good inhibitory effect on *Escherichia coli*, *Bacillus subtilis*, *Staphylococcus aureus*, *Aerobacter aerogenes,* and *Proteusbacillus vulgaris*, and the minimum inhibitory concentration (MIC) was 0.0443 mg/mL. In conclusion, ophiurasaponin from *Ophiopholis mirabilis* had obvious antioxidant activities and antimicrobial activities which could provide the theoretical basis for further research and development of antioxidant and antimicrobial marine drugs.

1. Introduction

Ophiopholis mirabilis is normally restricted to the shallow water of the northern and central Yellow Sea of China, such as along the coast of Dalian, Qingdao, and Yantai. Zoologically it belongs to Echinodermata, Ophiuroidea, Gnathophiurina, Ophiactidae, Ophiopholis Muller, and Troschel [1]. In this experiment, *Ophiopholis mirabilis* was harvested from Changdao archipelago (longitude 120°35′28″–120°56′36″, latitude 37°53′30″–38°23′58″), the interface between the Yellow Sea and the Bohai Sea.

Many kinds of active substances from echinoderms, such as saponins, polysaccharides, proteins, alkaloids, and fatty acids, have been isolated and reported by scholars both at home and abroad. However, they are mostly extracted from Asteroidea, Holothuroidea, and Echinoidea [2, 3]. These researches on Ophiuroidea from Echinodermata focus more on the morphology, taxonomy, regeneration incidence on species level, wrist-regeneration, and ecological fields [4, 5]. Recently, the studies on the preparation and characteristics of the Ophiurasaponin from *Ophiura kinbergi* have been reported [6]. The four compounds are isolated from *Axtroclarus conferus* and identified by spectroscopic analysis [7]. However, there has been no report about antioxidant and antimicrobial activities of ophiurasaponin from *Ophiopholis mirabilis*.

2. Experiments

2.1. Extraction and Purification of Ophiurasaponin from Ophiopholis mirabilis. Commonly-used solvent extraction method was applied in the experiment. The marine sample was naturally air-dried and then finely crushed. Afterwards the crushed sample was soaked in 85% ethanol three times. The collected ethanol-extract was concentrated in rotary evaporator. Equal volume of petroleum ether was added to the concentration extracted six times for degreasing and

equal volume of *n*-butanol was added to the water extracted six times as well. Then the supernatant was collected and concentrated in the rotary evaporator. After concentration, ophiurasaponin was precipitated by adding 10 times of volume of acetone and then centrifuged. After the precipitate was dried, the crude ophiurasaponin was obtained. Subsequently, some crude ophiurasaponin was purified through AB-8 macroporous resin, eluted with water, 20% ethanol, 40% ethanol, 60% ethanol, and 80% ethanol in turn. The eluted part of 40% ethanol was collected, silica gel column chromatography with elution (trichloromethane : methanol: H_2O = 82 : 16 : 2), Sephadex LH-20 gel column chromatography with methanol elution, and C18 ODS column chromatography with elution (methanol : H_2O = 1 : 1) were applied to purify ophiurasaponin, and then the refined ophiurasaponin was obtained after being concentrated. The colorimetric method was adopted in this experiment to determinate ophiurasaponin content, compared with the standard saponins.

2.2. Identification of Ophiurasaponin. Liebermann-Burchard reaction, melting test, UV-VIS determination of characteristic absorption peak, and infrared spectrum scanning were used to the identification of ophiurasaponin.

2.3. Detection of Antioxidation Capabilities

2.3.1. Determination of the Capacity of Scavenging Hydroxyl Free Radicals. According to the chemiluminescence system of copper sulfate-luminol-vitamin C-hydrogen peroxide [8], Ultra-Weak Luminescence Analyzer was used to detect the capability of the ophiurasaponin scavenging hydroxyl free radicals. The following reagents were added into the sample cell: ophiurasaponin 50 μL (1 mmol/L) (blank sample used as control), ascorbic acid 20 μL (1 mmol/L), luminol 50 μL (1 mmol/L), borate 780 μL (pH 9.24), and hydrogen peroxide 50 μL (1 mmol/L). The analyzers were immediately started and the illumination-intensity was tested within 100 s under the test conditions of T = 30°C and Hi-V: −800 V. The luminescence kinetic curves of hydroxyl inhibited by ophiurasaponin were indicated with illumination time as X-axis and illumination intensity integral as Y-axis. Origin 7.5 was applied to draw the kinetic curve of inhibited hydroxyl illumination by ophiurasaponin. According to the luminescence kinetic curves, the ratio of the inhibition capacities to ophiurasaponin concentration was calculated, and the value of IC_{50} was determined as well.

2.3.2. Determination of the Capacity of Scavenging Superoxide Anion Free Radicals. According to the chemiluminescence system of pyrogallol-luminol [9], various concentrations of ophiurasaponin 50 μL (blank sample used as control) and pyrogallol 50 μL (6.25 mmol/L) were added into the sample cell. The analyzers were started immediately and the illumination-intensity was tested within 20 s under the test conditions of T = 30°C and Hi-V: −900 V. The luminescence kinetic curves of superoxide anion inhibited by ophiurasaponin were indicated with illumination time as X-axis and illumination intensity integral as Y-axis. Origin 7.5 was applied to draw the kinetic curve of inhibited superoxide anion illumination by ophiurasaponin. According to the luminescence kinetic curves, the ratio of the inhibition capacities to ophiurasaponin concentration was calculated, and the value of IC_{50} was determined as well.

2.3.3. Determination of the Capacity of Scavenging Hydrogen Peroxide Free Radicals. According to the chemiluminescence system of hydrogen peroxide-luminol [10], the following reagents were added into the sample cell: various concentrations of ophiurasaponin 50 μL (blank sample used as control), luminol 50 μL (1 mmol/L), carbonate buffer 800 μL (pH 9.5), and 3% hydrogen peroxide 100 μL. The analyzers were started immediately and the illumination-intensity was tested within 100 s under the test conditions of T = 30°C and Hi-V: −850 V. The luminescence kinetic curves of hydrogen peroxide inhibited by ophiurasaponin were indicated with illumination time as X-axis and illumination intensity integral as Y-axis. Origin 7.5 was applied to draw the kinetic curve of inhibited hydrogen peroxide illumination by ophiurasaponin. According to the luminescence kinetic curves, the ratio of the inhibition capacities to ophiurasaponin concentration was calculated, and the value in IC_{50} was determined as well.

2.4. Detection of Antimicrobial Activity. The antimicrobial activity of ophiurasaponin was detected by using circular filter paper method [11]. Cell suspensions were finally diluted to 10^5 CFU/mL in order to be used in the activity assays. Potato Sucrose Agar (PSA) medium (fungi) and Beef Extract Peptone medium (bacteria) were incubated at 25°C for 48 h (fungi) and 37°C for 24 h (bacteria). Chloramphenicol (0.04 g/mL) and miconazole nitrate (0.04 g/mL) were used as the positive control and normal saline (NS) was used as the negative control. The minimum inhibitory concentration (MIC) of ophiurasaponin was determined by modified agar dilution method [12]. The concentration of ophiurasaponin was prepared to 0.06 g/mL, and then it was diluted into 10^{-1}, 10^{-2}, 10^{-3}, 10^{-4}, 10^{-5}, and 10^{-6}, respectively. All the tests were performed in triplicate (n = 3) and the results were expressed as mg/mL.

2.5. Statistical Data Processing. SPSS 11.0 software was used in the single factor analysis of variance by statistically analyzing experimental data, and the results were indicated by the mean standard deviation of plus or minus (+/−s).

3. Results and Discussion

3.1. The Chemical Features of Ophiurasaponin. Measured with ultraviolet absorption method, the content of crude ophiurasaponin was 46.75% and content of the refined ophiurasaponin was 96.72%. Identified by color reaction, ophiurasaponin was determined as steroidal saponins, whose melting points range from 245.4°C to 260.6°C. With ultraviolet visible light scanning within the scope of the 200 nm to 800 nm wavelength, compared with the standard saponins, a maximum absorption peak was identified at 276 nm. In

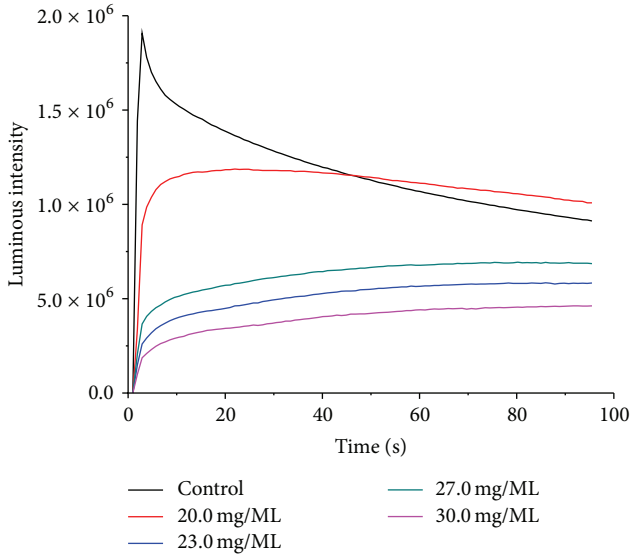

Figure 1: Inhibition of different concentrations of ophiurasaponin to hydroxyl: 20 mg/mL, 23 mg/mL, 25 mg/mL, 27 mg/mL, and 30 mg/mL.

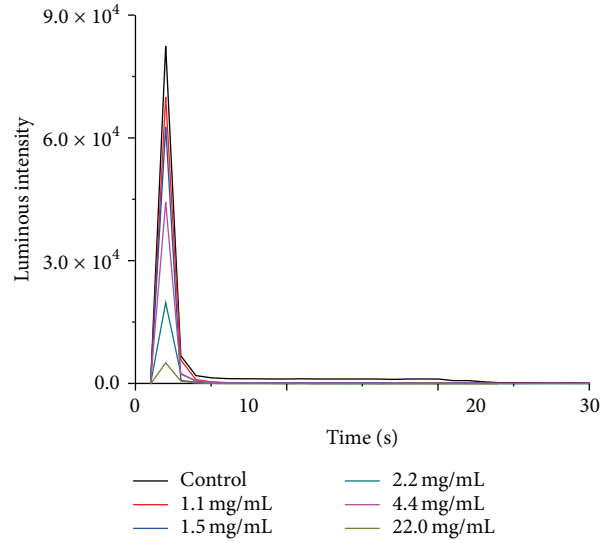

Figure 2: Inhibition of different concentrations of ophiurasaponin to superoxide anion: 1.1 mg/mL, 1.5 mg/mL, 2.2 mg/mL, 4.4 mg/mL, and 22 mg/mL.

400 cm^{-1} ~4000 cm^{-1} range scan, characteristic absorption peak was found similar to the standard saponins in 1030 cm^{-1}, 1336 cm^{-1}, and 1610 cm^{-1}. The result suggested that ophiurasaponin and standard saponins were analogous, but ophiurasaponin showed some differences in the fact that *Ophiopholis mirabilis* came from marine environment and had special structure.

3.2. Antioxidant Capacity. Metabolism of normal physiological process in human body could produce a small quantity of Oxo-free radicalism such as hydroxyl, superoxide anion, and hydrogen peroxide. The amount of free radicals in human body is usually in a homeostasis. A small amount of ROS (reactive oxygen species) free radicals can help transmit energy to maintain the vitality, strengthen the immunity, rid of inflammation, and inhibit tumor, and so forth, while excessive free radicals could interfere with the normal metabolism of human body and lead to sickness [13]. Therefore, the study of free radical scavengers on disease prevention and control is of great significance.

The luminescence kinetic curves of ophiurasaponin inhibiting hydroxyl, superoxide anion, and hydrogen peroxide were shown in Figures 1, 2, and 3, respectively.

The results showed that the antioxidant capabilities increased linearly with the increase of the concentration of ophiurasaponin from *Ophiopholis mirabilis* in a certain range. The inhibition was constant when it increased to a specific concentration. Usually the concentration of ophiurasaponin at 50% of illumination inhibition (IC_{50}) is taken to measure antioxidant capacity of the samples. Lower IC_{50} indicates that it has stronger antioxidant capacity.

As shown in Table 1, the result showed that ophiurasaponin from *Ophiopholis mirabilis* had the strongest inhibition to hydroxyl, the weakest to hydroxyl radicals, and medium to superoxide.

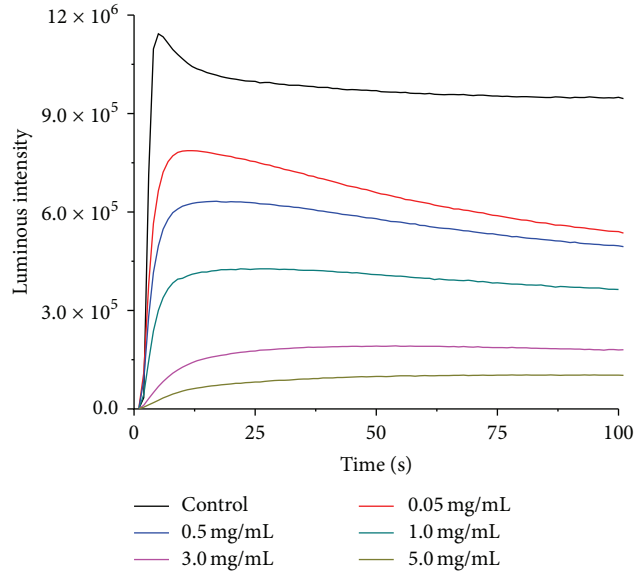

Figure 3: Inhibition of different concentrations of ophiurasaponin to hydrogen peroxide: 0.05 mg/mL, 0.5 mg/mL, 1 mg/mL, 3 mg/mL, and 5 mg/mL.

3.3. Results of Antimicrobial Activity. The antimicrobial activity was expressed as the size of the inhibition zone. The larger the size of inhibition zone is, the stronger the antimicrobial activities. As is shown in Table 2, the inhibitory effect on the tested bacteria of refined ophiurasaponin was enhanced significantly compared with the crude. The result showed that the refined ophiurasaponin had stronger antibacterial activity. what is more, the antibacterial ability of *Aerobacter aerogenes* (28.2 mm) was close to the positive control (31 mm), which declared that ophiurasaponin had strong inhibition effect on *Aerobacter aerogenes*.

Table 1: Capacities of antioxidation of ophiurasaponin $n = 6$.

Superoxide anion		Hydroxyl		Hydrogen peroxide	
Concentration (mg/mL)	Inhibition (%)	Concentration (mg/mL)	Inhibition (%)	Concentration (mg/mL)	Inhibition (%)
22	98.32 ± 0.09	30	77.28 ± 0.10	5	94.01 ± 0.07
4.4	32.05 ± 0.15	27	59.63 ± 0.11	3	72.14 ± 0.08
2.2	19.83 ± 0.06	25	47.45 ± 0.10	1	49.19 ± 0.11
1.5	16.32 ± 0.11	23	34.36 ± 0.05	0.5	38.58 ± 0.06
1.1	10.17 ± 0.08	20	10.14 ± 0.13	0.05	31.86 ± 0.12
The linear regression	$Y = 0.04x + 0.1012$	$Y = 0.0666x - 1.2017$		$Y = 0.1239x + 0.335$	
	$R^2 = 0.9928$	$R^2 = 0.9941$		$R^2 = 0.9918$	
IC_{50} (mg/mL)	9.98 ± 0.12	25.54 ± 0.07		1.37 ± 0.03	

Table 2: Inhibition of ophiurasaponin from *Ophiopholis mirabilis* to bacteria $n = 3$.

Species	Positive control (chloramphenicol)	Crude (mm)	Ophiurasaponin MIC (mg/mL)	Refined (mm)	Ophiurasaponin MIC (mg/mL)
Bacillus subtilis	44.5 ± 0.02	12.2 ± 0.10	1.1 ± 0.05	26.9 ± 0.01	0.0443 ± 0.03
Escherichia coli	51.0 ± 0.04	11.5 ± 0.08	1.1 ± 0.03	32.5 ± 0.03	0.0443 ± 0.03
Staphylococcus aureus	46.0 ± 0.06	11.2 ± 0.07	0.11 ± 0.01	30.9 ± 0.09	0.0443 ± 0.07
Proteusbacillus vulgaris	48.0 ± 0.05	11.2 ± 0.01	—	29.6 ± 0.05	—
Aerobacter aerogenes	31.0 ± 0.06	16.0 ± 0.05	1.1 ± 0.01	28.2 ± 0.04	0.0443 ± 0.01

Note: —: no inhibitory effect.

Table 3: Inhibition of ophiurasaponin from *Ophiopholis mirabilis* on fungi $n = 3$.

Species	Positive control (miconazole nitrate)	Crude (mm)	Ophiurasaponin MIC (mg/mL)	Refined (mm)	Ophiurasaponin MIC (mg/mL)
Penicillium digitatum	21.4 ± 0.03	—	—	—	—
Mucor circinelloides	30.7 ± 0.02	11.5 ± 0.06	1.1 ± 0.03	13.0 ± 0.02	4.43 ± 0.02
Aspergillus flavus	28.7 ± 0.01	—	—	—	—
Saccharomyces cerevisiae	20.7 ± 0.04	—	—	—	—
Saccharomyces cerevisiae Hansen	19.8 ± 0.03	11.2 ± 0.04	1.1 ± 0.04	—	—

Note: —: no inhibitory effect.

As shown in Table 3, ophiurasaponin from *Ophiopholis mirabilis* could inhibit Mucor circinelloides proliferation; however, it had no inhibition on *Penicillium digitatum*, *Aspergillus flavus*, and *Saccharomyces cerevisiae*. The result showed thatcrude ophiurasaponin inhibited the growth of *Saccharomyces cerevisiae* Hansen, but the refined ophiurasaponin did not inhibit its growth, because saponins of other substances in crude ophiurasaponin may be reactive. In addition, theinhibition of ophiurasaponin from *Ophiopholis mirabilis* on fungi was much less effective than that on bacteria.

The minimum inhibitory concentration (MIC) was defined as the lowest concentration of ophiurasaponin that inhibited growth. The MIC value of ophiurasaponin was evidently demonstrated in Table 3. The MIC of refined ophiurasaponin was 0.0443 mg/mL, much lower than that of the crude on bacterial. *Staphylococcus aureus* was the most sensitive bacteria to ophiurasaponin, the MIC value of the crude ophiurasaponin was 0.11 mg/mL, and the MIC value of the refined ophiurasaponin was 0.0443 mg/mL. *Mucor circinelloides* was less sensitive to ophiurasaponin (4.43 mg/mL MIC). Ophiurasaponin was not sensitive to *Proteusbacillus vulgaris, Penicillium digitatum, Aspergillus flavus, and Saccharomyces cerevisiae*. The result illuminated that the antimicrobial ability of ophiurasaponin had a certain selectivity and the antimicrobial ability of ophiurasaponin had a stronger effect on bacteria.

4. Conclusions

The paper showed that ophiurasaponin extracted from *Ophiopholis mirabilis* had excellent antioxidant activity and inhibition on microbial activity. Although further studies are needed to better evaluate its activities and mechanism(s), our

data suggest that ophiurasaponin might be a candidate for the antioxidant and antimicrobial marine drugs.

Conflict of Interests

The authors declare that there is no conflict of interests regarding the publication of this paper.

Acknowledgments

This work was supported by the Shandong province Natural Science Foundation (no. ZR2013DM002). The authors thank Professor Qiusheng Zheng and Huiling Leng for their critical reading of this paper.

References

[1] Y. L. Liao, *Fauna Sinica Invertebrata Echinodermata Ophiuroidea*, vol. 40, Science Press, Beijing, China, 2004.

[2] F. Kisa, K. Yamada, T. Miyamoto, M. Inagaki, and R. Higuchi, "Constituents of holothuroidea, 17. Isolation and structure of biologically active monosialo-gangliosides from the sea cucumber *Cucumaria echinata*," *Chemical and Pharmaceutical Bulletin*, vol. 54, no. 7, pp. 982–987, 2006.

[3] K.-S. Nam and Y.-H. Shon, "Chemopreventive effects of polysaccharides extract from *Asterina pectinifera* on HT-29 human colon adenocarcinoma cells," *BMB Reports*, vol. 42, no. 5, pp. 277–280, 2009.

[4] R. Bannister, I. M. McGonnell, A. Graham, M. C. Thorndyke, and P. W. Beesley, "Afuni, a novel transforming growth factor-β gene is involved in arm regeneration by the brittle star *Amphiura filiformis*," *Development Genes and Evolution*, vol. 215, no. 8, pp. 393–401, 2005.

[5] T. Fujita and S. Ohta, "Spatial structure within a dense bed of the brittle star *Ophiura sarsi* (Ophiuroidea: Echinodermata) in the bathyal zone off otsuchi, Northeastern Japan," *Journal of the Oceanographical Society of Japan*, vol. 45, no. 5, pp. 289–300, 1989.

[6] C. H. Guo, H. Z. Jin, X. J. Ni et al., "Preparation and primary identification of ophiurasaponin from *Ophiura kinbergi*," *Current Zoology*, vol. 47, pp. 131–133, 2001.

[7] C. W. Lin, J. Y. Su, L. M. Zeng et al., "Chemical constituents of axtroclarus conferus," *Journal of Instrumental Analysis*, vol. 7, pp. 59–61, 2002.

[8] S. Hanaoka, J.-M. Lin, and M. Yamada, "Chemiluminescence behavior of the decomposition of hydrogen peroxide catalyzed by copper(II)-amino acid complexes and its application to the determination of tryptophan and phenylalanine," *Analytica Chimica Acta*, vol. 409, no. 1-2, pp. 65–73, 2000.

[9] L. Jian, "Increased carbon disulfide-stimulated chemiluminescence in the pyrogallol-luminol system," *Luminescence*, vol. 16, no. 4, pp. 281–283, 2001.

[10] F. J. Pérez and S. Rubio, "An improved chemiluminescence method for hydrogen peroxide determination in plant tissues," *Plant Growth Regulation*, vol. 48, no. 1, pp. 89–95, 2006.

[11] H. D. Chludil, A. M. Seldes, and M. S. Maier, "Antifungal steroidal glycosides from the Patagonian starfish *Anasterias minuta*: structure—activity correlations," *Journal of Natural Products*, vol. 65, no. 2, pp. 153–157, 2002.

[12] R. Kumar, A. K. Chaturvedi, P. K. Shukla, and V. Lakshmi, "Antifungal activity in triterpene glycosides from the sea cucumber *Actinopyga lecanora*," *Bioorganic and Medicinal Chemistry Letters*, vol. 17, no. 15, pp. 4387–4391, 2007.

[13] H. Ahsan, A. Ali, and R. Ali, "Oxygen free radicals and systemic autoimmunity," *Clinical and Experimental Immunology*, vol. 131, no. 3, pp. 398–404, 2003.

Hindawi Publishing Corporation
Journal of Chemistry
Volume 2014, Article ID 525141, 9 pages
http://dx.doi.org/10.1155/2014/525141

Research Article

Purification and Characterization of Bioactive Compounds from *Styela clava*

Bao Ju,[1] Bin Chen,[2] Xingrong Zhang,[1] Chunling Han,[1] and Aili Jiang[1]

[1] *Department of Bioengineering, Yantai University, Yantai, Shandong 264005, China*
[2] *Yantai Institute of Coastal Zone Research Chinese Academy of Sciences, Yantai, Shandong 264003, China*

Correspondence should be addressed to Aili Jiang; jal9035@live.cn

Received 17 March 2014; Accepted 1 April 2014; Published 30 April 2014

Academic Editor: Qiusheng Zheng

The immunomodulatory activity of extract from *Styela clava* was studied systematically based on activity tracking *in vitro* in order to find out novel-structured secondary metabolite. The proliferation rates of mouse splenic lymphocytes and peritoneal macrophages were used as screening index, as well as NO release promoting activities. The crude extract (CE) and its different polar fractions from *S. clava* all exhibited proliferative activity of splenolymphocytes and mouse macrophages, as well as NO release promoting activities, among which petroleum ether fraction (PE) showed the strongest effect. The antioxidant experiment *in vitro* showed that CE demonstrated antioxidant ability in 1,1-diphenyl-2-picrylhydrazyl (DPPH) system and the beta carotene-linoleic acid system; the activity of ethyl acetate fraction (ET) was much stronger than that of the others. Further isolated by silica gel column chromatography, ET was classified into seven sub-components (E1~E7) listed in the order of activity as E5 > E6 > E4 > E3 > E7 > E2 > E1. Five compounds were separated as (1) cholesteric-7-en-3β-ol, (2) cholesteric-4-en-3β,6β-diol, (3) cholesterol, (4) batilol, and (5) ceramide, among which (1), (2), and (4) were isolated for the first time from *S. clava*.

1. Introduction

The ascidians are commonly found in waters all over the world, along the coasts and deep to the bottoms, which is the most important marine source for active agents except sponge. In the early 1970s, it had been found that the extract from ascidians had a variety of bioactivities such as cytotoxicity, antitumor *in vivo*, and immune regulation. Since 1980s, a greater variety of bioactive substances were extracted from the ascidians with the activities of antitumor, antivirus, antimicrobial, immune regulation, and biocatalysis. Further studies showed that those active chemical compounds in sea squirt mainly included peptides, alkaloids, polyethers, macrolides, terpenes, and polysulfides [1–9], among which some have been tested at the clinical phase as anticancer reagents [10–13].

By strengthening organisms' defense and host immune system against tumor cells, cell immunity can improve its overall antitumor ability to inhibit tumor and thus play an important role in immune antitumor treatment. Alcohol from *Styela clava* (5α,8α-cyclicobioxygen-24-bimethyl-6-vinyl-3β-cholesterol, SC), a lead compound against a variety of viruses, has a wide application to immune regulation as a supplement to maintain normal immune response for the removal of viruses and recovery [14].

The ascidian has become the hot topic for research and development both at home and abroad for its numerous active agents with high activity. *Styela clava*, the dominant population in the Yellow Sea and the Bohai Sea, has a negative impact on marine culture for its wide distribution and large quantity while the changes in its population may be regarded as an index for environment contamination. If fed in sea water in proper conditions, *S. clava* may grow and reproduce very fast with low cost; therefore, with rational exploitation, *S. clava* can become treasures instead of waste to benefit both economy and environment protection.

S. clava remains neglected as a potential marine chemical resource, and there are few reports on its components

worldwide besides few individual components without in-depth investigation. Up to now, there have been no reports of the systemic in-depth study on *S. clava*'s compounds and their activity. Integrated exploitation of its active agents may on one hand provide theoretical basis for resource exploitation to achieve maximum economic results and on the other improve our lives and medical care to achieve direct social results.

This paper is a study on *S. clava* in terms of its chemical structure and bioactivity to obtain novel-structured active agents as a theoretical basis for new drugs or lead compound for new drugs. These studies may be used as references for the research and development of marine functional food and drugs.

2. Materials and Methods

2.1. Materials. *Styela clava* was collected from Yantai Sishiliwan Bay, Shandong Province, China, in August 2010; adherents were removed and frozen.

Kunming mice of clean grade were purchased from Shandong Animal Experiment Center, with weight being 18–22 g for each.

ConA, LPS, MTT, peptone, 1,1-DPPH, β-carotene, and linoleic acid were purchased from Sigma Chemical Co. (USA), RPMI1640 from Gibco, fetal bovine serum from HyClone, DMSO from AMRESCO, and penicillin and streptomycin from Shandong Lukang Pharmaceutical Group Co., Ltd. Other analytical reagents were purchased from home markets.

2.2. Methods

2.2.1. Extraction of Active Agents from S. clava. Tissue of *S. clava* (15 kg) was minced, centrifuged, and then soaked in 95% ethanol three times in volume for 1 week at room temperature. The extraction was repeated three times. The combined extract was concentrated under vacuum to give a crude extract (CE) as brown extractum of 205 g. The crude extract was suspended in distilled water of 2000 mL and then further extracted with petroleum ether, chloroform, ethyl acetate, and butanol (800 mL ×3), respectively, resulting in petroleum ether extract (PE) 78.7 g, ethyl acetate extract (ET) 18.6 g, butyl alcohol extract (BU) 40.2 g, and the remainder (AR) 64.7 g.

2.2.2. Isolation, Purification, and Structural Identification of the Chemical Components from S. clava. After activity screening, normal phase silica gel column chromatography (CC) and ODS reversed phase silica gel column chromatography were adopted, respectively, for the most active ET, while petroleum ether and acetone, chloroform and carbinol were used for silica gel column chromatography gradient elution. Seven components (E1–E7) were isolated, among which components E2, E3, E4, and E5 for their large quantity were further purified by Sephadex LH-20, PTLC, Amberlite XAD-2, and recrystallization and 5 compounds were obtained and their structures were identified by IR (Nicolet impact 400), MS (HP 5988A GC/MS), and 1D NMR and 2D NMR (Bruker-500 MHz-FT-NMR).

2.2.3. Proliferation of Spleen Lymphocyte. Ten days after vaccinated S180, Kunming mice of clean grade were killed by cervical dislocation and spleens were taken out under asepsis for the preparation of lymphocyte suspension which was incubated in the 96-well plates (Coastar, USA) at the concentration of 1×10^7 cells/mL with 100 μL for each well and six repeats for each treating. Medium of 100 μL was added to the control group, 10 μg/mL ConA to the positive group and the sample solutions of different concentration to the experiment groups resulting in the concentrations of 12.5, 25, 50, 100 and 200 μg/mL, cultured at 37°C in 5% CO_2 incubators (by SHEL LAB) for 44 h, and, afterwards, 5 mg/mL of MTT was added with 20 μL for each well and further cultured for 4 h. After the media were removed, 0.15 mL of DMSO was added to each well and shaken for 10 min for complete mixture at room temperature for 10 min before ELX-800 (BioTek Instruments Inc.) was used to measure absorbance at 570 nm. Consider

$$\text{Proliferation ratio of lymphocytes (\%)} = \left[\frac{A_{\text{sample}} - A_{\text{control}}}{A_{\text{control}}}\right] \times 100\%, \quad (1)$$

where A_{sample} is the absorbance of tested sample and A_{control} is the absorbance of control group.

2.2.4. Proliferation of Macrophages. 2% (w/v) peptone of 2 mL was injected into the mice's peritoneal cavity every day for three days. After cervical dislocation, precooled Hank's of 5 mL was injected into the peritoneal cavity; then abdominal fluid was sucked and the supernatant was removed by centrifugation at 2000 rpm; the precipitate cells were washed twice.

1×10^6/mL of cell suspension was made with 10% of calf serum in RPMI 1640, incubated in the tissue culture plate with 100 μL for each well and cultured at 37°C in 5% CO_2 incubators for 2 h. The upper medium was removed and the wells were washed with PBS twice to remove the nonadherent cells; so macrophage monolayers were obtained. Fresh medium was put into the 96-well plates, following with fresh medium of 100 μL to the control group, 100 μL LPS to the positive group (with final concentration of 2 μg/mL), and 100 μL different samples of different concentrations to the other groups (the sample concentrations are as in Section 2.2.3), and cultured at 37°C in 5% CO_2 incubators for 24 h. Afterwards, upper medium was removed and new medium was added with 100 μL for each hole as well as 5 mg/mL of MTT with 20 μL, further cultured for 4 h; then the supernatant was carefully sucked and 150 μL DMSO was added before shaking for 10 min for complete mixture. After

placing at room temperature for 10 min, ELX-800 was used to measure absorbance at 570 nm. Consider

$$\text{Proliferation ratio of macrophages (\%)} = \left[\frac{A_{\text{sample}} - A_{\text{control}}}{A_{\text{control}}}\right] \times 100\%, \quad (2)$$

where A_{sample} is the absorbance of tested sample and A_{control} is the absorbance of control group.

2.2.5. NO Release Activities of Macrophages. Macrophages were prepared with the same method as in Section 2.2.4.

2.5×10^5/mL of cell suspension was made with 10% of calf serum in RPMI 1640, in sterile conditions inoculated on the tissue culture plate with 100 μL for each well and three wells for each sample were cultured at 37°C in 5% CO_2 incubators for 2 h. Then LPS solution (with final concentration of 2 μg/mL) of 100 μL was put into the positive group, medium 1640 of 100 μL was added to the control group, and 100 μL with different samples of different concentrations was added to the other groups, and further cultured for 48 h. Afterwards, upper medium of 50 μL from each well was removed and transferred to a new 96-well plate and measured according to the following method.

Standard Curve. Standard solution nitrite of 0.1 mol/L was diluted in 1 : 1000 with medium. A1~H3 on the tissue culture plate were used for standard curve. Standard solution nitrite of 100 μL was put into A1~A3, respectively, and medium of 50 μL was put into B1-H3, respectively. Doubling dilution was conducted to A–G in turn and the final fluid from G was removed and nitrite concentration coefficient (100, 50, 25, 12.5, 6.25, 3.13, 1.56, and 0 μmol/L) was obtained. Standard curve was necessary before each test with the same medium as for the samples.

Measurement. NED solution and sulfanilamide solution were kept at room temperature for 15 to 30 min. Each of tested samples of 100 μL was placed on the tissue culture plate, 2 to 3 repeated wells were used for every sample. Sulfanilamide solution of 50 μL was put into all standard curve wells and sample wells were kept in dark place at room temperature for 5 to 10 min and then the same was done with NED solution of 50 μL. Absorbance at 540 nm was measured within 30 min and the nitrite concentration in the samples was calculated according to standard curve.

2.2.6. In Vitro Antioxidant Activity

(1) DPPH Radical Scavenging Assay. Modified Binsan's method [15] was adopted. 1.5 mL sample in different concentrations was added to 1.5 mL of 0.2 mM DPPH in ethanol.

1.5 mL DPPH of 0.2 mmol in anhydrous ethanol was added to all the samples of 1.5 mL, after mixing vigorously, and kept at room temperature in dark for 30 min. The absorbance of the resulting solution was measured at 517 nm with water as the control and the ability to scavenge the DPPH radical was expressed by clearance rate (E) in the following formula:

$$E\,(\%) = \left[1 - \frac{A_{\text{sample}} - A_{\text{sample blank}}}{A_{\text{control}}}\right] \times 100\%, \quad (3)$$

where A_{sample} means the absorbance of test sample solution (DPPH + sample), $A_{\text{sample blank}}$ means the absorbance of the sample only (ethanol + sample), and A_{control} means the absorbance of control (DPPH + ethanol).

The half clean concentration (EC_{50}) is calculated by regression equation of E and sample concentration.

(2) β-Carotene-Linoleic Acid System. Modified Jayaprakasha's method [16] was adopted. β-carotene of 0.2 mg was dissolved in 0.2 mL trichloromethane, into which linoleic acid of 20 mg and Tween-40 of 200 mg were added and mixed completely. After chloroform was removed under vacuum at 40°C, distilled water of 50 mL (oxygenated for 2-3 min) was added. The reaction emulsion was prepared after vigorous agitation. The control was prepared as above except for the addition of β-carotene. Sample solution of 50 μL and reaction medium of 200 μL were added into 96-well plates, respectively, and the absorbance was measured at 450 nm immediately ($t = 0$), and remeasured every 20 min until the color of β-carotene faded in the control (about 240 min). Three parallel measurements were conducted and the antioxidant activity (AA) was expressed in the following formula:

$$\text{AA} = \left[1 - \frac{A_0 - A_t}{A_0' - A_t'}\right] \times 100, \quad (4)$$

where A_0 and A_t were the absorbance of the sample, while $t = 0$ and $t = 240$ min, respectively, and A_0' and A_t' were the absorbance of the control, while $t = 0$ and $t = 240$ min, respectively.

(3) Reducing Power. The reducing power was determined according to Yen and Duh's method [17]. All samples were dissolved with phosphate buffer solution (0.2 mol/L, pH 6.6) of 2.5 mL, and 1% potassium ferricyanide (w/v) of 2.5 mL was added before reacting at 50°C for 20 min; then 10% trichloroacetic acid (w/v) of 2.5 mL was added to stop reaction. Reaction mixture was centrifuged at 650 ×g for 10 min; supernatant of 2.5 mL was mixed with distilled water of 2.5 mL and 0.1% $FeCl_3$(w/v) of 0.5 mL. The absorbance was measured at 700 nm and the higher absorbance means the stronger reducing power. The reducing power is converted in ascorbic acid and expressed as ascorbic acid equivalent (AscAE) in milligrammes of ascorbic acid per gramme of sample (AscAE: mg/g AscA).

2.3. Statistical Analysis. All data were expressed by mean ± standard deviation. All statistical analyses were carried out using SPSS 13.0 for Windows. Tukey's multiple comparison tests were used to detect differences between groups, and a probability of $P < 0.05$ was taken as an acceptable level of significance.

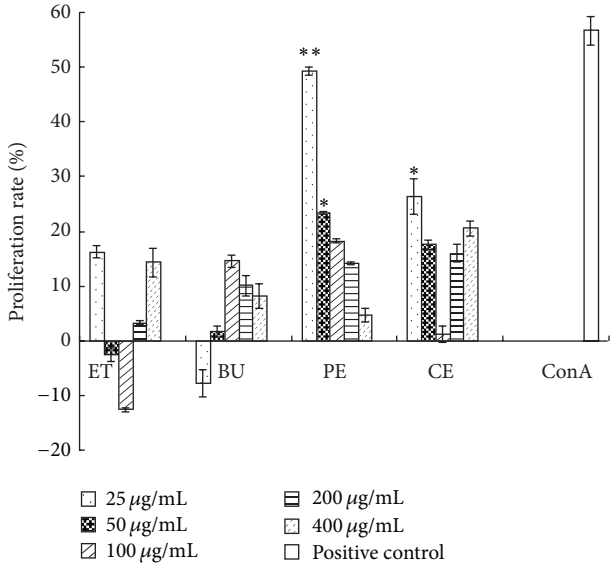

Figure 1: Effects of extracts on the proliferation of the mouse splenocytes. $^{*}P < 0.05$ and $^{**}P < 0.01$ compared with the control.

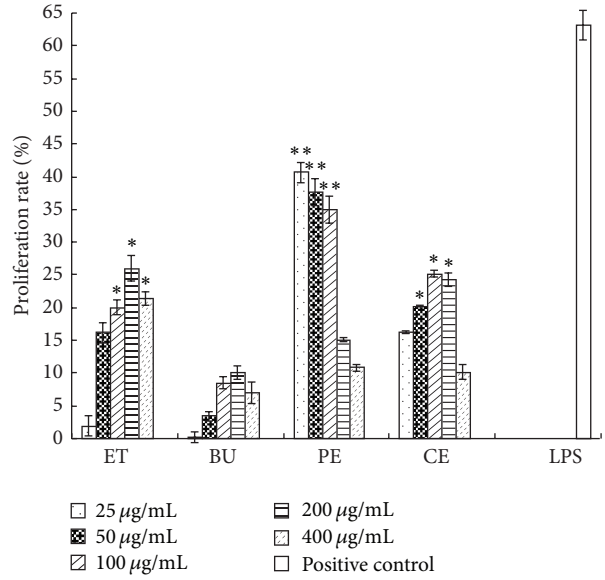

Figure 2: Effects of extracts on the proliferation of the mouse peritoneal macrophages. $^{*}P < 0.05$ and $^{**}P < 0.01$ compared with the control.

3. Results and Discussion

3.1. Proliferation of Spleen Lymphocyte. As organism's first line defending tumor, immune system plays an important role in the recognition and removal of malignant cells. The immune status evaluation of the body bearing neoplasm is important for mechanism study of antitumor drugs.

As shown in Figure 1, four extracts of *S. clava* demonstrate significant activity on splenocytes proliferation (compared with the control, $P < 0.05$, or $P < 0.01$), among which the proliferation effect of PE is the most active, with proliferation rate being near 50% at a concentration of 25 μg/mL, close to the positive control group ConA (56.71%). However, its proliferation rate reduces with the increasing concentration, and the proliferation rate is only 4.76% when the concentration reaches 400 μg/mL, which shows that PE inhibits the proliferation of the mouse splenocytes at high concentration. CE is less active than PE on the proliferation of the mouse splenocytes, demonstrating a rising trend at first and then a falling one. The effects of ET and BU are relatively weak, and ET shows distinctive inhibition at 50 μg/mL and 100 μg/mL with the inhibition rate of 12.62% at 100 μg/mL, but, on the contrary, BU reaches the strongest level at this concentration with the proliferation rate of 14.52%, while distinctive inhibition was shown below this point.

3.2. Proliferation of Macrophages. Figure 2 shows the effects of *S. clava*'s extracts on the proliferation of the mouse peritoneal macrophages. The four extracts all show significant effect on the proliferation of the mouse macrophages at all designed concentrations (compared with the control, $P < 0.05$ or $P < 0.01$), but it is weaker than that of the positive control LPS as proliferation rate of 63.19%. PE is the most active extract on the proliferation at concentration of 25 μg/mL, with proliferation rate 40.70%, but, afterwards, the proliferation rate drops with the increasing concentration and the proliferation rate is only 10.85% when the concentration reaches 400 μg/mL, showing similar trend as on the lymphocytes.

ET and CE are close on the effect of proliferation. ET reaches the lowest point at 25 μg/mL with the proliferation rate of 1.94% and the highest point at 200 μg/mL with the proliferation rate of 25.97%. CE shows similar trend as ET, reaching the highest and lowest points at 100 μg/mL and 400 μg/mL with the proliferation rate of 25.19% and 10.17%, respectively. BU shows the weakest effect, with the highest proliferation rate of only 10.08% at 200 μg/mL and the same effect as the control at 25 μg/mL; the proliferation rates at all the other concentrations are all below 10%.

3.3. NO Release Activities of Macrophages. Macrophages are the important components in the body immune system, functioning as immunization effect regulating the immune system, and NO is one of the active agents produced by macrophages, after they are activated [18]. Figure 3 shows effects of extract from *S. clava* on the NO release activities of mouse macrophages. The effects of ET, PE, and CE are all in positive correlation with concentration in promoting the release of NO. PE shows the strongest effect among them, reaching the highest point of 16.14 μmol/mL at 400 μg/mL. CE is less effective with NO releasing the highest point of 14.76 μmol/mL at 400 μg/mL. The effects of BU and ET are rather weak, only 8.70 μmol/mL for ET at 400 μg/mL as the highest point, while, at the other concentrations, the NO releasing abilities for ET and BU are close to and approaching 6 μmol/mL.

Table 1: DPPH scavenging activity of different components isolated from *S. clava*.

Component	DPPH scavenging rate (%)			
	50 (μg/mL)	100 (μg/mL)	150 (μg/mL)	200 (μg/mL)
CE	19.2 ± 0.37	30.12 ± 0.60	37.9 ± 0.64	42.6 ± 0.88
PE	4.83 ± 0.11	10.11 ± 0.22	14.24 ± 0.38	18.50 ± 0.37
ET	22.90 ± 0.70	38.10 ± 1.14	47.48 ± 1.30	50.64 ± 1.12
BU	8.38 ± 0.21	19.29 ± 0.37	25.32 ± 0.49	30.77 ± 0.62
AR	2.10 ± 0.05	3.05 ± 0.11	4.26 ± 0.08	4.89 ± 0.10

Table 2: DPPH scavenging activity of subcomponents E1–E7 isolated from ET of *S. clava*.

Subcomponent	DPPH scavenging rate (%)			
	50 (μg/mL)	100 (μg/mL)	150 (μg/mL)	200 (μg/mL)
ET	22.90 ± 0.70	38.10 ± 1.14	47.48 ± 1.30	50.64 ± 1.12
E1	8.24 ± 0.26	14.17 ± 0.40	18.64 ± 0.59	20.80 ± 0.65
E2	11.37 ± 0.38	18.19 ± 0.88	24.30 ± 1.62	29.18 ± 1.25
E3	18.46 ± 0.64	25.30 ± 1.24	34.28 ± 1.22	45.80 ± 0.99
E4	22.80 ± 0.32	38.20 ± 1.02	49.37 ± 1.57	56.78 ± 1.01
E5	30.26 ± 0.88	46.20 ± 0.92	59.16 ± 1.11	67.31 ± 1.65
E6	24.92 ± 0.77	42.00 ± 1.06	53.40 ± 0.70	64.42 ± 1.62
E7	14.00 ± 0.31	20.29 ± 0.66	27.13 ± 0.48	32.50 ± 1.01

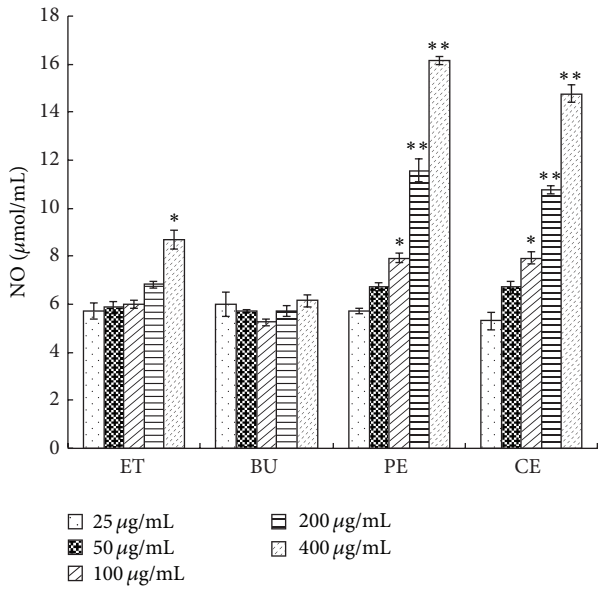

Figure 3: Effects of extracts on NO production. $^{*}P < 0.05$ and $^{**}P < 0.01$ compared with the control.

3.4. In Vitro Antioxidant Activity

3.4.1. DPPH Radical Scavenging Assay. The DPPH free radicals scavenging method is a colorimetric assay and can be used to evaluate the radical scavenging activity in a short time. DPPH is an organic free radical with maximal absorption at 517 nm. When with free radical scavenger, DPPH's lone electron will be paired and its absorbance will decrease, which can be used to evaluate its antioxidant activity. As shown in Table 1, there was a positive correlation between DPPH scavenging activity of CE and its concentration. Among the four extracted components, PE and BU demonstrate poor scavenging activity, while AR shows no scavenging activity. The scavenging activity of ET reaches 50.64% at 200 μg/mL, much higher than CE ($P < 0.05$), indicating that compounds with DPPH scavenging activity in *S. clava* are mostly medium polar.

E1–E7 subcomponents are isolated from ET with silica gel column chromatography, whose DPPH scavenging activity is shown in Table 2. At all experiment concentrations, E5 shows the strongest scavenging activity followed by E6, E4, E3, E7, and E2 with E1 the weakest. E5 and E6 show much stronger scavenging activity than ET ($P < 0.05$), while E4 is close to ET in scavenging activity. EC_{50} of E5 and E6 are 122.06 μg/mL and 139.68 μg/mL, respectively.

3.4.2. Antioxidant Activity in β-Carotene-Linoleic Acid System. β-carotene is a polyene pigment apt to be oxidized to fade. In the reaction medium, the superoxide produced by the oxidized linoleic acid results in β-carotene's fading, and, as time goes on, the absorbance decreases. The degree of β-carotene's fading depends on the antioxidant activity in the system. Table 3 shows antioxidant activities of different components isolated from *S. clava* in the β-carotene-linoleic acid system. CE has some antioxidation activities, positively correlated with its concentration. ET is much higher in its antioxidant activity than other components, reaching 50% at 200 μg/mL and is even higher than the positive control AscA at all experimental concentrations, which further indicates that compounds with higher antioxidant activity in the β-carotene-linoleic acid system are mostly medium-polar components.

Table 3: Antioxidant activity of different components isolated from *S. clava* in the β-carotene-linoleic acid system.

Component	Antioxidant activity (%)			
	10 (μg/mL)	50 (μg/mL)	100 (μg/mL)	200 (μg/mL)
CE	10.62 ± 0.38	20.10 ± 1.12	29.48 ± 1.30	40.35 ± 1.12
PE	4.60 ± 0.21	10.22 ± 0.44	16.50 ± 0.49	22.40 ± 0.68
ET	12.70 ± 0.65	28.76 ± 1.12	37.42 ± 0.88	48.37 ± 1.55
BU	7.20 ± 0.48	14.39 ± 0.62	22.60 ± 0.77	26.00 ± 0.89
AR	2.15 ± 0.05	6.90 ± 0.14	8.20 ± 0.18	9.80 ± 0.11
AscA	10.50 ± 0.12	20.70 ± 0.31	32.90 ± 0.18	46.60 ± 0.32

Table 4: Antioxidant activity of subcomponents E1–E7 isolated from ET in the β-carotene-linoleic acid system.

Subcomponent	Antioxidant activity (%)			
	10 (μg/mL)	50 (μg/mL)	100 (μg/mL)	200 (μg/mL)
ET	12.70 ± 0.65	28.76 ± 1.12	37.42 ± 0.88	48.37 ± 1.55
E1	6.46 ± 0.50	13.80 ± 0.46	28.20 ± 0.64	22.19 ± 0.97
E2	7.42 ± 0.31	15.40 ± 0.74	24.74 ± 1.07	30.90 ± 1.21
E3	9.30 ± 0.37	17.78 ± 0.87	27.41 ± 1.03	32.77 ± 1.27
E4	12.38 ± 0.67	24.72 ± 1.18	32.70 ± 0.79	43.65 ± 1.98
E5	20.24 ± 1.44	40.60 ± 1.25	54.10 ± 1.57	68.92 ± 1.67
E6	15.20 ± 0.79	34.40 ± 0.85	48.52 ± 1.71	62.36 ± 1.68
E7	10.70 ± 0.47	20.10 ± 0.27	28.42 ± 0.80	36.80 ± 0.98
AscA	10.50 ± 0.72	20.70 ± 0.31	32.90 ± 0.18	46.60 ± 0.32
GA	21.80 ± 0.41	42.80 ± 1.88	58.61 ± 1.20	70.10 ± 1.46

Table 5: Reducing power of extract and subcomponents E1–E7 isolated from ET.

Component	AscAE (mg/g AscA)
CE	40.20 ± 1.10
PE	14.32 ± 0.42
ET	62.60 ± 1.55
BU	26.60 ± 0.51
WT	5.72 ± 0.26
E1	20.40 ± 0.77
E2	28.20 ± 1.22
E3	46.20 ± 1.18
E4	61.60 ± 1.11
E5	84.40 ± 2.10
E6	75.20 ± 1.50
E7	41.60 ± 0.95

The antioxidant activity of subcomponents E1–E7 isolated from ET in the β-carotene-linoleic acid system is shown in Table 4. At all experiment concentrations, E5 shows the strongest antioxidant activity followed by E6, E4, E7, E3, and E2 with E1 being the weakest. Among the seven subcomponents E5 and E6 show much stronger antioxidant activity than ET ($P < 0.05$), while the antioxidant activity of E5 is 68.92% at 200 μg/mL close to the synthesized antioxidant GA.

3.4.3. Reducing Power. Table 5 shows the reducing power of the extract from *S. clava* and subcomponents E1–E7 isolated from ET. The reducing powers of all the samples demonstrate a pattern similar to DPPH scavenging activity and antioxidant activity in the β-carotene-linoleic acid system. Among all the extracted components, ET is the highest in the reducing power ($P < 0.05$) and the reducing power of the seven subcomponents isolated from ET is in the following order: E5 > E6 > E4 > E3 > E7 > E2 > E1.

3.5. Structural Identification of Compound. Compound 1, colorless needle crystal, is identified as $C_{27}H_{46}O$ with EI-MS and NMR. δ3.47 in ^{1}H NMR, δ7.18 in ^{13}C NMR, and DEPT show that there is hydroxyl in the molecule. δ5.31 in ^{1}H NMR, δ140.18 and δ121.7 in ^{13}C NMR, and DEPT further confirm the double bond in the molecule. m/z 255 and 147 in MS combined with δ5.31 (1H, H-7), δ3.56 (1H, m, H-3), δ1.01 (3H, s, Me-19), and δ0.88 (3H, s, Me-18) in ^{1}HMMR, δ140.8 (s, C-8), δ121.7 (d, C-7), and δ71.8 (d, C-3) in ^{13}C NMR, and DEPT referred to the physical constant and spectral data reported by Tsuda and Schroepfer Jr [19]; compound 1 was identified as cholesteric-7-en-3β-ol, which was isolated from *S. clava* for the first time.

Compound 2, colorless needle crystal, mp 244~246°C is identified as $C_{27}H_{46}O_2$ with EI-MS and NMR. The two signals of methyl group connected with quaternary carbon (δ1.26, s; δ0.71, s) and three signals of methyl group connected with tertiary carbon (δ0.91, d; δ0.87, d; δ0.85, d) show that this compound is sterol. The signal of 19-Me at δ1.26 shifts to a lower field in contrast to cholesterol, which proves the existence of 6β-OH. Meanwhile, in contrast to cholesterol, signal (δ4.18) of 3α-H also shifts to a lower field and so is

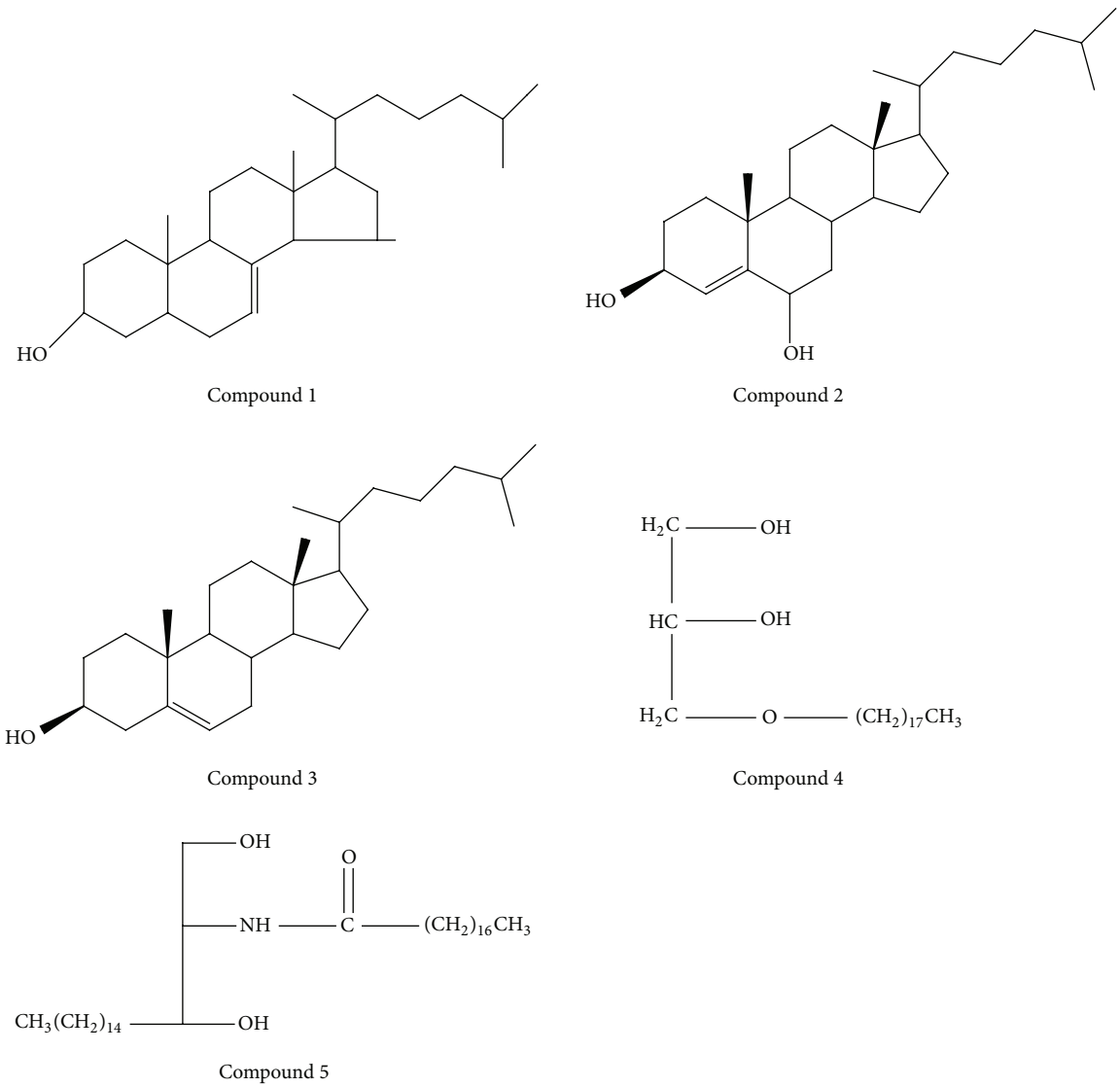

Figure 4: Structures of compounds.

proved of 4,5-double bond considering single peak δ5.55. Compound 2 is identified as cholesteric-4-en-3β, 6β-diol, referring to the physical constant and spectral data reported by Wahidullah et al. [20], which is isolated from *S. clava* for the first time.

Compound 3 is a white needle crystal, mp 148~149°C, purplish red at 10% sulfuric acid-ethanol solution. The multiple peaks at δ3.53 in ^{1}H NMR is the characteristic signal of 3α-H in sterol, while the multiple peaks at δ5.35 is signal of H-6. In addition, five methyl group signals appear in high field of ^{1}H NMR, among which the δ1.01, s and δ0.68, s belong to 19-Me and 18-Me, respectively, δ0.91, d is the signal of 21-Me, and δ0.84, d and δ0.82, d belong to 26-Me and 27-Me, respectively. Contrasting the physical constant and spectral data with Su et al. [21], compound 3 is identified as cholesterol.

Compound 4 is white powder, mp 68~69°C, purplish red at 10% sulfuric acid-ethanol solution. The molecular weight is 345 according to EI-MS. As shown in ^{13}C NMR spectrum, δ64.1 (t, C-1), δ31.9 (t, C2), δ29.6 (t, C3-C15), δ26.0 (t, C16), δ22.6 (t, C17), and δ14.1 (t, C18) are characteristic signals of long chain fatty acid, and δ72.2 (C-1), δ70.6 (C-2), and δ71.8 (C-3) belong to glycerol; so this compound should be a long chain triglyceride. However, there is no signal of ester carbonyl; therefore, this compound is identified as glycidyl ether, agreeing with Yang et al. [22] and Wang et al. [23], and is confirmed as batilol, which is isolated from *S. clava* for the first time.

Compound 5, molecular formula is $C_{36}H_{71}NO_3$ according to EI-MS and NMR. δ6.37 (1H) in ^{1}H NMR spectrum and δ173.9 (C=O) in ^{13}C NMR spectrum proves the existence of acylamino, and δ54.5 in ^{13}C NMR spectrum indicates that what is connected with nitrogen is methyne. δ2.02 (2H) in ^{1}H NMR indicates that there are two –OH in the compound, and δ74.74 and δ62.40 in ^{13}C NMR indicate that –CH– and –CH_2– connect with –OH, respectively. Meantime, a strong

hydrogen signal of δ1.26 in ^{1}H NMR spectrum and two signals $-CH_3-$ of δ0.84 (6H) determine two long chain alkyl groups. This compound is identified as ceramide referring to the physical constant and spectral data reported by Yu and Yang [24].

The structures of these compounds are shown in Figure 4. As reported by Cai et al. [25], the number and position of hydroxyl groups largely determined radical scavenging activity of phenolic compounds. Compounds 1, 2, and 3 all have only one phenolic hydroxyl group, and there is no functional groups in orthoposition; little steric hindrance effect increased their contact with free radicals.

4. Conclusion

The immunomodulatory and antioxidant activity of crude and fractionated extracts of the ascidian *Styela clava* were determined by *in vitro* screening. All these extracts demonstrate immunomodulatory activity through increasing the proliferation rate of spleen lymphocyte and macrophages, as well as the NO release activities of macrophages. Among them the petroleum ether fraction shows the strongest immune active *in vitro*. The ethyl acetate fraction (ET) was much higher in its antioxidant activity in DPPH system, reducing power assay and β-carotene-linoleic acid system compared with the other fractions, and its subcomponent E5 demonstrated the strongest antioxidant activity as well as reducing power, higher than the positive control AscA and close to the synthesized GA. ET was isolated systemically and five compounds were separated as (1) cholesteric-7-en-3β-ol, (2) cholesteric-4-en-3β,6β-diol, (3) cholesterol, (4) batilol, and (5) ceramide, among which (1), (2), and (4) were isolated for the first time from *S. clava*.

Conflict of Interests

The authors declare that there is no conflict of interests regarding the publication of this paper.

Authors' Contribution

Ju Bao and Chen Bin contributed equally to this project.

Acknowledgments

This study was supported by the National Natural Science Foundation of China (no. 31070368) and the Science and Technology Department of Shandong Province (BS2010HZ022 and ZR2011DL008).

References

[1] T. M. Zabriskie and C. M. Ireland, "The isolation and structure of modified bioactive nucleosides from *Jaspis johnstoni*," *Journal of Natural Products*, vol. 52, no. 6, pp. 1353–1356, 1989.

[2] J. Kobayashi, M. Tsuda, M. Ishibashi et al., "Amphidinolide F, a new cytotoxic macrolide from the marine dinoflagellate *Amphidinium sp*.," *Journal of Antibiotics*, vol. 44, no. 11, pp. 1259–1261, 1991.

[3] B. S. Davidson and C. M. Ireland, "Lissoclinolide, the first non-nitrogenous metabolite from a *Lissoclinum* tunicate," *Journal of Natural Products*, vol. 53, no. 4, pp. 1036–1038, 1990.

[4] T. N. Makarieva, V. A. Stonik, A. S. Dmitrenok et al., "Varacin and three new marine antimicrobial polysulfides from the far-Eastern ascidian *Polycitor sp*," *Journal of Natural Products*, vol. 58, no. 2, pp. 254–258, 1995.

[5] P. W. Ford and B. S. Davidson, "Plakinidine D, a new pyrroloacridine alkaloid from the ascidian *Didemnum rubeum*," *Journal of Natural Products*, vol. 60, no. 10, pp. 1051–1053, 1997.

[6] C. Ireland and P. J. Scheuer, "Ulicyclamine and ulithiacyclamide, two new small peptides from a marine tunicate," *Journal of the American Chemical Society*, vol. 102, no. 17, pp. 5688–5691, 1980.

[7] H. G. Chun, B. Davies, and D. Hoth, "Didemnin B: the first marine compound entering clinical trials as an antineoplastic agent," *Investigational New Drugs*, vol. 4, no. 3, pp. 279–284, 1986.

[8] M. A. Baker, D. R. Grubb, and A. Lawen, "Didemnin B induces apoptosis in proliferating but not resting peripheral blood mononuclear cells," *Apoptosis*, vol. 7, no. 5, pp. 407–412, 2002.

[9] M. D. Vera and M. M. Joullie, "Natural products as probes of cell biology: 20 Years of didemnin research," *Medicinal Research Reviews*, vol. 22, no. 2, pp. 102–145, 2002.

[10] S. Jin, B. Gorfajn, G. Faircloth, and K. W. Scotto, "Ecteinascidin 743, a transcription-targeted chemotherapeutic that inhibits MDR1 activation," *Proceedings of the National Academy of Sciences of the United States of America*, vol. 97, no. 12, pp. 6775–6779, 2000.

[11] C. van Kesteren, E. Cvitkovic, A. Taamma et al., "Pharmacokinetics and pharmacodynamics of the novel marine-derived anticancer agent ecteinascidin 743 in a phase I dose-finding study," *Clinical Cancer Research*, vol. 6, no. 12, pp. 4725–4732, 2000.

[12] E. G. C. Brain, "Safety and efficacy of ET-743: the French experience," *Anti-Cancer Drugs*, vol. 13, supplement 1, pp. S11–S14, 2002.

[13] J. C. M. Waterval, J. C. Bloks, R. W. Sparidans et al., "Degradation kinetics of aplidine, a new marine antitumoural cyclic peptide, in aqueous solution," *Journal of Chromatography B: Biomedical Sciences and Applications*, vol. 754, no. 1, pp. 161–168, 2001.

[14] C. K. Cai, *Research of anti-HBV activity and pharmacodynamic action and toxicity of SC [Ph.D. thesis]*, Beijing University of Chinese Medicine, Beijing, China, 2006.

[15] W. Binsan, S. Benjakul, W. Visessanguan, S. Roytrakul, M. Tanaka, and H. Kishimura, "Antioxidative activity of Mungoong, an extract paste, from the cephalothorax of white shrimp (*Litopenaeus vannamei*)," *Food Chemistry*, vol. 106, no. 1, pp. 185–193, 2008.

[16] G. K. Jayaprakasha, R. P. Singh, and K. K. Sakariah, "Antioxidant activity of grape seed (*Vitis vinifera*) extracts on peroxidation models *in vitro*," *Food Chemistry*, vol. 73, no. 3, pp. 285–290, 2001.

[17] G. C. Yen and P. D. Duh, "Antioxidative properties of methanolic extracts from peanut hulls," *Journal of the American Oil Chemists' Society*, vol. 70, no. 4, pp. 383–386, 1993.

[18] R. N. Albrecht, *Immunologie Tolerance and Macrophage Function*, Aeademie, New York, NY, USA, 1 edition, 1979.

[19] M. Tsuda and G. J. Schroepfer Jr., "Carbon-13 nuclear magnetic resonance studies of C27 sterol precursors of cholesterol," *Journal of Organic Chemistry*, vol. 44, no. 8, pp. 1290–1293, 1979.

[20] S. Wahidulla, L. D'Souza, and M. Govenker, "Lipid constituents of the red alga *Acantophora spicifera*," *Phytochemistry*, vol. 48, no. 7, pp. 1203–1206, 1998.

[21] G. C. Su, S. Zhang, and S. H. Qi, "Chemical constituents of *Amtipathes dichotoma*," *Chinese Traditional and Herbal Drugs*, vol. 39, no. 11, pp. 1606–1609, 2008.

[22] J. Yang, S.-H. Qi, S. Zhang, and Q.-X. Li, "Chemical constituents from the south China sea gorgonian coral *Subergorgia reticulata*," *Journal of Chinese medicinal materials*, vol. 29, no. 6, pp. 555–558, 2006.

[23] G. S. Wang, Q. Liu, and L. M. Zeng, "The chemical constituents of soft *Cladiella densa* from South China Sea," *Acta Scientiarum Naturalium Universitatis Sunyatseni*, vol. 34, no. 1, pp. 110–112, 1995.

[24] D. Q. Yu and J. S. Yang, *Handbook of Analytical Chmuistry*, vol. 7 of *123*, Chemical Industry Press, Beijing, China, 2nd edition, 1999.

[25] Y. Z. Cai, M. S. M. Sun, J. X. J. Xing, Q. Luo, and H. Corke, "Structure-radical scavenging activity relationships of phenolic compounds from traditional Chinese medicinal plants," *Life Sciences*, vol. 78, no. 25, pp. 2872–2888, 2006.

Hindawi Publishing Corporation
Journal of Chemistry
Volume 2014, Article ID 249485, 6 pages
http://dx.doi.org/10.1155/2014/249485

Research Article

Evaluation on Antioxidant Effect of Xanthohumol by Different Antioxidant Capacity Analytical Methods

Xiu-Li Zhang,[1] Yong-Dong Zhang,[1] Tao Wang,[1] Hong-Yun Guo,[1] Qi-Ming Liu,[2] and Hai-Xiang Su[1]

[1] *Gansu Academic Institute for Medical Research, Lanzhou, Gansu 730050, China*
[2] *Yumen Tuopu Scientific and Technological Development Co., Ltd., Yumen, Gansu 735000, China*

Correspondence should be addressed to Hai-Xiang Su; haixiangsu@163.com

Received 29 January 2014; Revised 30 March 2014; Accepted 30 March 2014; Published 17 April 2014

Academic Editor: Li Ji

Several assays have been frequently used to estimate antioxidant capacities including $ABTS^{\bullet+}$, DPPH, and FRAP assays. Xanthohumol (XN), the major prenylated flavonoid contained in beer, witnessed various reports on its antioxidant capacity. We systematically evaluated the antioxidant activity of XN using three systems, 2,2,-azino-bis-3-ethylbenzthiazoline-6-sulphonic acid ($ABTS^{\bullet+}$) scavenging assays, 1,1-diphenyl-2-picrylhydrazyl (DPPH) radical assays, and ferric reducing antioxidant power (FRAP) assays. The results are expressed as Trolox equivalent antioxidant capacity (TEAC). The TEAC of XN was $0.32 \pm 0.09\ \mu mol \cdot l^{-1}$ by the ABTS assay and $0.27 \pm 0.04\ \mu mol \cdot l^{-1}$ by the FRAP. Meanwhile, the XN did not show obviously scavenging effect on DPPH radical reaction system. These results showed that different methods in the evaluation of compound antioxidant capicity, there may be a different conclusion.

1. Introduction

Antioxidant capacity analysis is an important indicator to evaluate the antioxidation of the component. Several assays have been frequently used to estimate antioxidant capacity in free radical biology including 2,2,-azino-bis-3-ethylbenzthiazoline-6-sulphonic acid ($ABTS^{\bullet+}$) scavenging assays, 1,1-diphenyl-2-picrylhydrazyl (DPPH) radical assays, and ferric reducing antioxidant power (FRAP) assays. The difference of these methods is the use of different free radical. Xanthohumol (XN) is a natural prenylated chalcone derived from hops (*Humulus lupulus L.*). Over the past decade, anticancer, antimutagenic, and anti-inflammatory [1–5] properties of XN have been studied by many researchers, and all of these biological properties are based on its antioxidant effect.

ROS play a crucial role in the pathogenesis of several human diseases, such as cancer, rheumatoid (rheumatoid) arthritis, neurodegenerative diseases, and pulmonary diseases [6]. It seems crucial to quench ROS as fast as possible before they attack biomolecules and cause harm. Antioxidants play an important role to eliminate ROS and other radicals; meanwhile, the antioxidant capacity is positively correlated with the ability of scavenging free radicals. There are many different kinds of evaluation reports for the antioxidant capacity of XN against ROS and other radicals. XN showed high antioxidant activity in inhibiting LDL oxidation [7], was able to scavenge reactive radicals including hydroxyl and peroxyl radicals, and inhibited superoxide anion and nitric oxide production [1]. However, it has also been reported that XN to be prooxidant, was able to rapidly induces $O_2^{\bullet-}$ [8]. In this paper, we compared with different methods for XN antioxidant capacity, to clarify whether methodology resulted in the conclusion differences. We have assessed the antioxidant capacity with attention to the following proposals: (1) Niki and Noguchi reported that there are two types of antioxidants that scavenge radicals quickly and quench many radicals, and they proposed assessing reactivity based on both reaction rate and stoichiometry [9]; (2) the activities of some antioxidants vary depending on the assay method, and thus use of multiple methods is recommended [9–12]; and (3) comparative studies using common antioxidants are essential to clarify the biological significance of the activities of sample.

Trolox equivalent antioxidant capacity (TEAC) assay has been widely accepted for assessing "antioxidant power" as its inexpensive, highly reproducible, straightforward, and speedy procedure [13–16]. The TEAC method is based on the ability of antioxidant compounds to scavenge the long-lived stable radical cation chromophore of 2,2-azinobis (3-ethylbenzothiazoline 6-sulfonate; ABTS). Nowadays, TEAC value can be assigned to all compounds by comparing their scavenging capacity to that of Trolox, a water soluble vitamin E analogue [17], by several free radical reaction systems.

2. Materials and Methods

2.1. Chemicals. 2,2-Azinobis (3-ethylbenzothiazoline 6-sulfonate acid) diammonium salt (ABTS), 6-hydroxy-2,5,7,8-tetramethylchromane-2-carboxylic acid (Trolox), hydrogen peroxide, 2,4,6-tripyridy-s-triazine (TPTZ), and 1,1-diphenyl-2-picrylhydrazyl (DPPH) were purchased from Sigma (ShangHai, Sigma, China). All chemicals were of analytical grade. Reagents were used without further purification. Milli-Q grade water was used in the whole process.

Xanthohumol was extracted from hop pellets (*Humulus lupulus*) in Yumen Tuopu Scientific and Technological Development Co. The briefly procedure as the following description. The purity was 98.64% by high performance liquid chromatography.

2.2. Sample Preparation. Stock solutions of each XN ($100\,\mu g{\cdot}mL^{-1}$) and Trolox ($1\,mg{\cdot}mL^{-1}$) were prepared in 100% ($v{\cdot}v^{-1}$) ethanol and stored at $-20 \pm 2^{\circ}C$ until analysis.

2.3. Xanthohumol (Figure 1) Extraction and Isolation. The air-dried spent hop pellets (*Humulus lupulus*, 1.0 kg) were extracted three times with 70% acetone in water at room temperature; after filtration and evaporation, the residue (150 g) was dissolved in water (2.0 L) and the solution was extracted three times by ethyl acetate (EtOAc) and N-butyl alcohol (n-BuOH), respectively. The EtOAc portion (18 g) was chromatographed on a silica gel column (200–300 mesh 170 g) using CHCl3 : MeOH (100 : 1–2 : 1) gradient to provide 7 fractions (Fr A–G). Fr C was subjected to column chromatography (CC), eluted with CHCl3 : MeOH (100 : 1–3 : 1) to give five fractions (Fr C1–C5). Fr C5 (1.5 g) was subjected to CC eluted with petroleum ether: CH3COCH3 (4 : 1–2 : 1) to give four fractions (C5-1–C5-4). C5-4 was subjected to CC eluted with petroleum ether: CH3COCH3 (4 : 1–2 : 1) and then on a Sephadex LH-20 column (CHCl3 : MeOH, 2 : 1) to obtain Xanthohumol (50 mg).

2.4. Measurement of XN Antioxidant Capacity. Three types of radical scavenging capacity analytical methods were employed in the study as the following description. Each concentration of XN was run in triplicate, respectively. Mean and standard deviation ($n = 3$) were calculated.

2.5. $ABTS^{\bullet+}$ Radical Cation Scavenging Activity of XN. The assay is based on the inhibition of the absorbance of the radical cation of 2,2-azinobis (3-ethylbenzothiazoline 6-sulfonate; ABTS) which has characteristic long-wavelength absorption spectrum showing maximum at 734 nm [17, 18] slightly modified by Erel [19]. 150 μL of ABTS test reagent [17, 18] and 50 μL of sample were added to each well in a 96-well microtiter plate. As unpaired electrons are sequestered by antioxidants in the sample, the ABTS test reagent turns colourless. The absorbance of reaction system at 734 nm with microplate reader is reduced. The percentage inhibition of $ABTS^{\bullet+}$ by the sample was calculated according to the following formula:

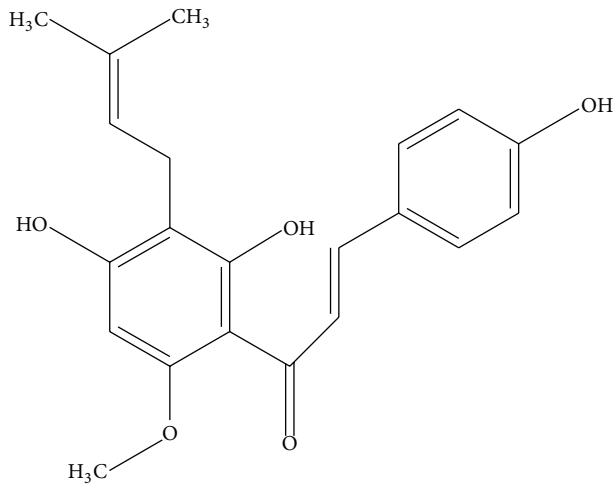

Figure 1: The molecular structure of Xanthohumol.

$$\%\ \text{Inhibition} = \left[\frac{A_0 - A_i}{A_0}\right] \times 100. \quad (1)$$

A_0 is the absorbance of the control, and A_i is the absorbance of the sample.

The free radical scavenging capacity of the XN, calculated as percentage inhibition of $ABTS^{\bullet+}$, was equated against a Trolox standard curve ($10–60\,\mu mol{\cdot}L^{-1}$). Results are expressed in TEAC ($\mu mol{\cdot}L^{-1}$). Necessary dilution was done to ensure the ABTS value fell in the linear range of the standard curve.

2.6. $DPPH^{\bullet}$ Radical Scavenging Activity Assay of XN. The DPPH assay was performed according to the method developed by Brand-Williams et al. [20]. The percentage inhibition of $DPPH^{\bullet}$ by the sample was calculated according to the following formula:

$$\%\ \text{Inhibition} = \left[\frac{A_0 - A_i}{A_0}\right] \times 100. \quad (2)$$

A_0 is the absorbance of the control, and A_i is the absorbance of the sample.

The free radical scavenging capacity of the XN, calculated as percentage inhibition of $DPPH^{\bullet}$, was equated against

a Trolox standard curve (10–60 μmol·L^{-1}). Results are expressed in TEAC concentration (μmol·L^{-1}). Necessary dilution was done to ensure the DPPH value fell in the linear range of the standard curve.

2.7. Ferric-Ion Reducing Antioxidant Power. A slightly modified FRAP method was used to test the total antioxidant capacity of XN [13]. In Benzie and Strain's original FRAP protocol [13, 21], 300 μL of FRAP reagent and 40 μL of sample were used in the reaction system. Half the amounts of FRAP reagent (150 μL) and sample (20 μL) were applied in this study to minimize the amount of sample needed to run the assay [22]. Briefly, the FRAP reagent was produced by mixing 300 mmol·L^{-1} acetate buffer (pH 3.6), 10 mmol·L^{-1} TPTZ solution, and 20 mmol·L^{-1} $FeCl_3 \cdot 6H_2O$ in a 10 : 1 : 1 ration and was prepared freshly at 37°C [21, 23, 24]. A total of 150 μL of working FRAP reagent and 20 μL of sample were added into each well in a 96-well microtiter plate and incubated at room temperature for 30 min in dark [25]. Reading of the colored product (ferrous tripyridyltriazine complex) was taken at 593 nm with microplate reader [22]. The Trolox standard curve was linear between 10 and 60 μmol·L^{-1} Trolox. The initial blank reading for each well with just FRAP reagent was then subtracted from the final reading of FRAP reagent with sample to determine the FRAP value for sample [25]. Results are expressed in TEAC (μmol·L^{-1}). Necessary dilution was done to ensure the FRAP value fell in the linear range of the standard curve. Sample was measured in triplicate. Mean and standard deviation ($n = 3$) were calculated.

2.8. Statistical Analysis. All data are presented as means (±SD) of at least three independent experiments, each experiment having a minimum of three replicates of sample. Student's paired t-test, correlation analyses, and linear regression analyses were performed using SPSS (version 13). The level of statistical significance was set at $P < 0.05$ for two-side testing.

3. Results and Discussion

In the ABTS$^{\bullet+}$ radical cation scavenging assay system, the final concentrations of XN used in the analysis are 60, 50, 40, 30, 20, 10 μmol·L^{-1} with 100% (v·v^{-1}) ethanol, and there was significant linear correlation in the percentage inhibition of concentrations of the XN (15.1%–47%). The maximum inhibition was 47% at the concentration of XN being 60 μmol·L^{-1}. The calibration curve (Figure 2) revealed a highly positive linear ($R^2 = 0.999$) correlation between the mean ABTS$^{\bullet+}$ inhibition percentage and Trolox concentration. This curve was therefore employed to reliably estimate antioxidant potential of the tested samples, and the curve revealed a highly positive linear ($R^2 = 0.9821$) correlation between mean ABTS$^{\bullet+}$ inhibition percentage and concentration of XN too (Figure 3). The TEAC value of XN was 0.32 ± 0.09 μmol·L^{-1} by the ABTS assay (Table 1).

DPPH$^{\bullet}$ radical scavenging activity was quantified in terms of percentage inhibition of a preformed free radical by antioxidants in each sample. Trolox was used as standard antioxidant too. There was a highly positive linear

Table 1: TEAC values of XN as determined by ABTS$^{\bullet+}$, DPPH$^{\bullet}$, and FRAP.

	ABTS$^{\bullet+}$	DPPH$^{\bullet}$	FRAP
TEAC	0.31 ± 0.09 μmol·L^{-1}	—	0.27 ± 0.09 μmol·L^{-1}

Data are expressed as mean ± SD. Each assay was run three times ($n = 3$).

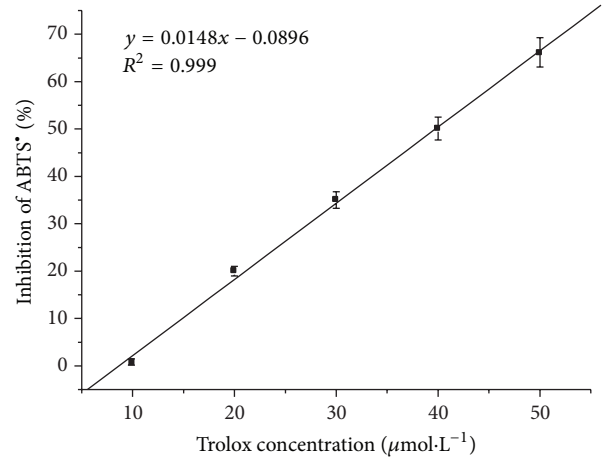

Figure 2: A representative calibration curve of ABTS$^{\bullet+}$ inhibition by Trolox standards (10, 20, 30, 40, 50 μmol·L^{-1}). $Y = 0.0148x - 0.0896$ and $R^2 = 0.999$ ($n = 3$).

($R^2 = 0.9968$) correlation between the mean inhibition value and the Trolox concentration (Figure 4). However, there was no statistic signification on the inhibition (10.7%–11.9%) of the DPPH$^{\bullet}$ radical by the various concentrations of XN (250, 200, 150, 100, 50 μmol·L^{-1} in 100% (v·v^{-1}) ethanol) (Figure 5), with no clear linear correlation between the mean inhibition value and the XN concentration and no clear linear correlation between the mean inhibition value and the XN concentration ($R^2 = 0.6668$).

The calibration curve (Figure 6) revealed a highly positive linear ($R^2 = 0.9992$) relation between mean FRAP value and concentration of Trolox. Figure 7 showed the correlation between FRAP and XN concentrations (125, 100, 75, 50, 25 μmol·L^{-1} in 100% (v·v^{-1}) ethanol), revealed a highly positive linear ($R^2 = 0.9938$). The maximum FRAP value appeared at the 125 μmol·L^{-1} of XN. The TEAC value of XN was 0.27 ± 0.04 μmol·L^{-1} by the FRAP (Table 1).

We evaluated the antioxidant capacity of XN by the TEAC assay through ABTS$^{\bullet+}$, DPPH$^{\bullet}$, and FRAP system and found significant difference for reducing ability of tested sample. Results showed that XN has stronger antioxidant activity in the ABTS$^{\bullet+}$ free radical inhibition and FRAP assay system. In the ABTS$^{\bullet+}$ radical cation scavenging assay system, the 10 μmol·L^{-1} of XN has 16.3% inhibition rate. The inhibition rate of XN reached 46.8% when its concentration was increased to 60 μmol·L^{-1}. There was a highly positive linear ($R^2 = 0.9839$) correlation between mean inhibition value and concentrations of XN which showed that XN significantly

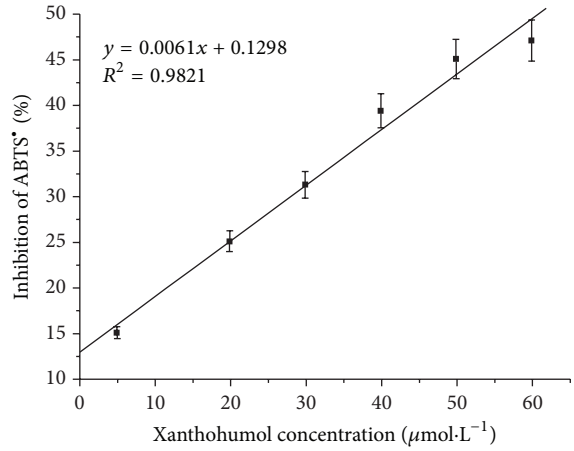

Figure 3: A linear correlation curve between Xanthohumol concentration and ABTS$^{\bullet+}$ inhibition percentage rate. $Y = 0.0061x + 0.1298$ and $R^2 = 0.9821$ ($n = 3$).

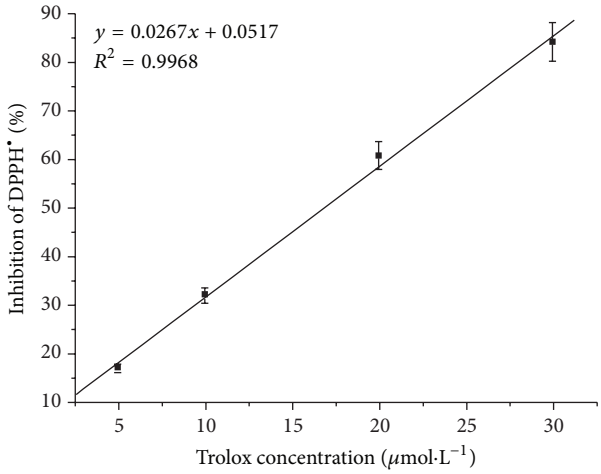

Figure 4: A representative calibration curve of inhibition DPPH$^{\bullet}$ by Trolox standards (5, 10, 20, 30 μmol·L^{-1}). $Y = 0.0267x + 0.0517$ and $R^2 = 0.9968$ ($n = 3$).

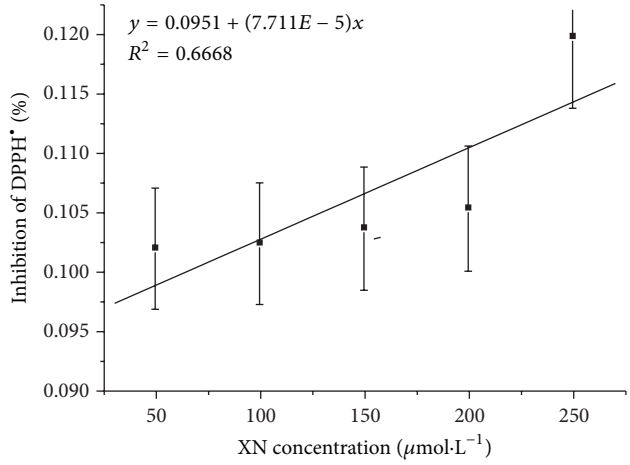

Figure 5: A linear correlation curve between Xanthohumol concentration and DPPH$^{\bullet}$ inhibition percentage rate. $Y = 0.0951 + (7.711E - 5)X$ and $R^2 = 0.6668$ ($n = 3$).

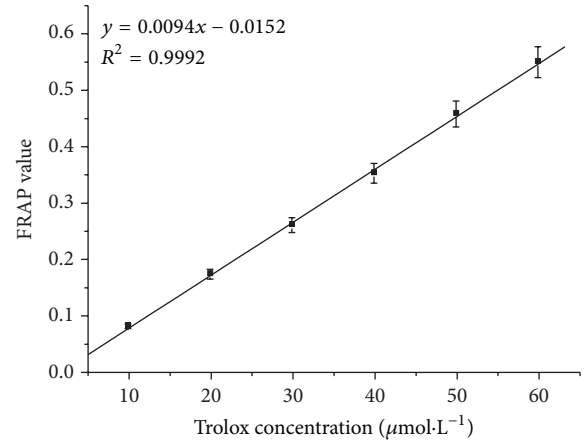

Figure 6: A representative calibration curve of FRAP values by Trolox standards (10, 20, 30, 40, 50, 60 μmol·L^{-1}). $Y = 0.0094x - 0.0152$ and $R^2 = 0.9992$ ($n = 3$).

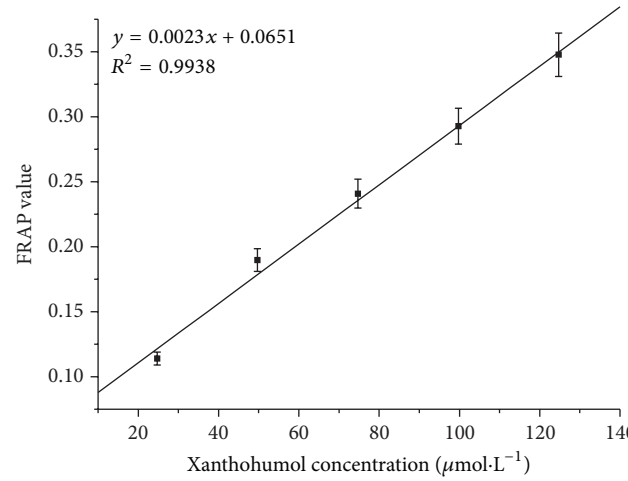

Figure 7: A representative calibration curve between Xanthohumol concentration and FRAP values percentage rate. $Y = 0.0023x + 0.0651$ and $R^2 = 0.9938$ ($n = 3$).

inhibited ABTS$^{\bullet+}$ in a concentration-dependent manner. Since FRAP measures the reduction of FeIII-TPTZ to FeII-TPTZ, the reduction values were 49.2%, 42.3%, 37.2%, 31.5%, and 23.5% with final concentrations of XN (25, 50, 75, 100, and 125 μmol·L^{-1}). Comparing ABTS$^{\bullet+}$ with FRAP radical assay system, XN has stronger scavenging capacity in ABTS$^{\bullet+}$ than FRAP system. In the DPPH assay system, XN showed that the maximum inhibitory is 11.9% with any concentration of XN. Therefore, XN has no or little scavenging effect on DPPH radical cation. Danila et al. have reported that a DPPH does not react with flavonoids without substituted OH in the B-ring or with aromatic acids with a single OH group; consequently, it could be said that DPPH scavenging highly depends on the degree of electron delocalization in a structure-activity study [26, 27]. XN possesses OH phenolics in the B-ring. The Bors's found cannot be used to explain XN's weak DPPH free radical system scavenging effect therefore. The farther studies are needed to clarify the relationship

between the structure of XN and its free radical scavenging capacity in DPPH assay system.

4. Conclusion

The findings of the present study based on different analytical principals suggest that the ABTS, DPPH, and FRAP assays gave comparable results for the antioxidant activity measured of XN. XN is able to scavenge many types of ROS, has stronger free radical scavenging capacity in $ABTS^{\bullet+}$ than FRAP system, and has no or little scavenging effect on DPPH radical cation reaction. So, we need to pay attention to the choice of methods when evaluating the antioxidant capacity of XN.

Conflict of Interests

The authors declare that there is no conflict of interests regarding the publication of this paper.

Acknowledgment

This study was supported by the project supported by the Science-Technology Foundation for Middle-Aged and Young Scientists of Gansu Province, China, no.1170RJY031.

References

[1] C. Gerhauser, A. Alt, E. Heiss et al., "Cancer chemopreventive activity of Xanthohumol, a natural product derived from hop," *Molecular Cancer Therapeutics*, vol. 1, no. 11, pp. 959–969, 2002.

[2] C. Gerhäuser, "Beer constituents as potential cancer chemopreventive agents," *European Journal of Cancer*, vol. 41, no. 13, pp. 1941–1954, 2005.

[3] C. L. Miranda, Y. H. Yang, M. C. Henderson et al., "Prenylflavonoids from hops inhibit the metabolic activation of the carcinogenic heterocyclic amine 2-amino-3-methylimidazo[4,5-f]quinoline, mediated by cDNA-expressed human CYP1A2," *Drug Metabolism and Disposition*, vol. 28, no. 11, pp. 1297–1302, 2000.

[4] R. Monteiro, C. Calhau, A. O. E. Silva et al., "Xanthohumol inhibits inflammatory factor production and angiogenesis in breast cancer xenografts," *Journal of Cellular Biochemistry*, vol. 104, no. 5, pp. 1699–1707, 2008.

[5] F. Ferk, W. W. Huber, M. Filipič et al., "Xanthohumol, a prenylated flavonoid contained in beer, prevents the induction of preneoplastic lesions and DNA damage in liver and colon induced by the heterocyclic aromatic amine amino-3-methylimidazo[4,5-f]quinoline (IQ)," *Mutation Research - Fundamental and Molecular Mechanisms of Mutagenesis*, vol. 691, no. 1-2, pp. 17–22, 2010.

[6] B. Halliwell and J. M. C. Gutteridge, *Free Radicals in Biology and Medicine*, Oxford University Press, New York, NY, USA, 3rd edition, 1999.

[7] C. L. Miranda, J. F. Stevens, V. Ivanov et al., "Antioxidant and prooxidant actions of prenylated and nonprenylated chalcones and flavanones in vitro," *Journal of Agricultural and Food Chemistry*, vol. 48, no. 9, pp. 3876–3884, 2000.

[8] J. Strathmann, K. Klimo, S. W. Sauer, J. G. Okun, J. H. M. Prehn, and C. Gerhäuser, "Xanthohumol-induced transient superoxide anion radical formation triggers cancer cells into apoptosis via a mitochondria-mediated mechanism," *FASEB Journal*, vol. 24, no. 8, pp. 2938–2950, 2010.

[9] E. Niki and N. Noguchi, "Evaluation of antioxidant capacity. What capacity is being measured by which method?" *IUBMB Life*, vol. 50, no. 4-5, pp. 323–329, 2000.

[10] K. Schlesier, M. Harwat, V. Böhm, and R. Bitsch, "Assessment of antioxidant activity by using different in vitro methods," *Free Radical Research*, vol. 36, no. 2, pp. 177–187, 2002.

[11] A. Janaszewska and G. Bartosz, "Assay of total antioxidant capacity: comparison of four methods as applied to human blood plasma," *Scandinavian Journal of Clinical and Laboratory Investigation*, vol. 62, no. 3, pp. 231–236, 2002.

[12] R. L. Prior and G. Cao, "In vivo total antioxidant capacity: comparison of different analytical methods," *Free Radical Biology and Medicine*, vol. 27, no. 11-12, pp. 1173–1181, 1999.

[13] I. F. F. Benzie and J. J. Strain, "The ferric reducing ability of plasma (FRAP) as a measure of "antioxidant power": the FRAP assay," *Analytical Biochemistry*, vol. 239, no. 1, pp. 70–76, 1996.

[14] G. Cao, C. P. Verdon, A. H. B. Wu, H. Wang, and R. L. Prior, "Automated assay of oxygen radical absorbance capacity with the COBAS FARA II," *Clinical Chemistry*, vol. 41, no. 12, pp. 1738–1744, 1995.

[15] N. J. Miller, C. Rice-Evans, M. J. Davies, V. Gopinathan, and A. Milner, "A novel method for measuring antioxidant capacity and its application to monitoring the antioxidant status in premature neonates," *Clinical Science*, vol. 84, no. 4, pp. 407–412, 1993.

[16] C. Rice-Evans and N. J. Miller, "Total antioxidant status in plasma and body fluids," *Methods in Enzymology*, vol. 234, pp. 279–293, 1994.

[17] R. Re, N. Pellegrini, A. Proteggente, A. Pannala, M. Yang, and C. Rice-Evans, "Antioxidant activity applying an improved ABTS radical cation decolorization assay," *Free Radical Biology and Medicine*, vol. 26, no. 9-10, pp. 1231–1237, 1999.

[18] R. van den Berg, G. R. M. M. Haenen, H. Van Den Berg, and A. Bast, "Applicability of an improved Trolox equivalent antioxidant capacity (TEAC) assay for evaluation of antioxidant capacity measurements of mixtures," *Food Chemistry*, vol. 66, no. 4, pp. 511–517, 1999.

[19] O. Erel, "A novel automated direct measurement method for total antioxidant capacity using a new generation, more stable ABTS radical cation," *Clinical Biochemistry*, vol. 37, no. 4, pp. 277–285, 2004.

[20] W. Brand-Williams, M. E. Cuvelier, and C. Berset, "Use of a free radical method to evaluate antioxidant activity," *LWT-Food Science and Technology*, vol. 28, no. 1, pp. 25–30, 1995.

[21] I. F. F. Benzie and J. J. Strain, "Ferric reducing/antioxidant power assay: direct measure of total antioxidant activity of biological fluids and modified version for simultaneous measurement of total antioxidant power and ascorbic acid concentration," *Methods in Enzymology*, vol. 299, pp. 15–27, 1998.

[22] K. Thaipong, U. Boonprakob, K. Crosby, L. Cisneros-Zevallos, and D. Hawkins Byrne, "Comparison of ABTS, DPPH, FRAP, and ORAC assays for estimating antioxidant activity from guava fruit extracts," *Journal of Food Composition and Analysis*, vol. 19, no. 6-7, pp. 669–675, 2006.

[23] C. Guo, J. Yang, J. Wei, Y. Li, J. Xu, and Y. Jiang, "Antioxidant activities of peel, pulp and seed fractions of common fruits as determined by FRAP assay," *Nutrition Research*, vol. 23, no. 12, pp. 1719–1726, 2003.

[24] A. Jiménez-Escrig, M. Rincón, R. Pulido, and F. Saura-Calixto, "Guava fruit (Psidium guajava L.) as a new source of antioxidant dietary fiber," *Journal of Agricultural and Food Chemistry*, vol. 49, no. 11, pp. 5489–5493, 2001.

[25] S. P. Griffin and R. Bhagooli, "Measuring antioxidant potential in corals using the FRAP assay," *Journal of Experimental Marine Biology and Ecology*, vol. 302, no. 2, pp. 201–211, 2004.

[26] W. Bors, C. Michel, and K. Stettmaier, "Antioxidant effects of flavonoids," *BioFactors*, vol. 6, no. 4, pp. 399–402, 1997.

[27] A. O. Danila, F. Gatea, and G. L. Radu, "Polyphenol composition and antioxidant activity of selected medicinal herbs," *Chemistry of Natural Compounds*, vol. 47, no. 1, pp. 22–26, 2011.